# Heavy Baryons\*

J.G.KÖRNER<sup>1</sup>, M.KRÄMER<sup>1,2</sup> and D.PIRJOL<sup>1</sup>

<sup>1</sup>Johannes Gutenberg-Universität, Institut für Physik, D-55099 Mainz, Germany

#### Abstract

We review the experimental and theoretical status of baryons containing one heavy quark. The charm and bottom baryon states are classified and their mass spectra are listed. The appropriate theoretical framework for the description of heavy baryons is the Heavy Quark Effective Theory, whose general ideas and methods are introduced and illustrated in specific examples. present simple covariant expressions for the spin wave functions of heavy baryons including p—wave baryons. The covariant spin wave functions are used to determine the Heavy Quark Symmetry structure of flavour-changing current-induced transitions between heavy baryons as well as one-pion and one-photon transitions between heavy baryons of the same flavour. We discuss  $1/m_Q$  corrections to the current-induced transitions as well as the structure of heavy to light baryon transitions. Whenever possible we attempt to present numbers to compare with experiment by making use of further model-dependent assumptions as e.g. the constituent picture for light quarks. We highlight recent advances in the theoretical understanding of the inclusive decays of hadrons containing one heavy quark including polarization. For exclusive semileptonic decays we discuss rates, angular decay distributions and polarization effects. We provide an update of the experimental and theoretical status of lifetimes of heavy baryons and of exclusive nonleptonic two body decays of charm baryons.

#### KEYWORDS

Angular distributions, heavy baryon decays, heavy quark effective theory, lifetimes, nonleptonic decays, polarization effects, semileptonic decays.

<sup>&</sup>lt;sup>2</sup>Deutsches Elektronen-Synchrotron DESY, D-22603 Hamburg, Germany

<sup>\*</sup> to appear in "Progress in Particle and Nuclear Physics"

# Contents

1	Introduction and Motivation	2
2	Classification of States and Mass Measurements	6
3	Outline of Heavy Quark Effective Theory	8
4		19
	4.1 Ground State Spin Wave Function	
	4.2 Excited Heavy Baryon States	
	4.4 Contribution of Transition Form Factors to the Bjorken Sum Rule	
	4.5 Pion Transitions Between Heavy Baryons	
	4.6 Photon Transitions Between Heavy Baryons	
5	Semileptonic Decays	51
	5.1 Inclusive Semileptonic Rates	. 51
	5.2 Exclusive Semileptonic Decays	. 55
	5.2.1 Amplitudes, Rates and Angular Decay Distributions	
	5.2.2 Model Results $c \to s$	
	5.2.3 Model Results $b \to c$	
	5.3 Polarization effects	. 67
6	Lifetimes and Inclusive Nonleptonic Decays	72
	6.1 Experimental Lifetimes	. 72
	6.2 Theoretical Lifetime Estimates	. 72
7	Exclusive Nonleptonic Decays	76
	7.1 Decay Rates and Decay Distributions	. 76
	7.2 Symmetry Considerations	. 77
	7.3 Quark Model and Current Algebra Results	. 78
8	Summary and Outlook	84

## 1 Introduction and Motivation

This year marks the  $20^{th}$  anniversary of the discovery in 1974 of the  $J/\psi$ , a narrow meson resonance of mass 3.1 GeV [1,2]. With the discovery of the  $J/\Psi$  a new era in particle physics began. In subsequent years this state was successfully interpreted as a bound state composed of the heavy charm quark with mass  $m_c \approx 1.5$  GeV and charge 2/3, and its antiparticle. Soon after the discovery of the so–called hidden charm state  $J/\Psi$  further so–called open charm hadrons composed of a charm quark and light (u:up, d:down, s:strange) quarks/antiquarks were found. The first candidate charm baryon states were detected in 1975 in neutrino interactions [3] soon to be followed by the identification of charm meson states at the SPEAR  $e^+e^-$ –ring in 1976 [4,5]. In retrospect, charm hadrons had probably made their appearance several years earlier in cosmic ray interactions [6].

The discovery [7] in 1977 of the  $\Upsilon$  family of mesons was the first indication of the existence of a fifth quark, the bottom quark b, with mass  $m_b \approx 5$  GeV and a charge -1/3. Again, open bottom meson states composed of a heavy bottom quark and a light antiquark were identified at a somewhat later stage [8,9]. Concerning bottom baryons the experimental situation is not yet quite conclusive. There have been reports on low statistics direct evidence for  $\Lambda_b$  in the channels  $\Lambda_b \to \Lambda \psi$  [10] and  $\Lambda_b \to \Lambda_c \pi^-$  [11]. These results need confirmation from other experiments. Some indirect evidence for semileptonic  $\Lambda_b$  and  $\Xi_b$  decays exists in the form of the detection of enhanced  $\Lambda_c \ell^-$  (high  $p_{\perp}$ ) [12] and  $\Xi_c \ell^-$  (high  $p_{\perp}$ ) [13] correlations from Z-decays at LEP. An early 1981 claim to the first observation of the  $\Lambda_b$  (at a rather low mass of  $\simeq 5425$  MeV) in an ISR experiment has not been upheld and probably was due to a statistical fluctuation [14]. Finally, a third species of heavy flavour quarks is anticipated but not yet identified in the top quark with a mass  $m_t \approx 140$  GeV and charge 2/3.

Recent measurements and theoretical calculations have substantially enhanced our understanding of charm meson states, their spectroscopy and decays. Experimental results on charm baryons and their decays are beginning to be good enough to apply and test what has been learned in the charm meson sector to the charm baryon sector. Furthermore, there is a very active ongoing experimental program at various laboratories to study charm and bottom baryons, their masses, lifetimes and weak decays. The present experiments and further planned future experiments will produce a wealth of data on heavy baryons. It is therefore timely to review what we know now about these states and what we can expect to learn from these experiments. How can we extrapolate theoretical calculations from mesons to baryons, and how do they translate to heavy flavour baryons with bottom quantum numbers?

The heavy charm and bottom quarks and the heavy hadrons composed of them are quite distinct in their properties from the light flavoured hadrons composed of u, d and s quarks. The large mass of the heavy flavoured quarks introduces a mass scale much larger than the confinement scale  $\Lambda \approx 400$  MeV which governs the physics of the light hadrons.

Although heavy hadrons with different heavy flavours have distinctly different masses, they are in some sense quite similar to one another once the appropriate mass scale including possible anomalous dimension factors have been taken care of. Recently this notion has been given a more precise meaning in the Heavy Quark Effective Theory (HQET). The HQET provides a systematic expansion of QCD in terms of inverse powers of the heavy quark mass. The leading term in this expansion gives rise to a new spin– and flavour–symmetry, termed Heavy Quark Symmetry.

Nature has been very accommodating in that it has divided its six quarks into a heavy and a light quark sector. The "heavy" c, b, t quarks are much heavier than the QCD scale  $\Lambda_{QCD} = 400$  MeV whereas the "light" u, d, s quarks are much (except for the s quark) lighter than  $\Lambda_{QCD}$ , i.e. one has

$$m_c, m_b, m_t \gg \Lambda_{QCD} \gg m_u, m_d, m_s$$
 (1)

In the heavy quark sector it then makes sense to first consider QCD in the limit where the heavy quark masses become very large and then, in the second stage, to consider power corrections to this limit in terms of a systematic  $1/m_Q$  expansion. Likewise, one can profitably first study the light quark sector in the zero mass limit, i.e. in the chiral symmetry limit, and then add corrections to the chiral limit at a later stage.

It is quite important to realize that the Heavy Quark Symmetry is not a spectrum symmetry but it is a new type of equal velocity symmetry. That one cannot expect a spectrum symmetry to hold in the heavy quark sector should be quite clear from the fact that there are two orders of magnitude difference between the masses of the c and t quarks! The new type of symmetry at equal velocities takes a little bit of getting used to. But once one has gotten into the habit of thinking in terms of quark and particle velocities the Heavy Quark Symmetry will in fact look quite natural.

The basic physics leading to the new spin and flavour symmetries at equal velocity can easily be appreciated in nontechnical terms by considering a bottom and charm baryon at rest as shown in Fig.1.

The heavy bottom quark and the charm quark at the center are surrounded by a cloud corresponding to a light diquark system. The only communication between the cloud and the center is via gluons. But since gluons are flavour blind the light cloud knows nothing about the flavour at the center. Also, for infinitely heavy quarks, there is no spin communication between the cloud and the center. Thus one concludes that, in the heavy mass limit, a bottom baryon at rest is identical to a charm baryon at rest regardless of the spin orientation of the heavy quarks, i.e. one has

Bottom baryon at 
$$rest(\downarrow\uparrow) = Charm baryon at  $rest(\uparrow\downarrow)$ . (2)$$

One then just needs to boost the rest configuration by a Lorentz boost from velocity zero to velocity v to conclude

Bottom baryon at velocity 
$$v(\downarrow\uparrow) = \text{Charm baryon at velocity } v(\uparrow\downarrow)$$
, (3)

remembering that a Lorentz boost depends only on relative velocities. Eq.(3) exposes the existence of a new spin and flavour symmetry of QCD at equal velocities which holds true in the large mass limit. This is nothing but the advertised Heavy Quark Symmetry.

In fact, everyone should be quite familiar with the existence of such a symmetry in the context of QED. Take a hydrogen, deuterium and tritium atom at rest as also shown in Fig.1.

Figure 1: Portrayal of bottom and charm baryon wave functions at rest. Upper right corner: wave functions of the hydrogen, deuterium and tritium atoms.

When hyperfine interactions are neglected they possess identical wave functions and thus identical atomic properties. The Coulombic interaction between the electron cloud and the nucleus at the center is sensitive only to the total charge of the nucleus which is the same for all three isotopes.

It is quite intriguing that many of the ideas of the HQET date back as far as 1937, then of course in the context of QED [15,16]. In the Bloch–Nordsieck approach to soft photon radiation it was the electron that was "infinitely" heavy (on the scale of the soft photons) so it could be treated as a classical source of radiation. In fact the Bloch–Nordsieck model was already formulated in terms of an effective theory with the electron degrees of freedom removed from the field theory. The quantum mechanical Foldy–Wouthuysen transformation has turned into the field–theoretical 1/m expansion. What used to be called the eikonal approximation is now referred to as on–mass shell propagation of heavy quarks with no velocity change ("velocity superselection rule").

We begin in Sec.2 with a discussion of the ground–state charm and bottom baryons. We list experimental mass values whenever they have been measured. For the missing mass values we give theoretical extrapolations. In Sec.3 we give a brief outline of HQET where we focus on heavy baryon applications. In Sec.4 we write down covariant forms of the heavy baryon spin wave functions including those of the p–wave excited heavy baryon states. Using the covariant spin wave functions we calculate current–induced transitions between heavy baryons of different flavours and discuss their contributions to the sum rule of Bjorken. We also compute one–pion and one–photon transitions between heavy baryons. In Sec.5 we review recent advances in the field of inclusive semileptonic decays of heavy hadrons and hope to convey some of the excitement that has been spawned by these recent developments. Sec.5 also contains a treatment of exclusive  $c \to s$  and  $b \to c$  semileptonic heavy baryon decays including a discussion of polarization effects where there have been some recent experimental and theoretical advances. Sec.6 deals with inclusive nonleptonic decays where we discuss lifetime hierarchies suggested by the interplay of various theoretical mechanisms contributing to the decays. Sec.7 treats exclusive nonleptonic charm baryon decays where there has been a wealth of recent data to

compare with theoretical modelling. Sec.8 contains our theoretical summary and an outlook on the heavy baryon physics that lies ahead of us.

From the point of view of phenomenological applications, the main emphasis in this review is on charm baryons and their decays. The obvious reason is that there already exists enough data on charm baryon decays to make their study worthwhile, while we are just entering the decade of experimental bottom baryon physics.

The charm baryons, being the lightest of the heavy baryons, may not be the best candidates to test and apply the predictions of HQET formulated for infinitely heavy quarks. But certainly charm hadrons and their decays will be the best studied experimentally in the next few years, at least what concerns baryons. Also they are an ideal laboratory to study the influence of preasymptotic 1/m effects to the heavy quark limit. And last, but not least, the quality of the  $b \rightarrow c$  physics to be extracted from bottom baryon to charm baryon transitions depends on the detailed knowledge of the decay properties of charm baryons.

Space limitations preclude an exhaustive treatment of charm and bottom baryon physics and of the many fascinating aspects of heavy hadron physics in general. In particular we do not discuss the physics of charm and bottom baryon production. Instead we focus on the properties of charm and bottom baryons as revealed in their decays. We refer the reader to earlier reviews on heavy baryon physics and on heavy hadron physics in general [17–25].

## 2 Classification of States and Mass Measurements

The ground–state charm baryons are classified as usual as members of the SU(4) multiplets 20' and 20. The  $J^P = 1/2^+$  ground–state baryons (containing the ordinary C = 0 octet baryons) comprise the 20' representation and the  $J^P = 3/2^+$  ground–state baryons (containing the ordinary C = 0 decuplet baryons) make up the 20 representation. For the bottom baryons we limit our attention to the lower mass B = 1 and C = 0 states, which can be classified in analogy to the charm baryon states. In Tables 1, 2, and 3 we list the quantum number content and masses of the charm baryon members of the 20' and 20 representation and of the B = 1, C = 0 bottom baryon states. We use the same notation as the Particle Data Group [26]. I and I<sub>3</sub> denote the isospin; S, C and B refer to the strangeness, charm and bottom quantum numbers.

There exist now precise mass measurements for the charm  $J^P=1/2^+$  baryon states  $\Lambda_c^+$ ,  $\Xi_c^+$ ,  $\Xi_c^0$ ,  $\Sigma_c^{++}$ ,  $\Sigma_c^+$ ,  $\Sigma_c^0$ ,  $\Sigma_c^0$  [26],  $\Omega_c^0$  [27,28] and a first determination of the mass of the  $J^P=3/2^+$  state  $\Sigma_c^*$  [29] at 2530 MeV. The  $\Omega_c^0$  mass listed in Table 1 is an average of the two results [27,28]. Because of the preliminary nature of the  $\Sigma_c^*$  mass determination [29] we do not list the experimental mass in Table 2. Discussion of the recently discovered excited  $\Lambda_c$ -states is deferred to Sec.4.

For the bottom baryons so far only the lowest lying state  $\Lambda_b$  has been observed [10]. The theoretical predictions of the  $\Lambda_b$  mass range from 5547 to 5660 MeV [30] and have to be compared with the experimental mass value of 5641  $\pm$  50 MeV quoted in [26]. Using the symmetry properties of the static theory for heavy quarks simple relations between heavy hadron masses can be derived (see e.g. [31]): from the relation  $M_{\Lambda_c} - 1/4(M_D + 3M_{D^*}) = M_{\Lambda_b} - 1/4(M_B + 3M_{B^*})$  the  $\Lambda_b$  mass is predicted to be  $\cong$  5630 MeV in good agreement with the experimental value. The remaining mass entries in Tables 1, 2, and 3 have been estimated in the framework of the one–gluon–exchange model of [32] where isospin splitting effects are not taken into account. In the non–relativistic Breit–Fermi reduction the one–gluon–exchange contribution leads to a spin–spin interaction of the form

$$H_{ss} = \sum_{i < j} \frac{16\pi\alpha_s}{9m_i m_j} \vec{s}_i \cdot \vec{s}_j \delta^3(\vec{r}_i - \vec{r}_j) \quad . \tag{4}$$

Starting with the seminal work of [32] many authors have emphasized the fact that the hyperfine splitting resulting from (4) is crucial in understanding the mass breaking pattern of both heavy and light hadrons [18,33]. As long as the spin–spin interaction term is taken into account a variety of models with differing degrees of sophistication will basically reproduce the heavy baryon mass pattern in Tables 1, 2, and 3. However, for our estimates of charm and bottom baryon masses in Tables 1, 2, and 3, we have retained the original version of the one–gluon–exchange model as detailed in [32].

Table 1: Charm  $1/2^+$  baryon states. [ab] and  $\{ab\}$  denote antisymmetric and symmetric flavour index combinations.

Notation	Quark	SU(3)	$(I,I_3)$	S	С	Mass
	content					
$\Lambda_c^+$	c[ud]	3*	(0, 0)	0	1	$2285.0 \pm 0.6 \; \mathrm{MeV}$
$\Xi_c^+$	c[su]	3*	(1/2, 1/2)	-1	1	$2466.2 \pm 2.2~\mathrm{MeV}$
$\Xi_c^0$	c[sd]	3*	(1/2, -1/2)	-1	1	$2472.8\pm1.7~\mathrm{MeV}$
$\Sigma_c^{++}$	cuu	6	(1, 1)	0	1	$2453 \pm 0.7 \; \mathrm{MeV}$
$\Sigma_c^+$	$c\{ud\}$	6	(1, 0)	0	1	$2453 \pm 3.0~\mathrm{MeV}$
$\Sigma_c^0$	cdd	6	(1, -1)	0	1	$2452.5\pm0.9~\mathrm{MeV}$
$\Xi_c^{+'}$	$c\{su\}$	6	(1/2, 1/2)	-1	1	$2.57~{ m GeV}$
$\Xi_c^{0'}$	$c\{sd\}$	6	(1/2, -1/2)	-1	1	$2.57~{ m GeV}$
$\Omega_c^0$	css	6	(0, 0)	-2	1	$2719.0 \pm 7.0 \pm 2.5 \text{ MeV}$
$\Xi_{cc}^{++}$	ccu	3	(1/2, 1/2)	0	2	3.61 GeV
$\Xi_{cc}^{+}$	ccd	3	(1/2, -1/2)	0	2	$3.61~{\rm GeV}$
$\Omega_{cc}^{+}$	ccs	3	(0, 0)	-1	2	$3.71~{\rm GeV}$

Of the observed charm and bottom baryons, the  $\Lambda_c$ ,  $\Xi_c$ ,  $\Omega_c$ , and  $\Lambda_b$  states are weakly decaying. According to theoretical expectations, the unobserved  $\Xi_{cc}$ ,  $\Omega_{cc}$  and  $\Omega_{ccc}$  as well as the  $\Xi_b$  and  $\Omega_b$  states in Tables 1 and 3 are also anticipated to be weakly decaying.

Because of the spatial  $\delta$ -function in Equation (4) the matrix elements of the spin-spin interaction term are proportional to the square of the baryon wave function at the origin. The experimental hyperfine splittings thus provide a reliable measure of the wave function at the origin of the ground-state baryons, the value of which is needed in lifetime estimates (cf. Sec.6.2).

Table 2: Charm  $3/2^+$  baryon states.

Notation	Quark	SU(3)	$(I,I_3)$	S	С	Mass
	content					
$\Sigma_c^{*++}$	cuu	6	(1, 1)	0	1	2.51 GeV
$\Sigma_c^{*+}$	cud	6	(1, 0)	0	1	$2.51~{\rm GeV}$
$\Sigma_c^{*0}$	cdd	6	(1, -1)	0	1	$2.51~{\rm GeV}$
<u>=</u> *+	cus	6	(1/2, 1/2)	-1	1	$2.63~{\rm GeV}$
$\Xi^{*0}$	cds	6	(1/2, -1/2)	-1	1	$2.63~{\rm GeV}$
$\Omega_c^{*0}$	css	6	(0, 0)	-2	1	$2.74~{\rm GeV}$
$\Xi_{cc}^{*++}$	ccu	3	(1/2, 1/2)	0	2	$3.68~{\rm GeV}$
$\Xi_{cc}^{*+}$	ccd	3	(1/2, -1/2)	0	2	$3.68~{\rm GeV}$
$\Omega_{cc}^{*+}$	ccs	3	(0, 0)	-1	2	$3.76~{\rm GeV}$
$\Omega_{ccc}^{++}$	ccc	1	(0, 0)	0	3	$4.73~{\rm GeV}$

# 3 Outline of Heavy Quark Effective Theory

Over the last past years it has become widely recognized that the fundamental theory of the strong interactions, quantum chromodynamics (QCD), simplifies enormously in the presence of a very heavy quark [35]. By heavy it is understood that the quark mass must be much larger than the typical scale of the strong interactions  $\Lambda_{QCD} \simeq 400$  MeV. The Heavy Quark Effective Theory (HQET) [36] is a set of rules which embodies in a natural way the new symmetries appearing in this limit and describes in a systematic manner the deviations from the symmetry limit.

There exist two quarks in nature to which the ideas of HQET can be applied: the charmed  $(m_c \simeq 1.5 \text{ GeV})$  and the bottom quark  $(m_b \simeq 4.8 \text{ GeV})$ . In this review we will mainly be concerned with applications of the HQET to the study of baryons made up of one of these two heavy quarks and two light quarks (denoted as Qqq, with Q = c,b and q = u,d,s). The scope of the method is, however, not limited to this situation. It is possible to regard a baryon of the type QQq as a bound state of the heavy pair QQ looking like a pointlike heavy object and the light quark q [37].

Table 3: Bottom baryon states with B=1, C=0 and  $J^P=1/2^+, 3/2^+$  quantum numbers.

Notation	Quark	$J^P$	SU(3)	$(I, I_3)$	S	В	Mass
	content						
$\Lambda_b$	b[ud]	$1/2^{+}$	3*	(0, 0)	0	1	$5641 \pm 50 \text{ MeV}$
$\Xi_b^0$	b[su]	$1/2^{+}$	3*	(1/2, 1/2)	-1	1	$5.80~{\rm GeV}$
$\Xi_b^-$	b[sd]	$1/2^{+}$	3*	(1/2, -1/2)	-1	1	$5.80~{\rm GeV}$
$\Sigma_b^+$	buu	$1/2^{+}$	6	(1, 1)	0	1	5.82 GeV
$\Sigma_b^0$	$b\{ud\}$	$1/2^{+}$	6	(1, 0)	0	1	$5.82~{\rm GeV}$
$\Sigma_b^-$	bdd	$1/2^{+}$	6	(1, -1)	0	1	$5.82~{\rm GeV}$
$\Xi_b^{0'}$	$b\{su\}$	$1/2^{+}$	6	(1/2, 1/2)	-1	1	$5.94~{\rm GeV}$
$\Xi_b^{-'}$	$b\{sd\}$	$1/2^{+}$	6	(1/2, -1/2)	-1	1	$5.94~{\rm GeV}$
$\Omega_b^-$	bss	$1/2^{+}$	6	(0, 0)	-2	1	$6.04~{\rm GeV}$
$\Sigma_b^{*+}$	buu	$3/2^{+}$	6	(1, 1)	0	1	5.84 GeV
$\Sigma_b^{*0}$	bud	$3/2^{+}$	6	(1, 0)	0	1	$5.84~{\rm GeV}$
$\Sigma_b^{*-}$	bdd	$3/2^{+}$	6	(1, -1)	0	1	$5.84~{\rm GeV}$
$\Xi_b^{*0}$	bus	$3/2^{+}$	6	(1/2, 1/2)	-1	1	$5.94~{\rm GeV}$
$\Xi_b^{*-}$	bds	$3/2^{+}$	6	(1/2, -1/2)	-1	1	$5.94~{\rm GeV}$
$\Omega_b^{*-}$	bss	$3/2^{+}$	6	(0, 0)	-2	1	$6.06~{\rm GeV}$

The idea of the Heavy Quark Symmetry is very simple and can be best explained using a quantum mechanical analogy. A bound state Qqq can be looked upon as consisting of the heavy quark Q surrounded by the two light valence quarks, gluons and vacuum pairs, which will be collectively referred to as the "light diquark system" or, more generally, as the "light degrees of freedom". The Heavy Quark Symmetry expresses the fact that the state of the "light degrees of freedom" is independent of that of the heavy quark, in the limit when the mass of the latter goes to infinity. In particular this means that the "light degrees of freedom" will look the same regardless of the flavour type and the spin orientation of the heavy quark. Thus, there are actually two distinct heavy quark symmetries, the flavour symmetry and the spin symmetry, and we will turn to a separate discussion of their properties and consequences.

Before doing this, it is convenient to introduce a formal field—theoretical description for the heavy quark in a hadron of the type Qqq or  $Q\bar{q}$ . The heavy quark in such a bound state continually exchanges momentum with the "light degrees of freedom", of the order  $\Lambda_{QCD}$ , and therefore its change in velocity is of the order  $\Lambda/m_Q$ , which vanishes when the quark is infinitely heavy. Let us consider for simplicity the rest frame of the hadron. Then the heavy quark will be also at rest and we can disregard all its dynamical degrees of freedom, except for colour. It can be then described in terms of the Lagrangian

$$L_{HQET} = \bar{Q}(iD_0 - m_Q)Q, \qquad (5)$$

where  $D_{\mu} = \partial_{\mu} + igA_{\mu}$ . This results from the QCD Lagrangian

$$L_{QCD} = \bar{Q}(i\not\!\!D - m_Q)Q, \qquad (6)$$

when the condition

$$Q = \frac{1 + \gamma_0}{2}Q\tag{7}$$

is imposed. This condition expresses the fact that the heavy quark is at rest and is equivalent to saying that such a quark is only described by the upper two components of the Dirac spinor, the Pauli spinor. The generalization of (5) to a heavy quark moving with velocity v is

$$L_{HQET} = \bar{Q}_v(iv \cdot D - m_Q)Q_v, \qquad (8)$$

where the field  $Q_v$  now satisfies the condition

$$Q_v = \frac{1+\psi}{2}Q_v. (9)$$

It is easy to see that in this limit the quark mass  $m_Q$  becomes irrelevant, as it can be completely removed from the Lagrangian through a simple field transformation

$$h_v = e^{im_Q v \cdot x} Q_v \,. \tag{10}$$

In terms of the new field  $h_v$ , the HQET Lagrangian becomes

$$L_{HQET} = \bar{h}_v(iv \cdot D)h_v. \tag{11}$$

The reader will have noticed that we labeled the heavy quark field  $h_v$  with the heavy quark velocity v. This is to say that for each possible velocity we introduce a distinct field, which duplicates the initial one, and for each such field we have one term in the Lagrangian similar to (11). There is no term in this Lagrangian which connects heavy quark fields of different velocities, so the quark velocity is a good quantum number. This statement is sometimes called the "velocity superselection rule".

Having developed the formalism of the HQET at zero<sup>th</sup> order in  $1/m_Q$ , we are in a position to discuss the two symmetries specific to the infinite mass limit. As discussed before, the flavour symmetry relates heavy hadrons containing different (heavy) quarks. Let us denote the two heavy quark species by b and c. Then the total Lagrangian is

$$L_{HQET} = \bar{h}_v^{(b)}(iv \cdot D)h_v^{(b)} + \bar{h}_v^{(c)}(iv \cdot D)h_v^{(c)}. \tag{12}$$

Note that the two heavy quarks must have the same velocity. It is easy to see that this Lagrangian is invariant under the transformation

$$\begin{pmatrix} h_v^{(c)} \\ h_v^{(b)} \end{pmatrix} \to U \begin{pmatrix} h_v^{(c)} \\ h_v^{(b)} \end{pmatrix}$$

where U is an arbitrary SU(2) matrix. This is the formal statement of the flavour symmetry. Any symmetry in quantum mechanics has in general two consequences: degeneracies and an associated conservation law, and this one is no exception to the rule. The degeneracy implied by the flavour symmetry can be expressed as

$$m_{bqq} - m_b = m_{cqq} - m_c \,, \tag{13}$$

that is, the mass of the light degrees of freedom (for given quantum numbers) is independent of the type of the heavy quark. The other consequence of this symmetry is the existence of a conserved operator, a kind of isospin, which we will denote by  $\vec{\tau}$ . It has the following properties

$$\tau_3|bqq\rangle = |bqq\rangle \qquad \tau_3|cqq\rangle = -|cqq\rangle$$
(14)

$$\tau_{-}|bqq\rangle = |cqq\rangle \qquad \tau_{+}|cqq\rangle = |bqq\rangle \tag{15}$$

where  $\tau_{\pm} = \tau_1 \pm i\tau_2$ . An explicit representation for  $\vec{\tau}$  is

$$\vec{\tau} = \frac{1}{2} \int d^3x (\bar{h}_v^{(b)}(x) \ \bar{h}_v^{(c)}(x)) \gamma_0 \vec{\sigma} \begin{pmatrix} h_v^{(b)}(x) \\ h_v^{(c)}(x) \end{pmatrix}$$
(16)

where  $\vec{\sigma}$  are the Pauli matrices. Note that they act in the flavour space, not on the Dirac indices of the fields. The conservation of  $\vec{\tau}$  can be used to relate amplitudes for processes involving b quarks to those involving c quarks, much in the same way as the conservation of the usual isospin can be used to relate processes involving protons to those involving neutrons.

Another symmetry appearing in the infinite mass limit is the spin symmetry: the "light degrees of freedom" are insensitive to the spin orientation of the heavy quark. This can be seen by noting that the HQET Lagrangian (11) is invariant under an arbitrary spin rotation of the heavy quark (for a heavy quark at rest)

$$h_v \to \exp(\frac{i}{2}\vec{\Sigma} \cdot \vec{n}\theta)h_v$$
 (17)

where  $\vec{n}$  and  $\theta$  are respectively, the rotation axis and the rotation angle, and  $\vec{\Sigma}$  is the spin operator. This symmetry implies a degeneracy between the two states of spin  $J = j \pm \frac{1}{2}$  obtained by coupling the heavy quark spin  $s = \frac{1}{2}$  with the angular momentum of the "light degrees of freedom" j. Such states are for example B and  $B^*$  for mesons and  $\Sigma_b$  and  $\Sigma_b^*$  for baryons. The corresponding conserved quantity is, of course, the heavy quark spin

$$\vec{s} = \frac{1}{2} \int d^3x \bar{h}(x) \gamma_0 \vec{\Sigma} h(x) . \tag{18}$$

The conservation of this operator can be used to relate amplitudes for processes involving the two partners of a multiplet described above.

As an example of how the HQET can relate various transition amplitudes, we consider the calculation of the matrix element [38,39]

$$M_{\mu} = \langle \Lambda_c(v_2, s_2) | \bar{c} \gamma_{\mu} b | \Lambda_b(v_1, s_1) \rangle \tag{19}$$

appearing in the description of the semileptonic decay  $\Lambda_b \to \Lambda_c e \bar{\nu}_e$ . It will be shown that, in the limit of infinitely heavy b and c quarks, it can be completely described in terms of  $\xi(\omega)$  ( $\omega = v_1 \cdot v_2$ ), which is one of the elastic form–factors of the  $\Lambda_c$  baryon, defined through

$$\langle \Lambda_c(v_2, s_2) | \bar{c} \gamma_{\mu} c | \Lambda_c(v_1, s_1) \rangle = \bar{u}(v_2, s_2) [\xi(\omega) \gamma_{\mu} + \zeta(\omega) (v_1 + v_2)_{\mu}] u(v_1, s_1) . \tag{20}$$

This is the most general form which is allowed for this matrix element from current conservation. Furthermore, in the infinite mass limit, the form–factor  $\zeta(\omega)$  will be shown to vanish.

The states in (20) are normalized according to

$$\langle \Lambda_O(p_1, s_1) | \Lambda_O(p_2, s_2) \rangle = 2E_1(2\pi)^3 \delta^{(3)}(\vec{p_1} - \vec{p_2})$$

and the spinors u(v,s) satisfy  $\bar{u}(v,s)u(v,s)=2m_{\Lambda_Q}$ .

Let us write the matrix element (20) in the HQET using the Lagrangian (8) and go to the reference frame where  $v_1 = (1, \vec{0})$ . Also, take  $s_1 = +\frac{1}{2}$  and consider the (1 + i2) component of the vector current. This gives

$$\langle \Lambda_c(v_2, s_2) | \bar{h}_{v_2}^{(c)} \gamma_{1+i2} h_{v_1}^{(c)} | \Lambda_c(\vec{0}, \uparrow) \rangle = \zeta(\omega) \bar{u}(v_2, s_2) u(\vec{0}, \uparrow) v_{2_{1+i2}}, \tag{21}$$

since  $\gamma_{1+i2}u(\vec{0},\uparrow)=0$ . We now use the commutation relation

$$[s_3^{(v_1)}, \bar{h}_{v_2}^{(c)} \gamma_{1+i2} h_{v_1}^{(c)}] = \frac{1}{2} \bar{h}_{v_2}^{(c)} \gamma_{1+i2} h_{v_1}^{(c)}$$
(22)

which can be obtained from the defining relation for  $\vec{s}^{(v_1)}$  (18). Here the fields  $h_{v_1}^{(c)}$  and  $\bar{h}_{v_2}^{(c)}$  must be considered as distinct, according to the discussion above, and therefore they anticommute. Thus we can write

$$\frac{1}{2} \langle \Lambda_c(v_2, s_2) | \bar{h}_{v_2}^{(c)} \gamma_{1+i2} h_{v_1}^{(c)} | \Lambda_c(\vec{0}, \uparrow) \rangle = 
\langle \Lambda_c(v_2, s_2) | s_3^{(v_1)} \bar{h}_{v_2}^{(c)} \gamma_{1+i2} h_{v_1}^{(c)} - \bar{h}_{v_2}^{(c)} \gamma_{1+i2} h_{v_1}^{(c)} s_3^{(v_1)} | \Lambda_c(\vec{0}, \uparrow) \rangle = 
-\frac{1}{2} \langle \Lambda_c(v_2, s_2) | \bar{h}_{v_2}^{(c)} \gamma_{1+i2} h_{v_1}^{(c)} | \Lambda_c(\vec{0}, \uparrow) \rangle = 0,$$
(23)

where we have used that  $s_3^{(v_1)}|\Lambda_c(v_2,s_2)\rangle = 0$  because this state contains no  $v_1$ -type heavy quarks. Comparing with (21), this gives that

$$\zeta(\omega) = 0. \tag{24}$$

We have seen in the above calculation the heavy quark spin symmetry in action. Next we make use of the flavour symmetry to relate the transition matrix element for  $c \to c$  to the matrix element for  $b \to c$ . The proof is entirely analogous to the preceding one, and makes use of the following commutation relation

$$[\tau_{-}, \bar{h}_{v_{2}}^{(c)} \gamma_{\mu} h_{v_{1}}^{(c)}] = -\bar{h}_{v_{2}}^{(c)} \gamma_{\mu} h_{v_{1}}^{(b)}. \tag{25}$$

This gives

$$\langle \Lambda_c(v_2, s_2) | \bar{h}_{v_2}^{(c)} \gamma_\mu h_{v_1}^{(b)} | \Lambda_b(v_1, s_1) \rangle = -\langle \Lambda_c(v_2, s_2) | \tau_- \bar{h}_{v_2}^{(c)} \gamma_\mu h_{v_1}^{(c)} - \bar{h}_{v_2}^{(c)} \gamma_\mu h_{v_1}^{(c)} \tau_- | \Lambda_b(v_1, s_1) \rangle$$

$$= \langle \Lambda_c(v_2, s_2) | \bar{h}_{v_2}^{(c)} \gamma_\mu h_{v_1}^{(c)} | \Lambda_c(v_1, s_1) \rangle = \bar{u}(v_2, s_2) \gamma_\mu u(v_1, s_1) \xi(\omega) . \tag{26}$$

This proves the promised result. Actually it is much more general: any matrix element between any  $\Lambda_Q$  baryon states can be expressed, in the infinite mass limit, in terms of the same function  $\xi(\omega)$ 

$$\langle \Lambda_c(v_2, s_2) | \bar{h}_{v_2}^{(c)} \Gamma h_{v_1}^{(b)} | \Lambda_b(v_1, s_1) \rangle = \bar{u}(v_2, s_2) \Gamma u(v_1, s_1) \xi(\omega) , \qquad (27)$$

with  $\Gamma$  an arbitrary gamma matrix. The universal function  $\xi(\omega)$  is called the Isgur–Wise function or the reduced form–factor. It encodes nonperturbative, long–distance properties of QCD, which are at present noncalculable (except on a lattice or from QCD sum rules) and has therefore to be extracted from experiment. There is one thing which can be said about this function, its value for  $\omega=1$  is known

$$\xi(1) = 1. \tag{28}$$

This may be seen by taking  $v_1 = v_2 = v$  in (20) and noting that the value of the matrix element on the l.h.s. is equal to  $2m_{\Lambda_c}v_{\mu}\delta_{s_1,s_2}$  because the vector current is conserved. Also, on the r.h.s.  $\bar{u}(v,s_2)\gamma_{\mu}u(v,s_1) = 2m_{\Lambda_c}v_{\mu}\delta_{s_1,s_2}$  (because  $\psi u(v,s) = u(v,s)$ ), which gives (28).

In principle, the relation (27) and its generalization to other baryon states could be proved by making use of commutation relations like the ones above. This procedure is rather tedious and, fortunately, there exists a more elegant method which allows one to do the same with considerably less effort. This is the covariant wave–function method, which will be presented later on in Sec.4.

In the infinite mass limit, the matrix element in (27) becomes independent of the heavy quark mass. This is to be expected, because it is a measure of the overlap between the "light degrees of freedom" of the initial and final baryons, which only depends on the velocity change  $\omega$  but not on the masses of the heavy quarks. There are two sorts of corrections to this result which induce a mass-dependence: i) radiative corrections and ii) power–suppressed mass corrections.

The first type of corrections are due to hard gluon exchange between the initial and final heavy quarks and bring about a logarithmic mass dependence of the matrix elements. Because of lack of space, we only quote the result in the leading logarithm approximation [40] and refer the reader to the literature for its derivation:

$$\langle \Lambda_c(v_2, s_2) | \bar{h}_{v_2}^{(c)} \Gamma h_{v_1}^{(b)} | \Lambda_b(v_1, s_1) \rangle =$$

$$\left( \frac{\alpha_s(m_b)}{\alpha_s(m_c)} \right)^{-\frac{6}{25}} \left( \frac{\alpha_s(m_c)}{\alpha_s(\mu)} \right)^{-\frac{8}{27} [\omega r(\omega) - 1]} [\bar{u}(v_2, s_2) \Gamma u(v_1, s_1)] \xi(\omega, \mu)$$

$$(29)$$

with

$$r(x) = \frac{1}{\sqrt{x^2 - 1}} \log(x + \sqrt{x^2 - 1}). \tag{30}$$

The Isgur–Wise function  $\xi(\omega, \mu)$  acquires a dependence on the renormalization scale  $\mu$ , which is exactly compensated by the  $\mu$ –dependence in the anomalous dimension factor, so that the matrix element is  $\mu$ –independent.

In contrast to the radiative corrections discussed above, which have left unchanged the prediction (27) (apart from multiplying it with a correction factor), the corrections suppressed by one or more powers of  $1/m_Q$  change its form. This will be seen to happen because these corrections break in general both the spin and the flavour heavy quark symmetries. To order  $1/m_Q$  they can be obtained in a simple way as follows. Consider the Dirac equation for the heavy quark field

$$(i \not\!\!D - m_Q)Q = 0. (31)$$

Decompose Q(x) into an "upper" and a "lower" component

$$Q(x) = e^{-im_Q v \cdot x} (h^{(+)}(x) + h^{(-)}(x)), \qquad \forall h^{(\pm)} = \pm h^{(\pm)}.$$
 (32)

Introducing this into the Dirac equation (31) and projecting the resulting relation onto the "upper" and "lower"—spaces gives two equations

$$i \mathcal{D}_{\perp} h^{(+)} - (iv \cdot D + 2m_Q) h^{(-)} = 0$$
 (33)

$$iv \cdot Dh^{(+)} + i \mathcal{D}_{\perp} h^{(-)} = 0.$$
 (34)

The first relation can be used to solve for  $h^{(-)}$  in terms of  $h^{(+)}$ :

$$h^{(-)} = \frac{i \not D_{\perp}}{2m_Q} h^{(+)} + \mathcal{O}(1/m_Q^2)$$
 (35)

which, when inserted into the second relation, gives the equation of motion for the  $h^{(+)}$  field

$$\left(iv \cdot D + \frac{(i\mathcal{D}_{\perp})^2}{2m_Q} + \cdots\right)h^{(+)} = 0. \tag{36}$$

This can be considered to have arisen from the Lagrangian [41–43]

$$\mathcal{L}_{HQET} = \bar{h}^{(+)} i v \cdot D h^{(+)} + \bar{h}^{(+)} \frac{(i \mathcal{D}_{\perp})^2}{2m_Q} h^{(+)} + \cdots$$
 (37)

which gives the generalization of (11) by including corrections of order  $1/m_Q$  (the derivation presented here has been taken from [25]). The relation of the QCD field Q(x) to the HQET field  $h^{(+)}$  can be found from (32,35) to be given by

$$Q(x) = e^{-im_Q v \cdot x} \left( 1 + \frac{i \mathcal{D}_{\perp}}{2m_Q} + \cdots \right) h^{(+)}(x). \tag{38}$$

We mention that the extension of this method to obtain the higher order corrections to the HQET Lagrangian (see also [43]) is not without risk [44,45]. This is due to the fact that the  $h^{(+)}(x)$  field has a mass-dependent normalization. The correct heavy quark field must be determined from the condition of its having the same normalization as the QCD field Q(x) [42].

We proceed now with investigating the effects of the new terms which appear in the HQET Lagrangian at order  $1/m_Q$ . They can be written in a slightly different form as

$$\mathcal{L}_{HQET} = \bar{h}^{(+)} i v \cdot D h^{(+)} + \frac{1}{2m_Q} \bar{h}^{(+)} \left( (iD)^2 - (iv \cdot D)^2 - \frac{g}{2} \sigma_{\mu\nu} F^{\mu\nu} \right) h^{(+)} + \cdots$$
 (39)

with

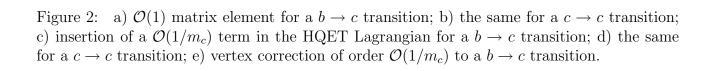
$$F^a_{\mu\nu} = \partial_\mu A^a_\nu - \partial_\nu A^a_\mu - g f_{abc} A^b_\mu A^c_\nu \,. \tag{40}$$

All three terms at order  $1/m_Q$  break the flavour symmetry. Indeed, one cannot rotate anymore the fields of two heavy quarks into each other, as before, because the mass factors  $1/m_Q$  are different for the two quarks. The last term breaks also the spin symmetry, because it is no longer invariant under the field transformation (17). One therefore expects corrections to the predictions (27), which have been obtained under the assumption that these two symmetries are valid. There is, however, one important kinematical point where these corrections vanish and the leading order result (27) remains valid. This happens for the zero recoil point  $v_1 = v_2$ . This result is called Luke's theorem [46,47,49,42]. We shall prove Luke's theorem for the special case of  $\Lambda_b \to \Lambda_c$  transitions. We will do this by explicitly calculating the form of the  $1/m_c$ -order correction to the matrix elements of the vector and axial transition currents away from the equal-velocity point [47]. The correction proportional to  $1/m_b$  can be calculated in a completely analogous manner.

There are two sources of corrections to the prediction (27): i) corrections due to the new terms in the Lagrangian (39) and ii) corrections due to the modified form of the current:

$$\bar{c}\Gamma b \to \bar{h}_{v_2}^{(c)}\Gamma h_{v_1}^{(b)} - \frac{1}{2m_c}\bar{h}_{v_2}^{(c)}(i\not\!\!\!\!D_\perp)\Gamma h_{v_1}^{(b)}.$$
 (41)

These corrections are represented into a graphical form in Fig.2. The insertion of a  $1/m_c$  term in the HQET Lagrangian is shown as a cross on the c propagator and contributes a



correction to (27) equal to

$$\frac{i}{2m_c} \langle \Lambda_c(v_2, s_2) | \int d^4x T(\bar{h}_{v_2}^{(c)}(iD)^2 h_{v_1}^{(c)})(x) (\bar{h}_{v_2}^{(c)} \Gamma h_{v_1}^{(b)})(0) | \Lambda_b(v_1, s_1) \rangle 
- \frac{i}{4m_c} \langle \Lambda_c(v_2, s_2) | \int d^4x T(\bar{h}_{v_2}^{(c)} g \sigma_{\mu\nu} F^{\mu\nu} h_{v_1}^{(c)})(x) (\bar{h}_{v_2}^{(c)} \Gamma h_{v_1}^{(b)})(0) | \Lambda_b(v_1, s_1) \rangle = 
\frac{1}{2m_c} \bar{u}(v_2, s_2) \Gamma u(v_1, s_1) \eta(\omega) + \frac{1}{2m_c} \bar{u}(v_2, s_2) \sigma^{\mu\nu} \frac{1 + \psi_2}{2} \Gamma u(v_1, s_1) \zeta_{\mu\nu}(\omega)$$
(42)

where  $\eta(\omega)$  is an unknown function and  $\zeta_{\mu\nu}$  is the most general antisymmetric tensor which can be built from  $v_1, v_2$  and hence is proportional to  $v_{1\mu}v_{2\nu} - v_{1\nu}v_{2\mu}$  (the combination  $\epsilon_{\mu\nu\lambda\xi}v_1^{\lambda}v_2^{\xi}$  is not allowed because it has the wrong parity, it transforms as a pseudotensor). Actually, this form for  $\zeta_{\mu\nu}$  vanishes when inserted in (42) because  $\sigma_{\mu\nu}v_2^{\nu} = 0$  when sandwiched between projectors  $(1 + \psi_2)/2$  and we are only left with the first term.

The correction to the current (41) is shown in Fig.2 as a cross on the upper vertex and contributes to the matrix element (27) the term

$$-\frac{1}{2m_c} \langle \Lambda_c(v_2, s_2) | (\bar{h}_{v_2}^{(c)}(i \not\!\!\!\!D_\perp) \Gamma h_{v_1}^{(b)})(0) | \Lambda_b(v_1, s_1) \rangle. \tag{43}$$

Let us first calculate the matrix element

$$\langle \Lambda_c(v_2, s_2) | \bar{h}_{v_2}^{(c)}(i \stackrel{\leftarrow}{D_{\mu}}) \Gamma h_{v_1}^{(b)} | \Lambda_b(v_1, s_1) \rangle = \bar{u}(v_2, s_2) \Gamma u(v_1, s_1) [Av_{1_{\mu}} + Bv_{2_{\mu}}], \tag{44}$$

in terms of which one can readily express (43). Here A, B are functions of  $v_1 \cdot v_2$  which we will compute now. Multiplying (44) with  $v_{2\mu}$  and using the equation of motion for the  $h_{v_1}^{(c)}$  field  $\bar{h}_{v_2}^{(c)}iv_2 \cdot \stackrel{\leftarrow}{D} = 0$ , one obtains

$$B = -Av_1 \cdot v_2 \,. \tag{45}$$

A can be obtained by noting that

$$\langle \Lambda_c(v_2, s_2) | i \partial_{\mu} (\bar{h}_{v_2}^{(c)} \Gamma h_{v_1}^{(b)}) | \Lambda_b(v_1, s_1) \rangle = \bar{\Lambda}(v_{1\mu} - v_{2\mu}) \langle \Lambda_c(v_2, s_2) | \bar{h}_{v_2}^{(c)} \Gamma h_{v_1}^{(b)} | \Lambda_b(v_1, s_1) \rangle 
= \bar{\Lambda}(v_{1\mu} - v_{2\mu}) \bar{u}(v_2, s_2) \Gamma u(v_1, s_1) \xi(\omega)$$
(46)

with  $\bar{\Lambda} = m_{\Lambda_Q} - m_Q$  the binding energy of the  $\Lambda_Q$  baryon, which is independent of Q in the infinite mass limit. On the other hand, the first matrix element in this equation can be written as

$$\langle \Lambda_c(v_2, s_2) | \bar{h}_{v_2}^{(c)}(i \stackrel{\leftarrow}{D_{\mu}}) \Gamma h_{v_1}^{(b)} | \Lambda_b(v_1, s_1) \rangle + \langle \Lambda_c(v_2, s_2) | \bar{h}_{v_2}^{(c)} \Gamma(i \stackrel{\rightarrow}{D_{\mu}}) h_{v_1}^{(b)} | \Lambda_b(v_1, s_1) \rangle$$

$$(47)$$

By contracting this with  $v_{1\mu}$  and comparing with (44,46), the following result emerges

$$A = \frac{\bar{\Lambda}\xi(\omega)}{1+\omega} \,. \tag{48}$$

Thus, for example the correction to (27) for  $\Gamma = \gamma_{\mu}$  can be obtained to be of the form

$$-\frac{1}{2m_c}\bar{u}(v_2, s_2)[2v_{1\mu} - \gamma_{\mu}(1+\omega)]u(v_1, s_1)\frac{\bar{\Lambda}\xi(\omega)}{1+\omega} + \frac{1}{2m_c}[\bar{u}(v_2, s_2)\gamma_{\mu}u(v_1, s_1)]\eta(\omega). \tag{49}$$

One can obtain a condition on  $\eta(1)$  by considering the same correction to the matrix element

$$\langle \Lambda_c(v, s_2) | \bar{h}_{v_1}^{(c)} \gamma_\mu h_{v_1}^{(c)} | \Lambda_c(v, s_1) \rangle$$

which, by current conservation, is known to vanish. This can be calculated in a completely analogous way, with the result

$$\frac{1}{m_c} [\bar{u}(v_2, s_2)\gamma_\mu u(v_1, s_1)] (\eta(\omega) + \bar{\Lambda}\xi(\omega)) - \frac{1}{m_c} \frac{\bar{\Lambda}\xi(\omega)}{1+\omega} [\bar{u}(v_2, s_2)u(v_1, s_1)] (v_{1\mu} + v_{2\mu}). \tag{50}$$

This should vanish for  $v_1 = v_2$ , whence  $\eta(1) = 0$ .

The correction to (27) for the other case of physical significance  $\Gamma = \gamma_{\mu} \gamma_{5}$ , is equal to

$$-\frac{1}{2m_c}\bar{u}(v_2, s_2)[2v_{1\mu} + \gamma_{\mu}(1-\omega)]\gamma_5 u(v_1, s_1)\frac{\bar{\Lambda}\xi(\omega)}{1+\omega} + \frac{1}{2m_c}[\bar{u}(v_2, s_2)\gamma_{\mu}\gamma_5 u(v_1, s_1)]\eta(\omega). \tag{51}$$

We can summarize our findings by introducing six form–factors  $f_{1,2,3}^V(\omega)$  and  $f_{1,2,3}^A(\omega)$ , defined by

$$\langle \Lambda_c(v_2, s_2) | \bar{c} \gamma_\mu b | \Lambda_b(v_1, s_1) \rangle = \bar{u}(v_2, s_2) [f_1^V \gamma_\mu + f_2^V v_{1\mu} + f_3^V v_{2\mu}] u(v_1, s_1)$$
 (52)

$$\langle \Lambda_c(v_2, s_2) | \bar{c} \gamma_\mu \gamma_5 b | \Lambda_b(v_1, s_1) \rangle = \bar{u}(v_2, s_2) [f_1^A \gamma_\mu + f_2^A v_{1\mu} + f_3^A v_{2\mu}] \gamma_5 u(v_1, s_1) . \tag{53}$$

In terms of these form–factors, the relations (27,49,51) can be compactly expressed as

$$f_1^V(\omega) = \xi(\omega) + \left(\frac{1}{2m_c} + \frac{1}{2m_b}\right) (\eta(\omega) + \bar{\Lambda}\xi(\omega))$$
 (54)

$$f_2^V(\omega) = -\frac{1}{m_c} \frac{\bar{\Lambda}\xi(\omega)}{1+\omega} \tag{55}$$

$$f_3^V(\omega) = -\frac{1}{m_b} \frac{\bar{\Lambda}\xi(\omega)}{1+\omega} \tag{56}$$

$$f_1^A(\omega) = \xi(\omega) + \left(\frac{1}{2m_c} + \frac{1}{2m_b}\right) \left(\eta(\omega) + \frac{\bar{\Lambda}\xi(\omega)(\omega - 1)}{1 + \omega}\right)$$
 (57)

$$f_2^A(\omega) = -\frac{1}{m_c} \frac{\Lambda \xi(\omega)}{1+\omega} \tag{58}$$

$$f_3^A(\omega) = \frac{1}{m_b} \frac{\bar{\Lambda}\xi(\omega)}{1+\omega} \,. \tag{59}$$

We have included here also the corrections proportional to  $1/m_b$ , which can be obtained from those of order  $1/m_c$  by taking the complex conjugate followed by the interchange of the quark labels  $c \leftrightarrow b$ .

For  $v_1 = v_2$  one can see, by making use of  $\xi(1) = 1$  and  $\eta(1) = 0$ , that

$$f_1^V(1) + f_2^V(1) + f_3^V(1) = 1 (60)$$

$$f_1^A(1) = 1 (61)$$

which is just the content of Luke's theorem for the  $\Lambda_{Q_1} \to \Lambda_{Q_2}$  transitions (the original derivation of the theorem [46] was given for the transition matrix elements between meson states  $B \to D^{(*)}$ ). The linear combination of vector current amplitudes in Eq.(60) and the axial vector current amplitude  $f_1^A$  in Eq.(61) are the partial wave s-wave amplitudes that survive in the limit  $\omega \to 1$  (see the discussion in Sec.5.2.2). We emphasize that Luke's theorem and the  $\mathcal{O}(1/m_Q)$  normalization condition applies to the s-wave amplitudes as written down in (60,61). We mention that the  $1/m_Q$  corrections have been worked out also for other baryonic

transitions of interest, like  $\Omega_b \to \Omega_c^{(*)}$  [48], for which simplifications similar to (60,61) hold true at the zero–recoil point  $v_1 = v_2$ .

We mention that Luke's theorem can be proved in a very general context using a diagrammatic language [42]. Referring to the  $b \to c$  and  $c \to c$  transitions drawn in Fig.2 one notes that there is a doubling up of the contributions of both the Lagrangian and the current insertion when going from the inelastic  $b \to c$  to the elastic  $c \to c$  case. Since one knows from current conservation that the elastic  $1/m_c$  corrections have to vanish at the zero recoil point (or, equivalently, at  $q^2 = 0$ ) one concludes that also the inelastic  $1/m_c$  corrections have to vanish at the zero recoil point — they are exactly one—half of the vanishing elastic  $1/m_c$  corrections. This way of proving Luke's theorem is independent of what happens on the light side and thus immediately applies to any heavy particle transition, be it baryons, mesons or even supersymmetric heavy particles. Using the diagrammatic language one can also immediately appreciate that Luke's theorem breaks down at  $\mathcal{O}(1/m_c^2)$ . The elastic  $\mathcal{O}(1/m_c^2)$  transition shown in diagram 2f has no analogue in the inelastic  $b \to c$  case and thus there is no longer a doubling up argument as was used in the  $\mathcal{O}(1/m_c)$  proof.

This concludes our brief presentation of the basic ideas and methods of the HQET. The reader can find more details and applications in the many good existing reviews on this subject [24,25].

# 4 Heavy Baryon Spin Wave Functions and Heavy Baryon Transitions

The heavy baryons that we are mainly concerned with in this review are bound states formed from a heavy quark and a light diquark system. The spin–parity quantum numbers  $j^P$  of the light diquark system are determined from the spin and orbital degree of freedom of the two light quarks that make up the diquark system. From the spin degrees of freedom of the two light quarks one obtains a spin 0 and a spin 1 state. The total orbital state of the diquark system is characterized by two angular degrees of freedom which we take to be the two independent relative momenta  $k = \frac{1}{2}(p_1 - p_2)$  and  $K = \frac{1}{2}(p_1 + p_2 - 2p_3)$  that can be formed from the two light quark momenta  $p_1$  and  $p_2$  and the heavy quark momentum  $p_3$ . The k-orbital momentum describes relative orbital excitations of the two light quarks, and the K-orbital momentum describes orbital excitations of the center of mass of the two light quarks relative to the heavy quark as drawn in Fig.3.

Figure 3: Orbital angular momenta of the light diquark system.  $l_k$  describes relative orbital momentum of the two light quarks and  $l_K$  describes orbital momentum of the center of mass of the light quarks relative to the heavy quark.

In this review we limit our discussion to the ground state baryons with  $l_k = l_K = 0$  and the p-wave baryons with  $(l_k = 0, l_K = 1)$  or  $(l_k = 1, l_K = 0)$ . A treatment of higher orbital excitations can be found in [50]. The flavour symmetry nature of the light diquark state can then be determined from the generalized Pauli principle as applied to the light quark sector. Totally antisymmetric (symmetric) spatial configurations are antisymmetric (symmetric) in

flavour space. The antisymmetric flavour configurations  $\Lambda_{[q_1q_2]Q}$  will be generically referred to as  $\Lambda$ -type states and the symmetric flavour configurations  $\Sigma_{\{q_1q_2\}Q}$  as  $\Sigma$ -type states. In SU(3) (q=u,d,s) the  $\Lambda$ -type states form an antitriplet  $3^*$  and the  $\Sigma$ -type states a sextet 6 according to the decomposition  $3\otimes 3=3^*\oplus 6$ .

Mass values of the ground state charm and bottom baryons have been listed in Tables 1,2 and 3. As concerns p-wave levels there are altogether seven  $\Lambda$ -type and seven  $\Sigma$ -type p-wave states for a given flavour configuration. According to a quark model calculation [51] done in the charm baryon sector the p-wave levels are well separated from the ground states. For the  $\Lambda_c$ -type p-wave states the two  $(l_k = 0, l_K = 1)$  states are lowest because orbital and spin-spin splitting effects work in the same direction to lower these two states while the five  $(l_k = 1, l_K = 0)$  states are raised. The total orbital and spin-spin splitting effect amounts to  $\cong 350$  MeV. For the  $\Sigma_c$ -type states, however, the orbital and spin-spin splitting effects work in opposite directions leading to a close level spacing of the seven  $\Sigma_c$ -type states.

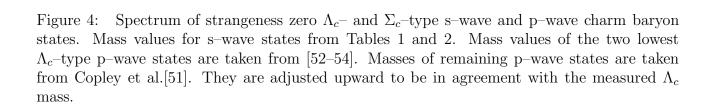
These qualitative features clearly show up in the  $\Lambda_c$ - and  $\Sigma_c$ -type charm baryon level plot in Fig.4 taken from the calculation of [51]. Copley et al. [51] used a constituent quark model based on harmonic oscillator interquark forces. The two recently found excited  $\Lambda_c$ -states at  $\cong 2593$  MeV [52] and at  $\cong 2627$  MeV [52–54] lie almost on top of the two ( $l_k = 0$ ,  $l_K = 1$ ) levels predicted by [51] thus inviting an interpretation of these two new states as forming the  $1/2^-$  and  $3/2^-$  members of the ( $l_k = 0$ ,  $l_K = 1$ ) Heavy Quark Symmetry spin doublet. The details of the closely spaced level ordering of the remaining five  $\Lambda_c$ -type and seven  $\Sigma_c$ -type p-wave states awaits to be unravelled by further experimental and theoretical effort.

There exists no universal agreement on how to label the excited heavy baryon states. In a spectroscopic notation one would write  ${}^{2s+1}_{j}(l;l_1,l_2)_J$  where  $l_1$  and  $l_2$  are the two light–side orbital degrees of freedom coupling to a total orbital momentum l. The total orbital momentum then couples with the spin singlet or triplet state 2s+1 to form a light diquark state with spin j. The total spin J of the heavy baryon is then obtained by coupling j with the heavy quark spin  $S_Q = 1/2$  to form  $J = j \pm 1/2$ . In order to avoid the cumbersome spectroscopic notation we use a more concise notation in this review which is i) tailored to the p–wave states and ii) uses the  $l_1 = l_k$  and  $l_2 = l_K$  basis which diagonalizes the Hamiltonian, at least in the harmonic oscillator approximation [51]. The  $(l_k = 0, l_K = 1)$  and the  $(l_k = 1, l_K = 0)$  states will be referred to as the K– and k–states, respectively. Heavy Quark Symmetry doublets will be denoted by  $\{B_{QKj}\}$  or  $\{B_{Qkj}\}$  (j=1,2) and the singlets (j=0) by  $B_{QK0}$  and  $B_{Qk0}$   $(B = \Lambda$ – or  $\Sigma$ –type). The two degenerate members of the doublets are denoted by  $\{B_{QKj}\}$  :=  $\{B_{QKj}, B_{QKj}^*\}$  (and the same for  $K \to k$ ) for total heavy baryon spins  $\{J = j - 1/2, J = j + 1/2\}$ . When summarily referring to excited heavy baryon states these will be called  $B_Q^*$  as in  $\Lambda_Q^*$  or  $\Sigma_Q^*$ .

## 4.1 Ground State Spin Wave Function

The ground state heavy baryons  $(l_k = l_K = 0)$  are made from the heavy quark Q with spin-parity  $J^P = \frac{1}{2}^+$  and a light diquark system with spin-parity  $0^+$  ( $\Lambda$ -type) and  $1^+$  ( $\Sigma$ -type) moving in a s-wave state relative to the heavy quark. The spin wave functions of the light diquark system will be denoted by  $\chi^0$  and  $\chi^{1,\mu}$  for the spin 0 and spin 1 diquark, respectively. When one combines the diquark spin with the heavy quark's spin one obtains the ground state heavy baryons  $\Lambda_Q$  and  $\{\Sigma_Q, \Sigma_Q^*\}$  according to the coupling scheme

$$0^+ \otimes \frac{1}{2}^+ \to \frac{1}{2}^+ \qquad \Lambda_Q \tag{62}$$



$$1^{+} \otimes \frac{1}{2}^{+} \setminus \frac{\frac{1}{2}^{+}}{\frac{3}{2}^{+}} \quad \left\{\begin{array}{c} \Sigma_{Q} \\ \Sigma_{Q}^{*} \end{array}\right\}$$
 (63)

The two states  $\Sigma_Q$  and  $\Sigma_Q^*$  are exactly degenerate in the heavy quark limit since the heavy quark possesses no spin interaction with the light-side diquark system as  $m_Q \to \infty$ .

For the purposes of deriving the consequences of the Heavy Quark Symmetry the only information needed about the light diquark system is its spin and its parity. This entails the transversality condition on the 1<sup>+</sup> state  $v^{\mu}\chi^{1}_{\mu} = 0$ . Nevertheless it is convenient (but not necessary) to regard the spin 0 and spin 1 diquark system as being composed of two light quarks according to

$$\frac{1}{2}^{+} \otimes \frac{1}{2}^{+} = 0^{+} \oplus 1^{+} \quad . \tag{64}$$

The explicit forms of the covariant bispinor spin wave functions in the constituent quark model read (see [50])

$$\begin{array}{rcl}
0^{+}: & \hat{\chi}_{\alpha\beta}^{0} & = & \frac{1}{2\sqrt{2}}[(\psi+1)\gamma_{5}C]_{\alpha\beta} \\
1^{+}: & \hat{\chi}_{\alpha\beta}^{1,\mu} & = & \frac{1}{2\sqrt{2}}[(\psi+1)\gamma_{\perp}^{\mu}C]_{\alpha\beta}
\end{array} (65)$$

where  $\gamma_{\perp}^{\mu}$  is the (four–) transverse  $\gamma$ –matrix defined by  $\gamma_{\perp}^{\mu} = \gamma^{\mu} - \psi v^{\mu}$ , and  $v^{\mu}$  is the fourvelocity of the diquark system (equal to the heavy baryon's four velocity  $v^{\mu} = \frac{P^{\mu}}{M}$ ). C is the  $4 \times 4$  charge conjugation matrix  $C = i\gamma_0\gamma_2$  and serves to "pull down" the antispinor index in the remaining spinor–antispinor  $\gamma$ –matrix combination. In the following we shall drop explicit reference to the spin of the bispinor state and write  $\hat{\chi}$  and  $\hat{\chi}^{\mu}$  for  $\hat{\chi}^0$  and  $\hat{\chi}^{1,\mu}$ , respectively, where this does not lead to confusion.

The spin wave functions  $\hat{\chi}$  and  $\hat{\chi}^{\mu}$  satisfy the so-called Bargmann-Wigner equations on both labels, i.e.

$$\psi_{\alpha\alpha'}\hat{\chi}_{\alpha'\beta} = \psi_{\alpha\beta'}\hat{\chi}_{\beta\beta'} = \hat{\chi}_{\alpha\beta} \tag{66}$$

and similarly for  $\hat{\chi}^{\mu}$ . They further possess the symmetry properties

$$\hat{\chi}_{\alpha\beta} = -\hat{\chi}_{\beta\alpha} 
\hat{\chi}_{\alpha\beta}^{\mu} = \hat{\chi}_{\beta\alpha}^{\mu}$$
(67)

The transverse  $\gamma_{\mu}$ -matrix is used in the spin 1 part of Eq.(65) in order to ensure that the spin 1 wave function is transverse to the four-velocity  $v^{\mu}$ , i.e.

$$v_{\mu}\hat{\chi}^{\mu} = 0 \tag{68}$$

The transversality condition (68) insures that  $\hat{\chi}^{\mu}$  reduces to a three–component object in the particle's rest frame (r.f.)  $v_{\mu} = (1,0,0,0)$ . The Bargmann–Wigner condition (66) in turn implies that the bispinor wave functions reduce to an upper–left two by two matrix in the rest frame which, from the transversality condition (68), has the appropriate r.f. spin transformation behaviour. In fact one has

$$\hat{\chi}_{\alpha\beta}\Big|_{r.f.} = -\frac{1}{\sqrt{2}} \begin{pmatrix} i\sigma^2 & 0\\ 0 & 0 \end{pmatrix}$$

$$\hat{\chi}^{\mu}_{\alpha\beta}\Big|_{r.f.} = -\frac{1}{\sqrt{2}} \begin{pmatrix} \sigma^k i\sigma^2 & 0\\ 0 & 0 \end{pmatrix}$$
(69)

where the  $\sigma^k$  (k=1,2,3) are the usual Pauli matrices and  $i\sigma^2$  is the  $2\times 2$  charge conjugation matrix [55]. When reading Eq.(69) component—wise in the spherical basis (see Eq.(73)) one recovers the familiar spin wave functions  $\hat{\chi}\Big|_{r.f.} = \frac{1}{\sqrt{2}}(\uparrow\downarrow - \downarrow\uparrow)$  etc. The representations (65) can be seen to form a covariant way of writing the Clebsch–Gordan coupling in a moving frame  $v^{\mu}$  with  $\vec{v} \neq 0$  or, put differently, the covariant spin wave functions are just boosted rest frame spin wave functions.

Let us briefly have a look at the normalization of the bispinor diquark spin wave functions Eq.(65). The conjugate spin wave functions are given by (see e.g. [56])

$$\bar{\hat{\chi}}(v) = C^{-1}C^{-1}\hat{\chi}(-v) \tag{70}$$

such that

$$\bar{\hat{\chi}} = -\frac{1}{2\sqrt{2}} [C^{-1} \gamma_5 (\psi + 1)] 
\bar{\hat{\chi}}^{\mu} = -\frac{1}{2\sqrt{2}} [C^{-1} \gamma_{\perp}^{\mu} (\psi + 1)]$$
(71)

The normalization can then be calculated to be

$$\bar{\hat{\chi}}_{\alpha\beta}\hat{\chi}_{\alpha\beta} = 1 
\bar{\hat{\chi}}_{\alpha\beta}^{\mu}\hat{\chi}_{\alpha\beta}^{\nu} = -g_{\perp}^{\mu\nu}$$
(72)

where  $g^{\mu\nu}_{\perp} = g^{\mu\nu} - v^{\mu}v^{\nu}$ .

It is sometimes convenient to transform to the spherical basis for the spin 1 diquarks which can be done with the help of the spin 1 polarization vectors. One has  $(\lambda = \pm 1, 0)$ 

$$\hat{\chi}(1,\lambda) = \varepsilon_{\mu}(\lambda)\hat{\chi}^{\mu} \tag{73}$$

and the inverse

$$\hat{\chi}^{\mu} = \sum_{\lambda} \varepsilon^{*\mu}(\lambda) \hat{\chi}(1,\lambda) \tag{74}$$

where

$$\varepsilon_{\mu}(\pm) = \mp \frac{1}{\sqrt{2}}(0, 1, \pm i, o)$$

$$\varepsilon_{\mu}(0) = (|\vec{v}|, 0, 0, v_{0})$$
(75)

In as much as the spin wave functions  $\hat{\chi}$  and  $\hat{\chi}^{\mu}$  satisfy the Bargmann–Wigner equation on both spinor labels they are spin wave functions built from constituent on–mass shell quarks. While these do not adequately describe the actual physical situation of the light diquark system the on–mass shell spin wave functions are nevertheless quite useful when one wants to construct non–constituent spin wave functions with the correct spin and parity of the diquark system. To obtain the full light side spin wave functions one just multiplies the on–shell spin wave functions  $\hat{\chi}_{\alpha\beta}$  with a spinor valued matrix  $A_{\alpha\beta}^{\alpha'\beta'}$  such that the spin and parity of the light diquark system remain untouched. The resulting off–shell spin wave functions will be denoted by an unhatted object and reads

$$\chi_{\alpha\beta} = A_{\alpha\beta}^{\alpha'\beta'} \hat{\chi}_{\alpha'\beta'} \tag{76}$$

where the wave function matrix  $A_{\alpha\beta}^{\alpha'\beta'}$  in general depends on the nature of the diquark state as well as on the velocity  $v_{\mu}$  and the relative momenta k and K. The multiplication with the spin and parity neutral matrix  $A_{\alpha\beta}^{\alpha'\beta'}$  serves to soften the light-side spinor structure. This would e.g. be achieved by the replacement  $(\psi + 1) \to (A\psi + B + C\not k + D\not k \cdot \not v)$  for the positive energy projection in the spin wave functions (65). The off-shell spin wave functions  $\chi_{\alpha\beta}$  no longer

satisfy the Bargmann–Wigner equations but still represent a diquark system transforming as  $J^P=0^+$  and  $J^P=1^+$  under parity transformations and SO(3) rest frame rotations. The constituent quark model can be seen to be a special case of Eq.(76) where the matrix  $A_{\alpha\beta}^{\alpha'\beta'}$  takes the special form  $A_{\alpha\beta}^{\alpha'\beta'}=\delta_{\alpha}^{\alpha'}\delta_{\beta}^{\beta'}A$ .

The normalization of the wave function matrix  $A_{\alpha\beta}^{\alpha'\beta'}$  must be such that the normalization conditions Eq.(72) generalize to

$$(\chi, \chi) = 1 \tag{77}$$

$$(\chi^{\mu}, \chi^{\nu}) = -g_{\perp}^{\mu\nu} \tag{78}$$

where the inner product (,) is defined with regard to integrations and traces over the internal degrees of freedom of the diquark state. The exact form of the phase space integral, the spinor trace and the form of the integrand need not concern us here since we are only interested in the rest frame transformation properties of the spinor tensors  $\chi$  and  $\chi^{\mu}$ , and their correct normalization which we define through Eqs.(77) and (78).

We are now in the position to write down the spin wave functions  $\Psi_{\alpha\beta\gamma}$  of the ground state heavy baryons by writing down invariant couplings between the light–side spinor tensors  $\chi$  and  $\chi^{\mu}$  and the heavy–side spinor tensors  $\psi$  and  $\psi^{\mu}$  of the ground state baryons according to the coupling scheme

$$\underbrace{\frac{1}{2}^{+} \otimes \frac{1}{2}^{+}}_{light \ side} \otimes \underbrace{\frac{1}{2}^{+} \otimes J^{P}}_{heavy \ side} \Longrightarrow 0^{+}. \tag{79}$$

The heavy–side spinor tensors  $\psi$  and  $\psi^{\mu}$  involve the heavy baryon spinor u (for  $J^P = \frac{1}{2}^+$ ) and the Rarita–Schwinger spinor–vector  $u^{\mu}$  (for  $J^P = \frac{3}{2}^+$ ), and their couplings to the heavy quark spinor label. The rule is that if additional tensor structure is required on the heavy side one brings in a factor of  $\gamma^{\mu}_{\perp}$  (remember that  $v^{\mu}$  annihilates on the light side tensor). One then has

$$\Lambda_Q: \qquad \Psi_{\alpha\beta\gamma} = \chi_{\alpha\beta}\psi_{\gamma} \equiv \chi u \tag{80}$$

$$\{\Sigma_Q\}: \qquad \Psi_{\alpha\beta\gamma} = \chi^{\mu}_{\alpha\beta}\psi_{\mu,\gamma}$$

$$\equiv \chi^{\mu} \left\{ \begin{array}{c} \frac{1}{\sqrt{3}}\gamma^{\perp}_{\mu}\gamma_5 u \\ u_{\mu} \end{array} \right\}$$
(81)

where the curly bracket notation always implies a two-fold Heavy Quark Symmetry degeneracy. The Lorentz contraction on the r.h.s. of Eq.(81) is required because the total heavy baryon wave function  $\Psi_{\alpha\beta\gamma}$  on the l.h.s. of Eq.(81) transforms as a scalar in Lorentz space (but not in spinor space).<sup>1</sup>

The total spin wave functions  $\Psi_{\alpha\beta\gamma}$  satisfy the Bargmann–Wigner (or mass–shell) condition on the heavy quark spinor label  $\gamma$ , i.e.

$$\psi_{\gamma\gamma'}\Psi_{\alpha\beta\gamma'} = \Psi_{\alpha\beta\gamma} \tag{82}$$

showing that the heavy quarks appear in the theory as freely propagating on–mass shell quarks as is required in the Heavy Quark Symmetry limit. Note that a factor of  $\gamma_5$  is needed in the  $\Sigma_Q$  spin wave function in order to satisfy the mass–shell condition (82).

<sup>&</sup>lt;sup>1</sup>For added emphasis we keep the transversality labels in scalar products such as  $\chi^{\mu}\gamma^{\perp}_{\mu}$  most of the time even though the transversality label could be dropped since  $\chi^{\mu}\gamma^{\perp}_{\mu} = \chi^{\mu}\gamma_{\mu}$  since  $v^{\mu}\chi_{\mu} = 0$ .

The normalization of the heavy–side spin wave functions  $\psi$  and  $\psi^{\mu}$  can be seen to follow from the overall normalization condition

$$(\Psi, \Psi) = 2M \tag{83}$$

where the inner product (, ) is defined as in Eqs.(77) and (78). Using the fact that the light—side and heavy—side spin wave functions factorize in the sense of Eqs.(80) and (81) one then obtains the appropriate normalization conditions for the heavy—side spin wave functions  $\psi$  and  $\psi^{\mu}$ . In fact one has

$$\Lambda_Q : 2M = (\Psi, \Psi) = (\chi, \chi)\bar{\psi}\psi \tag{84}$$

$$\{\Sigma_Q\}$$
 :  $2M = (\Psi, \Psi) = (\chi^{\mu}, \chi^{\nu})\bar{\psi}_{\mu}\psi_{\nu}$  (85)

Using the normalization conditions Eqs. (77) and (78) for the light-side wave functions one obtains

$$\bar{\psi}\psi = 2M \tag{86}$$

$$-g^{\mu\nu}_{\perp}\bar{\psi}_{\mu}\psi_{\nu} = 2M. \tag{87}$$

The  $\Lambda$ - and  $\Sigma$ -type heavy-side spin wave functions  $\psi$  and  $\psi_{\mu}$  in Eqs.(80) and (81) can be seen to satisfy the normalization conditions (86) and (87) using  $\bar{u}u = 2M$  and  $\bar{u}^{\mu}u_{\mu} = -2M$ .

#### 4.2 Excited Heavy Baryon States

The spin wave function formalism introduced in Sec.(4.1) for the ground state baryons can easily be extended to describe excited baryon states. The coupling scheme (79) now involves also orbital angular momentum and reads

$$\underbrace{\frac{1}{2}^{+} \otimes \frac{1}{2}^{+} \otimes l_{k}^{P=(-)^{l_{k}}} \otimes l_{K}^{P=(-)^{l_{K}}}}_{light \ side} \otimes \underbrace{\frac{1}{2}^{+} \otimes J^{P}}_{heavy \ side} \Longrightarrow 0^{+}. \tag{88}$$

In the tensor formalism the orbital excitations are represented by tensor products of the relative momenta  $k_{\mu}^{\perp} = k_{\mu} - k \cdot v \, v_{\mu}$  and  $K_{\mu}^{\perp} = K_{\mu} - K \cdot v \, v_{\mu}$  where the transversality again reduces the relative four–momenta to relative three–momenta in the rest frame  $\vec{v} = 0$ . Here we shall only discuss p–wave orbital excitations.

Combining the p-wave negative parity orbital angular momentum state  $j^P = 1^-$  with the two  $j^P = 0^+, 1^+$  spin states one has the following spin–parity content for the total light–side diquark states:

$$0^{+} \otimes 1^{-} = 1^{-} \tag{89}$$

$$1^{+} \otimes 1^{-} = 0^{-} \oplus 1^{-} \oplus 2^{-} \tag{90}$$

For example, in the tensor formalism the decomposition (90) is achieved by writing e.g.

$$\hat{\chi}^{\mu_1} k_{\perp}^{\mu_2} = \frac{1}{3} \hat{\chi}^{\mu} k_{\perp \mu} g_{\perp}^{\mu_1 \mu_2} + \frac{1}{2} [\hat{\chi}^{\mu_1} k_{\perp}^{\mu_2}] + \frac{1}{2} {\{\hat{\chi}^{\mu_1} k_{\perp}^{\mu_2}\}_0}$$

$$\tag{91}$$

where  $\{\ \}_0$  stands for the traceless symmetric tensor product. Without any loss of generality we have taken  $k_{\mu}^{\perp}$  to represent the orbital excitation in the above example. For our purposes it is more convenient to represent the spin one piece of (91) by an one-index tensor according to

$$\frac{1}{2} [\hat{\chi}^{\mu_1} k_{\perp}^{\mu_2}] \approx -\frac{1}{2} \varepsilon_{\mu\mu_1\mu_2\alpha} \hat{\chi}^{\mu_1} k^{\mu_2} v^{\alpha} 
:= -\frac{1}{2} \varepsilon (\mu \, \hat{\chi} \, k \, v)$$
(92)

(we define  $\varepsilon_{0123} = 1$  as in Bjorken–Drell). In the following we use a concise notation for  $\varepsilon$ -tensor contractions, cf.

$$\varepsilon(\mu \hat{\chi} k v) := \varepsilon_{\mu \mu_1 \mu_2 \alpha} \hat{\chi}^{\mu_1} k^{\mu_2} v^{\alpha} \quad . \tag{93}$$

As in the case of the ground–state baryons we can now use the on–shell diquark states  $\hat{\chi}$  and  $\hat{\chi}^{\mu}$  together with the orbital momenta represented by  $k_{\perp}^{\mu}$  and  $K_{\perp}^{\mu}$  to build up the light–side states  $\hat{\phi}^{\mu_1...\mu_j}$  with the desired  $j^P$  quantum numbers. For illustrative purposes such explicit constructions have been listed in Tables 4 and 5 (where the spin zero metric contraction  $g_{\perp}^{\mu_1\mu}$  has been already absorbed into the heavy–side spin wave functions). The construction has to be such that the resulting spinor–tensors  $\hat{\phi}^{\mu_1...\mu_j}$  representing a spin j diquark state have to be i) transverse on all indices ii) totally symmetric in all indices and iii) traceless w.r.t. any pair of indices. This would be the approach that one would take in a constituent type quark model approximation.

The spinor–tensor spin wave functions  $\hat{\phi}^{\mu_1...\mu_j}$  listed in Tables 4 and 5 have the correct parity and spin angular momentum to describe the diquark states. As in the ground–state case the spinor–tensor has to be multiplied by a wave function matrix  $A_{\alpha\beta}^{\alpha'\beta'}$  in order to obtain the full diquark state wave functions. One thus has

$$[\phi^{\mu_1\dots\mu_j}]_{\alpha\beta} = A_{\alpha\beta}^{\alpha'\beta'} [\hat{\phi}^{\mu_1\dots\mu_j}]_{\alpha'\beta'} \tag{94}$$

where the wave function matrix  $A_{\alpha\beta}^{\alpha'\beta'}$  in general depends on the external and internal degrees of freedom of the diquark state, i.e. it is different for different diquark states. In the following we shall mostly suppress spinor labels.

The full diquark wave function  $\phi^{\mu_1...\mu_j}$  satisfies the normalization condition

$$(\phi^{\nu_1\dots\nu_j},\phi^{\mu_1\dots\mu_j}) = G^{\mu_1\dots\mu_j;\nu_1\dots\nu_j} \tag{95}$$

where the inner product is defined as an integration and trace over the internal degrees of freedom of the diquark state as in Eqs.(77) and (78).  $G^{\mu_1...\mu_j;\nu_1...\nu_j}$  is a generalized transverse metric tensor which is i) transverse in all indices, ii) symmetric in the sets of indices  $\{\mu_i\}$  and  $\{\nu_i\}$  and iii) traceless w.r.t. to any index pair in  $\{\mu_i\}$  or in  $\{\nu_i\}$ . Its general explicit form can be found in [50].

We emphasize again that all that is needed for the purposes of Heavy Quark Symmetry is the  $j^P$  transformation behaviour of the light–side diquark states together with the normalization condition (95). The constituent states listed in Tables 4 and 5 can be viewed as possible "interpolating fields" of the true diquark states. Furthermore explicit forms of the constituent states are needed in later applications if one wants to make reference to the constituent quark model approach.

Although we are dealing only with diquark spins j = 0, 1 and 2 in this review the generic notation introduced in (94) and (95) turns out to be quite convenient even for these simple cases. It is also easily generalized to higher spins [50] (see also [57]). To be explicit we list the subsidiary conditions and the normalization tensors for the light–side diquark states with spins j = 0, 1, 2. One has

$$i) \quad j = 0 : \phi; \qquad G = 1$$
 (96)

*ii*) 
$$j = 1$$
 :  $\phi^{\mu_1}$ ;  $G^{\mu_1\nu_1} = -g^{\mu_1\nu_1}_{\perp}$   
transversality:  $v^{\mu_1}\phi_{\mu_1} = 0$  (97)

Table 4: Spin wave functions (s.w.f.) of  $\Lambda$ -type s- and p-wave heavy baryons. Light-side spin wave functions are constituent spin wave functions.

	light side s.w.f. $\hat{\phi}^{\mu_1\mu_j}$	$j^P$	heavy side s.w.f. $\psi_{\mu_1\mu_j}$	$J^P$
$\Lambda_Q$	$\hat{\chi}$	0+	u	$\frac{1}{2}^{+}$
$\{\Lambda_{QK1}\}$	$\hat{\chi}^0 K_\perp^{\mu_1}$	1-	$\frac{\frac{1}{\sqrt{3}}\gamma_{\mu_1}^{\perp}\gamma_5 u}{u_{\mu_1}}$	$\frac{1}{2}^{-}$ $\frac{3}{2}^{-}$
$\Lambda_{Qk0}$	$\hat{\chi}^1 \cdot k_{\perp}$	0-	u	$\frac{1}{2}^{-}$
$\{\Lambda_{Qk1}\}$	$\frac{1}{2}\varepsilon(\mu_1\hat{\chi}^1k_\perp v)$	1-	$\frac{\frac{1}{\sqrt{3}}\gamma_{\mu_1}^{\perp}\gamma_5 u}{u_{\mu_1}}$	$\frac{1}{2}^{-}$ $\frac{3}{2}^{-}$
$\{\Lambda_{Qk2}\}$	$rac{1}{2}\hat{\chi}^{1\{\mu_1}k_{\perp}^{\mu_2\}_0}$	2-	$\frac{\frac{1}{\sqrt{10}}\gamma_5\gamma_{\{\mu_1}^{\perp}u_{\mu_2\}_0}}{u_{\mu_1\mu_2}}$	$\frac{3}{2}$ $\frac{5}{2}$ $\frac{5}{2}$

Table 5: Spin wave functions (s.w.f.) of  $\Sigma$ -type s- and p-wave heavy baryons. Light-side spin wave functions are constituent spin wave functions.

	light side s.w.f. $\hat{\phi}^{\mu_1\mu_j}$	$j^P$	heavy side s.w.f. $\psi_{\mu_1\mu_j}$	$J^P$
$\{\Sigma_Q\}$	$\hat{\chi}^{1\mu_1}$	1+	$\frac{\frac{1}{\sqrt{3}}\gamma_{\mu_1}^{\perp}\gamma_5 u}{u_{\mu_1}}$	$\frac{\frac{1}{2}^{+}}{\frac{3}{2}^{+}}$
$\{\Sigma_{Qk1}\}$	$\hat{\chi}^0 k_\perp^{\mu_1}$	1-	$\frac{\frac{1}{\sqrt{3}}\gamma_{\mu_1}^{\perp}\gamma_5 u}{u_{\mu_1}}$	$   \begin{array}{r}     \frac{1}{2} + \\     \frac{3}{2} + \\     \hline     \frac{1}{2} - \\     \frac{3}{2} - \\     \hline     \frac{3}{2} - \\     \hline   \end{array} $
$\Sigma_{QK0}$	$\hat{\chi}^1 \cdot K_{\perp}$	0-	u	$\frac{1}{2}^{-}$
$\{\Sigma_{QK1}\}$	$\frac{1}{2}\varepsilon(\mu_1\hat{\chi}^1K_{\perp}v)$	1-	$\frac{\frac{1}{\sqrt{3}}\gamma_{\mu_1}^{\perp}\gamma_5 u}{u_{\mu_1}}$	$\frac{\frac{1}{2}^{-}}{\frac{1}{2}^{-}}$ $\frac{3}{2}^{-}$
$\{\Sigma_{QK2}\}$	$\frac{1}{2}\hat{\chi}^{1\{\mu_1}K_{\perp}^{\mu_2\}_0}$	2-	$\frac{\frac{1}{\sqrt{10}}\gamma_5\gamma_{\{\mu_1}^{\perp}u_{\mu_2\}_0}}{u_{\mu_1\mu_2}}$	$\frac{3}{2}^{-}$ $\frac{5}{2}^{-}$

$$iii) \quad j=2 : \phi^{\mu_1\mu_2}; \qquad G^{\mu_1\mu_2;\nu_1\nu_2} = \frac{1}{2}(g_{\perp}^{\mu_1\nu_1}g_{\perp}^{\mu_2\nu_2} + g_{\perp}^{\mu_1\nu_2}g_{\perp}^{\mu_2\nu_1} - \frac{2}{3}g^{\mu_1\mu_2}g^{\nu_1\nu_2})$$

$$\text{symmetry: } \phi^{\mu_1\mu_2} = \phi^{\mu_2\mu_1}$$

$$\text{transversality: } v^{\mu_1}\phi_{\mu_1\mu_2} = 0$$

$$\text{tracelessness: } g_{\perp}^{\mu_1\mu_2}\phi_{\mu_1\mu_2} = 0 \tag{98}$$

It is a useful and instructive exercise to transform the cartesian tensors  $\phi^{\mu_1...\mu_j}$  to a spherical basis. First note that because of the normalization condition Eq.(95) the cartesian tensors  $\phi^{\mu_1...\mu_j}$  can be looked upon as forming a set of orthonormal vectors in a (2j+1) dimensional linear vector space. They can thus be represented by the state vectors  $|\mu_1...\mu_j\rangle$  which satisfy orthonormality and completeness relations. One has

orthonormality : 
$$\langle \nu_1 \dots \nu_j \mid \mu_1 \dots \mu_j \rangle = G^{\nu_1 \dots \nu_j}_{\mu_1 \dots \mu_j}$$
 (99)

completeness: 
$$|\mu_1 \dots \mu_j\rangle\langle\mu_1 \dots \mu_j| = \mathbb{1}$$
 (100)

where the Einstein summation convention is used in Eq.(100).

One can then transform to a spherical basis  $|\phi_i, \lambda\rangle := |j, \lambda\rangle$ 

$$|j,\lambda\rangle = \varepsilon^{\mu_1\dots\mu_j}(\lambda) |\mu_1\dots\mu_j\rangle$$
 (101)

where the  $\varepsilon_{\mu_1...\mu_j}$  are the usual spin–j polarization tensors. The inverse of (101) is given by

$$|\mu_1 \dots \mu_j\rangle = \sum_{\lambda} \varepsilon_{\mu_1 \dots \mu_j}^*(\lambda) |j,\lambda\rangle$$
 (102)

The spherical basis vectors  $|j,\lambda\rangle$  in turn satisfy orthonormality and completeness relations. One has

orthonormality : 
$$\langle j, \lambda \mid j, \lambda' \rangle = \delta_{\lambda \lambda'}$$
 (103)

completeness : 
$$\sum_{\lambda} |j,\lambda\rangle\langle j,\lambda| = 1$$
 (104)

From the above one can then derive orthonormality and completeness relation for the polarization tensors which read

$$\varepsilon_{\mu_1\dots\mu_j}^*(\lambda)\varepsilon^{\mu_1\dots\mu_j}(\lambda') = (-)^j \delta_{\lambda\lambda'} \tag{105}$$

$$\sum_{\lambda} \varepsilon^{\mu_1 \dots \mu_j}(\lambda) \varepsilon^*_{\nu_1 \dots \nu_j}(\lambda) = G^{\mu_1 \dots \mu_j}_{\nu_1 \dots \nu_j}$$
(106)

After this technical aside we return to the construction of the excited heavy baryon states. Using the diquark states  $\phi^{\mu_1...\mu_j}$  the heavy baryon spin wave functions can easily be obtained from the contraction

$$\Psi_{\alpha\beta\gamma} = [\phi^{\mu_1\dots\mu_j}]_{\alpha\beta}\psi_{\mu_1\dots\mu_j;\gamma} \tag{107}$$

The heavy–side spin wave functions  $\psi_{\mu_1...\mu_j}$  are then uniquely determined in terms of spinor–tensor forms that involve the heavy baryons Rarita–Schwinger spinor–tensors  $u^{\mu_1...\mu_j}$  and  $u^{\mu_1...\mu_{j-1}}$  for the  $j\pm 1/2$  high and low spin partners, respectively, in the degenerate Heavy Quark Symmetry baryon doublet. In the latter case an additional  $\gamma_{\perp}^{\mu_j}\gamma_5$  needs to be introduced to complete the tensor structure ( $v^{\mu_j}$  cannot be used because it annihilates on the light side). The  $\gamma_5$  enters since the  $\psi^{\mu_1...\mu_j}$  have to satisfy the heavy quark mass–shell condition

$$\psi\psi^{\mu_1\dots\mu_j} = \psi^{\mu_1\dots\mu_j} \tag{108}$$

The normalization of the heavy–side spin wave functions is fixed through the normalization condition

$$\bar{\psi}^{\nu_1 \dots \nu_j} \psi^{\mu_1 \dots \mu_j} G_{\mu_1 \dots \mu_j; \nu_1 \dots \nu_j} = 2M \tag{109}$$

by the same reasoning as in Eq.(86) and (87). The generalized Rarita-Schwinger spinor-tensors are normalized according to

$$\bar{u}^{\mu_1\dots\mu_j}u_{\mu_1\dots\mu_j} = (-)^j 2M.$$

In this way one can then write down all the spin wave functions of the excited heavy baryons. In Table 4 we have listed the spin wave functions for the excited  $\Lambda$ -type states together with the ground state  $\Lambda$  and in Table 5 we have done the same for the  $\Sigma$ -type states. The p-wave states are labelled according to the nature of their orbital state and their light-side diquark spin j. Of interest is also whether the states are in a spin singlet  $\chi^0$  or triplet  $\chi^{1,\mu}$  state. This can be determined by invoking the generalized Pauli principle for the light diquark system. One thus finds that one has a spin singlet configuration  $\chi^0$  for  $\{\Lambda_{QK1}\}$  and  $\{\Sigma_{QK1}\}$  and a spin triplet configuration  $\chi^{1,\mu}$  for  $\{\Lambda_{Qkj}; (j=0,1,2)\}$  and  $\{\Sigma_{QK1}\}$ . In the remaining part of Sec.4 we shall make repeated use of the covariant spin wave functions written down in Sec.4.1 and 4.2.

A last comment concerns flavour wave functions. The antisymmetric (antitriplet) and symmetric (sextet) light diquark flavour wave functions are given by  $[q_iq_j] = \frac{1}{\sqrt{2}}(q_iq_j - q_jq_i)$  and  $\{q_iq_j\} = \frac{1}{\sqrt{2}}(q_iq_j + q_jq_i)$  with  $q_i, q_j = u, d, s$ . It is sometimes convenient to represent the antisymmetric flavour wave function by an one-index object by raising indices with the help of  $\varepsilon^{ijk}$ , i.e.  $T^k = \varepsilon^{ijk}[q_iq_j]$ , as is appropriate for the antitriplet representation.

#### 4.3 Current-Induced Heavy Baryon Transitions

The exclusive semileptonic decays  $H_b \to H_c + l^- + \bar{\nu}_l$  have played a central role in the development of the Heavy Quark Symmetry. Originally the prime motivation for studying these decays was the desire to get a handle on the value of the Kobayashi–Maskawa matrix element  $V_{bc}$ . Once HQET was formulated it was noticed that the structure of these decays is sufficiently rich to put the predictions of the heavy quark limit and the  $1/m_Q$  corrections to this limit to a detailed test in these decays. Quite naturally in the beginning the main emphasis was on the mesonic  $b \to c$  transitions. But as more and more data is being collected on heavy baryon decays a new important field for the applications of Heavy Quark Symmetry has been opening from the investigation of current–induced heavy baryon transitions.

As explained in Sec.2 the following ground state to ground state weak semileptonic transitions are expected to be observable

$$\Lambda_{Q} - \text{type} : \Lambda_{b} \to \Lambda_{c} + l^{-} + \bar{\nu}_{l} 
\Xi_{b} \to \Xi_{c} + l^{-} + \bar{\nu}_{l} 
\Sigma_{Q} - \text{type} : \Omega_{b} \to \Omega_{c} + l^{-} + \bar{\nu}_{l} 
: \Omega_{b} \to \Omega_{c}^{*} + l^{-} + \bar{\nu}_{l}$$
(110)

The other ground state bottom baryons also have semileptonic modes but their semileptonic branching ratios are so small as to make their semileptonic decays unobservable for all practical purposes.

Further there are transitions to excited charm baryon states as in  $\Lambda_b \to \Lambda_c^{**}$ . One would then want to know how big the rate into the inelastic channels  $\Lambda_c^{**}$  is, in particular as the

Figure 5: Current-induced transition between heavy baryons. Heavy-side transition  $Q_1(v_1) \rightarrow Q_2(v_2)$  mediated by (V-A) heavy quark current. Light-side transition  $j_1^{P_1}(v_1) \rightarrow j_2^{P_2}(v_2)$  depends only on the invariant velocity transfer variable  $\omega = v_1 \cdot v_2$ .

elastic rate and the inelastic rates are intimately linked together by the sum rule of Bjorken. Again one would like to test the predictions of HQET also for the inelastic contributions. For example, the excited  $\Lambda_c^{**}$ -states produced in these decays (and for that matter the  $\Lambda_c$ ) will be polarized with definite predictions for the polarization density matrices from HQET. The polarization of the  $\Lambda_c^{**}$ 's would reveal itself by the angular decay distribution of its subsequent decay products. Such considerations can e.g. be used to pin down the  $J^P$  quantum numbers of the excited  $\Lambda_C^{**}$  states.

There are two ingredients that go into the Heavy Quark Symmetry description of the semileptonic transitions as shown in Fig.5. First there is the  $b \to c$  transition which is mediated through the known (V-A) structure. Second there is the transition from the initial diquark system to the final diquark system whose strength and structure is not known. The lack of knowledge concerning the light-side diquark transition can be parameterized in terms of independent transition amplitudes which are called reduced form factors. These can only depend on the one kinematical Lorentz invariant  $\omega = v_1 \cdot v_2$  that arises in the transition. Finally the heavy quarks and the light diquark system in the initial and final state have to combine to form heavy baryons with the correct spin-parity quantum numbers. The correct spin coupling factors that achieve this can be determined from products of C.G. coefficients [58,59] (or alternatively from 6-j symbols). Here we use the covariant approach to determine the correct spin coupling factors as in [50].

For the current–induced transitions we then obtain

$$M^{\lambda} = \langle B_{Q_2}(v_2) \mid J^{\lambda} \mid B_{Q_1}(v_1) \rangle = \bar{\psi}_{2,\alpha}^{\mu_1 \dots \mu_{j_1}} \Gamma_{\alpha\beta}^{\lambda} \psi_{1,\beta}^{\nu_1 \dots \nu_{j_2}} (\sum_i f_i(\omega) t_{\mu_1 \dots \mu_{j_1}; \nu_1 \dots \nu_{j_2}}^i)$$
(111)

where the  $\psi^{\mu_1...\mu_j}$  are the heavy-side spin wave functions.  $\Gamma^{\lambda}$  determines the structure of the  $Q_1 \to Q_2$  current transition (e.g.  $\gamma^{\lambda}(1-\gamma^5)$  for a (V-A) interaction). The tensors  $t^i_{\mu_1...\mu_{j_1};\nu_1...\nu_{j_2}}$  describe the diquark transition. They have to be build from the vectors  $v^{\mu_i}_1$  and  $v^{\nu_i}_2$ , the metric tensors  $g_{\mu_i\nu_k}$  and, depending on parity, from the Levi-Civita object  $\varepsilon(\mu_i\nu_k v_1v_2)$ . The  $f_i(\omega)$  are reduced form factors that depend only on the invariant velocity transfer variable  $\omega = v_1 \cdot v_2$ .

Note that the Heavy Quark Symmetry prediction for the current matrix element (111) has some structural similarity to the Wigner–Eckart theorem. The  $f_i(\omega)$  can be regarded as "reduced matrix elements" and the  $\bar{\psi}_2^{\mu_1...\mu_{j_1}}\Gamma^{\lambda}\psi_1^{\nu_1...\nu_{j_2}}t_{\mu_1...\mu_{j_1};\nu_{1_2}...\nu_{j_2}}^i$  are the Clebsch–Gordan coefficients that project onto the reduced matrix elements  $f_i(\omega)$ . The reduced form factors serve to parameterize our ignorance about the dynamics of the light–side transitions. Heavy Quark Symmetry can tell us nothing about the reduced form factors  $f_i(\omega)$  except for the existence of a normalization condition at zero recoil  $\omega = 1$  for the elastic transitions, as mentioned in Sec.3. The magnitude and the  $\omega$ –dependence of the reduced form factors would have to be calculated using nonperturbative methods such as QCD sum rules, lattice gauge theory or, more conventionally, explicit quark models.

The number of the independent tensors  $t^i_{\mu_1...\mu_{j_1},\nu_1...\nu_{j_2}}$  and their parity depend of course on the particular transition that is being considered. For the simple cases considered here they can easily be written down using the building blocks  $v^{\mu_i}_1$ ,  $v^{\nu_i}_2$ ,  $g_{\mu_i\nu_k}$  and  $\varepsilon(\mu_i\nu_k v_1v_2)$ , as mentioned before.

For the  $\Lambda$ -type transitions the tensor structure is particularly simple since the diquark in the initial state has  $j^P = 0^+$ . This implies that there is at most one reduced form factor for the  $\Lambda$ -type transitions. One has [50,60]

i) 
$$\Lambda_{Q_1} \to \Lambda_{Q_2}$$
 :  $\frac{1}{2}^+ \to \frac{1}{2}^+$ 

$$M^{\lambda} = \bar{u}_2 \Gamma^{\lambda} u_1 f^{(0)}(\omega)$$
form factor normalization:  $f^{(0)}(\omega = 1) = 1$  (112)

*ii*) 
$$\Lambda_{Q_1} \to \{\Lambda_{Q_2K1}\}$$
 :  $\frac{1}{2}^+ \to \left\{\begin{array}{c} \frac{1}{2}^- \\ \frac{3}{2}^- \end{array}\right\}$ 

$$M^{\lambda} = \left\{\begin{array}{c} -\frac{1}{\sqrt{3}} \bar{u}_2 \gamma_5 \gamma_{\perp 2}^{\mu} \\ \bar{u}_2^{\mu} \end{array}\right\} \Gamma^{\lambda} u_1 f_1^{(1)}(\omega) v_{1\mu}$$
 (113)

$$iii)$$
  $\Lambda_{Q_1} \to \Lambda_{Q_2k0}$  :  $\frac{1}{2}^+ \to \frac{1}{2}^ M^{\lambda} = 0$  (forbidden) (114)

$$iv) \quad \Lambda_{Q_1} \to \{\Lambda_{Q_2k1}\} \qquad : \quad \frac{1}{2}^+ \to \left\{\begin{array}{c} \frac{1}{2}^- \\ \frac{3}{2}^- \end{array}\right\}$$

$$M^{\lambda} = \left\{\begin{array}{c} -\frac{1}{\sqrt{3}} \bar{u}_2 \gamma_5 \gamma_{\perp 2}^{\mu} \\ \bar{u}_2^{\mu} \end{array}\right\} \Gamma^{\lambda} u_1 f_2^{(1)}(\omega) v_{1\mu} \qquad (115)$$

$$v)$$
  $\Lambda_{Q_1} \to \{\Lambda_{Q_2k2}\}$  :  $\frac{1}{2}^+ \to \left\{\begin{array}{c} \frac{3}{2}^-\\ \frac{5}{2}^- \end{array}\right\}$ 

$$M^{\lambda} = 0 \quad \text{(forbidden)}$$
 (116)

For the elastic transition there is a change of notation from the one used in Sec.3 ( $f^{(0)}(\omega) = \xi(\omega)$ ) to allow for the inclusion of the p-wave contributions.

Let us make a few comments about the structure of the current-induced matrix elements (112)–(116). An alternative way of determining the tensors  $t^i_{\mu_1...\mu_{j_1};\nu_1...\nu_{j_2}}$  and their associated reduced form factors  $f_i(\omega)$  consists in considering the structure of the light-side transitions.

For this purpose it is convenient to consider the light–side transition in the spherical basis (see Eq.(99)–(106)). One has

$$(\phi_2(j_2^{P_2}, \lambda, v_2), \phi_1(j_1^{P_1}, \lambda, v_1)) = \varepsilon^{*\nu_1 \dots \nu_{j_2}}(\lambda) (\sum_i f_i(\omega) t^i_{\nu_1 \dots \nu_{j_2}; \mu_1 \dots \mu_{j_1}}) \varepsilon^{\mu_1 \dots \mu_{j_1}}(\lambda)$$
(117)

where the tensors  $t^i_{\nu_1...\nu_{j_2};\mu_1...\mu_{j_1}}$  describe the light side transition. Explicitly one has

$$(\phi_{2\nu_1\dots\nu_{j_2}}(v_2),\phi_{1\mu_1\dots\mu_{j_1}}(v_1)) = \sum_i f_i(\omega)t^i_{\nu_1\dots\nu_{j_2};\mu_1\dots\mu_{j_1}}$$
(118)

In Eq.(117) we have made use of the fact that the helicity (or  $j_z$ ) is conserved in the light side diquark transition, i.e.  $\lambda_1 = \lambda_2 := \lambda$ . The inner product is defined as in Eq.(95), but now for the parity conserving inelastic transitions  $j_1^{P_1}(v_1) \to j_2^{P_2}(v_2)$ . It is evident that Eq.(117) possesses the same tensor structure as Eq.(111). Using the alternative form (117) it is then easy to understand the absence of  $\Lambda_{Q_1} \to \Lambda_{Q_2k_0}$ ,  $\{\Lambda_{Q_2k_2}\}$  transitions since there can be no parity conserving transitions  $0^+ \to 0^-$  and  $0^+ \to 2^-$ .

The form (117) also provides for the zero recoil normalization condition  $f(\omega = 1) = 1$  for the  $\Lambda_{Q_1} \to \Lambda_{Q_2}$  transition mentioned in Sec.3 and written down in (112). In this case one has an elastic  $0^+ \to 0^+$  transition which is evidently normalized to 1 at  $v_1 = v_2$  according to Eq.(95). Physically speaking, the normalization condition arises because there is a complete overlap of the wave function of the diquark system before and after the  $Q_1 \to Q_2$  transition at zero recoil.

The counting of the number of reduced form factors that describe the heavy baryon transitions can readily be done by referring to the number of independent diquark transition amplitudes N in Eq.(117). Defining the normality n of a diquark state with quantum numbers  $j^P$  by  $n = P(-)^j$  one has to differentiate between the two cases where the product of normalities of the two diquark states is even or odd. One finds

i) 
$$n_1 \cdot n_2 = 1$$
 :  $N = j_{min} + 1$   
ii)  $n_1 \cdot n_2 = -1$  :  $N = j_{min}$  (119)

where  $j_{min} = Min\{j_1, j_2\}$ . In closed form one has  $N = j_{min} + \frac{1}{2}(1 + n_1 \cdot n_2)$ . The above analysis agrees with Eqs.(112)–(116) as it must. Eq.(119) can be derived by counting the number of independent helicity amplitudes in the transition Eq.(117) [61]. The difference between the  $n_1 \cdot n_2$ —even and –odd case comes about because parity invariance forbids helicity zero transitions when  $n_1 \cdot n_2 = -1$ . An even more elementary way of deriving Eq.(119) is by performing a simple LS analysis in which the transition operator is treated as a  $0^+$  "spurion" state either in the initial or final state [58].

For the  $\Sigma$ -type transitions the form factor structure predicted by Heavy Quark Symmetry is a trifle more complex since now the initial diquark is a  $j^P = 1^+$  diquark state. For each of the  $\Sigma$ -type transitions there are now at most two reduced form factors.<sup>2</sup> One has

$$i)\{\Sigma_{Q_1}\} \to \{\Sigma_{Q_2}\} \qquad : \qquad \left\{\begin{array}{c} \frac{1}{2}^+ \\ \frac{3}{2}^+ \end{array}\right\} \to \left\{\begin{array}{c} \frac{1}{2}^+ \\ \frac{3}{2}^+ \end{array}\right\}$$
$$M^{\lambda} = \left\{\begin{array}{c} -\frac{1}{\sqrt{3}} \bar{u}_2 \gamma_5 \gamma_{\perp 2}^{\nu_1} \\ \bar{u}_2^{\nu_1} \end{array}\right\} \Gamma^{\lambda} \left\{\begin{array}{c} \frac{1}{\sqrt{3}} \gamma_{\perp 1}^{\mu_1} \gamma_5 u_1 \\ u_1^{\mu_1} \end{array}\right\} \left(-g_1^{(0)}(\omega) g_{\mu_1 \nu_1} + g_2^{(0)}(\omega) v_{1 \nu_1} v_{2 \mu_2}\right)$$

<sup>&</sup>lt;sup>2</sup>As a curious by line we would like to remind the reader that the full Heavy Quark Symmetry spin structure of the  $\Lambda_Q$ – and  $\Sigma_Q$ –type ground state transitions had already been written down some 17 years ago in the crossed  $e^+e^-$  channel [62].

form factor normalization:  $g_1^{(0)}(\omega=1)=1$ 

$$ii)\{\Sigma_{Q_{1}}\} \rightarrow \{\Sigma_{Q_{2}k1}\} : \left\{\frac{\frac{1}{2}^{+}}{\frac{3}{2}^{+}}\right\} \rightarrow \left\{\frac{\frac{1}{2}^{-}}{\frac{3}{2}^{-}}\right\}$$

$$M^{\lambda} = \left\{-\frac{1}{\sqrt{3}}\bar{u}_{2}\gamma_{5}\gamma_{\perp 2}^{\nu_{1}}}{\bar{u}_{2}^{\nu_{1}}}\right\} \Gamma^{\lambda} \left\{-\frac{1}{\sqrt{3}}\gamma_{\perp 1}^{\mu_{1}}\gamma_{5}u_{1}}{u_{1}^{\mu_{1}}}\right\} ig_{1}^{(1)}(\omega)\varepsilon(\mu_{1}\nu_{1}v_{1}v_{2})$$

$$iii)\{\Sigma_{Q_{1}}\} \rightarrow \Sigma_{Q_{2}K0} : \left\{\frac{\frac{1}{2}^{+}}{\frac{3}{2}^{+}}\right\} \rightarrow \frac{1}{2}^{-}$$

$$M^{\lambda} = \bar{u}_{2}\Gamma^{\lambda} \left\{-\frac{1}{\sqrt{3}}\gamma_{\perp 1}^{\mu_{1}}\gamma_{5}u_{1}}{u_{1}^{\mu_{1}}}\right\} g_{2}^{(1)}(\omega)v_{2\mu_{1}}$$

$$iv)\{\Sigma_{Q_{1}}\} \rightarrow \{\Sigma_{Q_{2}K1}\} : \left\{\frac{\frac{1}{2}^{+}}{\frac{3}{2}^{+}}\right\} \rightarrow \left\{\frac{\frac{1}{2}^{-}}{\frac{3}{2}^{-}}\right\}$$

$$M^{\lambda} = \left\{-\frac{1}{\sqrt{3}}\bar{u}_{2}\gamma_{5}\gamma_{\perp 2}^{\nu_{1}}}{\bar{u}_{2}^{\nu_{1}}}\right\} \Gamma^{\lambda} \left\{-\frac{1}{\sqrt{3}}\gamma_{\perp 1}^{\mu_{1}}\gamma_{5}u_{1}}{u_{1}^{\mu_{1}}}\right\} ig_{3}^{(1)}(\omega)\varepsilon(\mu_{1}\nu_{1}v_{1}v_{2})$$

$$v)\{\Sigma_{Q_{1}}\} \rightarrow \{\Sigma_{Q_{2}K2}\} : \left\{\frac{\frac{1}{2}^{+}}{\frac{3}{2}^{+}}\right\} \rightarrow \left\{\frac{\frac{3}{2}^{-}}{\frac{5}{2}^{-}}\right\}$$

$$M^{\lambda} = \left\{-\frac{1}{\sqrt{10}}\bar{u}_{2}^{(\nu_{1}}\gamma_{5}\gamma_{\perp 2}^{\nu_{2}})\sigma_{1}^{\nu_{2}}}{\bar{u}_{2}^{\nu_{1}\nu_{2}}}\right\} \Gamma^{\lambda} \left\{-\frac{1}{\sqrt{3}}\gamma_{\perp 1}^{\mu_{1}}\gamma_{5}u_{1}}{u_{1}^{\mu_{1}}}\right\} (-g_{4}^{(1)}(\omega)v_{1\nu_{1}}g_{\nu_{2}\mu_{1}} + g_{5}^{(1)}(\omega)v_{1\nu_{1}}v_{1\nu_{2}}v_{2\mu_{1}})$$

$$(121)$$

As discussed before the form factor counting can of course be done equally well by counting the number of form factors in the diquark transitions  $1^+ \to j_2^{P_2}$  using the general formula Eq.(119). The normalization condition for the "elastic" transition  $\{\Sigma_{Q_1}\} \to \{\Sigma_{Q_2}\}$  at zero recoil applies only to the metric form factor  $g_1^{(0)}(\omega)$  since the second form factor  $g_2^{(0)}(\omega)$  does not contribute when  $v_1 = v_2$ . The zero recoil normalization  $g_1^{(0)}(1) = 1$  follows directly from the normalization of the diquark state, cf. Eq.(95).

Equations (112)–(116) and (120)–(121) represent the most general transition form factor structure in the Heavy Quark Symmetry limit. We shall discuss some possible simplifications at the end of Sec.4.4 by resolving the diquark transitions into constituent quark transitions. It is important to keep in mind, though, that any simplification of the form factor structure predicted by Heavy Quark Symmetry necessarily involves further model dependent assumptions.

Before closing this subsection we briefly want to discuss the Heavy Quark Symmetry structure of current–induced transitions from a heavy baryon to a light baryon. This would be of relevance for e.g.  $c \to s$  or  $b \to u$  transitions. Here we limit ourselves to ground state transitions. For heavy to light transitions one must now allow for spin interactions of the light "active" quark coming from the weak interaction vertex with the light diquark system, i.e. now one has a factorization only in the initial state. The spin interaction can be introduced

by adding  $\gamma$ -structure to the light "active" fermion in the final state. This amounts to the replacements  $f^{(0)} \to f' + \psi_1 f''$ ,  $g_1^{(0)} \to g_1' + \psi_1 g_1''$  and  $g_2^{(0)} \to g_2' + \psi g_2''$  in Eq.(112) and (120). Explicitly one has [39,63]

$$\Lambda_Q \to \Lambda_q : M^{\lambda} = \bar{u}_2(p_2)(f'(p_2 \cdot v_1) + \psi_1 f''(p_2 \cdot v_1))\Gamma^{\lambda} u_1(v_1) 
\{\Sigma_Q\} \to \Sigma_q : M^{\lambda} = \frac{1}{\sqrt{3}} \bar{u}_2(p_2) \gamma_5 \gamma_{\perp_2}^{\nu_1} [-g_{\mu_1 \nu_1}(g'_1(p_2 \cdot v_1) + \psi_1 g''_1(p_2 \cdot v_1)) 
+ v_{1\nu_1} p_{2\mu_1}(g'_2(p_2 \cdot v_1) + \psi_1 g''_2(p_2 \cdot v_1))]$$
(122)

$$\Gamma^{\lambda} \left\{ \begin{array}{c} \frac{1}{\sqrt{3}} \gamma_{\perp_{1}}^{\mu_{1}} \gamma_{5} u_{1}(v_{1}) \\ u_{1}^{\mu_{1}}(v_{1}) \end{array} \right\}$$
(123)

and similarly for  $\{\Sigma_Q\} \to \Sigma_q^*$ , albeit with a new set of form factors. Now there is no normalization condition for any of the form factors, and the transitions  $\{\Sigma_Q\} \to \Sigma_q$  and  $\{\Sigma_Q\} \to \Sigma_q^*$  are not related.

# 4.4 Contribution of Transition Form Factors to the Bjorken Sum Rule

As mentioned before, Heavy Quark Symmetry says nothing about the  $\omega$ - dependence of the reduced form factors except for the normalization condition at zero recoil in the elastic case. However, Bjorken has pointed out [64] that one may extract useful information on the reduced form factors by considering the contribution of the heavy decay baryons  $B_{Q_2}, B_{Q_2}^{**}, \ldots$  to the structure functions  $H^i$  occurring in the semileptonic decay  $B_{Q_1} \to (B_{Q_2} + B_{Q_2}^{**}, \ldots) + \nu_l + l$  (for a definition of the structure functions  $H_i$  see Sec.5.2). Then, by invoking duality, one equates the sum of particle structure functions to the corresponding inclusive structure function calculated from the free quark decay  $Q_1 \to Q_2 + \nu_l + l$  for any value of  $\omega$ .

Technically, it is simplest to consider the contribution of the decay baryons to the longitudinal structure function  $H_L$ . One first calculates longitudinal helicity transition amplitudes and then squares them in order to obtain the contribution of a given final baryon to the Bjorken sum rule. This is an elegant method that avoids the tedium of having to do lengthy spin sums in squared covariant matrix elements.

In this way it is not difficult to obtain the contribution of the s– and p–wave baryons to the Bjorken sum rule. For the  $\Lambda$ –type transitions one has

$$1 = |f^{(0)}(\omega)|^2 + (\omega^2 - 1)(|f_1^{(1)}(\omega)|^2 + |f_2^{(1)}(\omega)|^2) + \dots$$

$$(124)$$

where the ellipsis stand for the contributions of higher radial and orbital excitations not considered here, and for continuum contributions.

The higher orbital and radial excitations, and the continuum will contribute to the sum rule with threshold powers  $(\omega^2 - 1)^n$  at least as high as the p-wave contributions, i.e.  $n \ge 1$ . For the zero recoil point  $\omega = 1$  all but the elastic contribution vanish and one recovers the normalization condition  $f^{(0)}(1) = 1$  for the elastic form factor. As one is moving away from the zero recoil point  $\omega = 1$  rate is disappearing from the elastic channel while it appears in the inelastic channels. Using positivity one obtains bounds for the elastic form factor and for its derivative at the zero recoil point  $\omega = 1$ . One has

$$f^{(0)}(\omega) \le 1 \tag{125}$$

$$\frac{df^{(0)}}{d\omega}\Big|_{\omega=1} \le -(|f^{(1)}(1)|^2 + |f^{(1)}(1)|^2) \le 0 \tag{126}$$

For the  $\Sigma$ -type transitions one finds [50,65]

$$1 = \frac{2}{3} |g_1^{(0)}(\omega)|^2 + \frac{1}{3} |\omega g_1^{(0)}(\omega) - (\omega^2 - 1)g_2^{(0)}(\omega)|^2 + (\omega^2 - 1)\{\frac{2}{3} |g_1^{(1)}(\omega)|^2 + \frac{1}{3} |g_2^{(1)}(\omega)|^2 + \frac{4}{3} |g_3^{(1)}(\omega)|^2 + \frac{2}{3} |g_4^{(1)}(\omega)|^2 + \frac{4}{9} |\omega g_4^{(1)}(\omega) - (\omega^2 - 1)g_5^{(1)}|^2\} + \dots$$

$$(127)$$

We have diagonalized the form factor contributions of the ground state and the  $\{\Sigma_{Q_2K_2}\}$  multiplet in terms of the longitudinal and the transverse diquark transitions,  $F_L = g_1^{(0)}$  and  $F_T = \omega g_1^{(0)} - (\omega^2 - 1)g_2^{(0)}$  and similarly for the  $1^+ \to 2^-$  transition.

The bounds on the elastic form factors and their derivatives now read

$$\frac{2}{3} |g_1^{(0)}(\omega)|^2 + \frac{1}{3} |\omega g_1^{(0)}(\omega) - (\omega^2 - 1)g_2^{(0)}(\omega)|^2 \le 1$$
(128)

and

$$\frac{dg_1^{(0)}(\omega)}{d\omega}\Big|_{\omega=1} \le -\frac{1}{3} + \frac{2}{3}g_2^{(0)}(1) \tag{129}$$

The bounds on the form factors (128) and (129) are not very strong. Still one of the bounds suffices to e.g. rule out the "quark confinement model (QCM)" of [66]. In the QCM model one finds  $f^{(0)}(\omega) = \Phi(\omega)$ ,  $g_1^{(0)} = \omega \Phi(\omega)$  and  $g_2^{(0)}(\omega) = \Phi(\omega)$  where the form factor function

$$\Phi = \frac{\ln(1 + \sqrt{\omega^2 - 1})}{\sqrt{\omega^2 - 1}} \tag{130}$$

has a similar origin as the one-loop correction to the current-quark-quark vertex discussed in Sec.3. Substituting the QCM results in the bound (128) the bound translates into

$$\Phi^2(\omega) \le \frac{3}{1 + 2\omega^2} \tag{131}$$

which can be checked to be wrong. One can check that the sum rule bounds (125), (126) and (132) are indeed satisfied by the QCM form factors ( $\Phi'(1) = -1$ ). However, in view of the violation of the bound (128) one concludes that the QCM model has to be ruled out as it predicts form factors which are too hard.

Let us consider the simplification that occur when one adopts a constituent quark model description for the ground state to ground state transitions  $\Lambda_{Q_1} \to \Lambda_{Q_2}$  and  $\{\Sigma_{Q_1}\} \to \{\Sigma_{Q_2}\}$ . As already mentioned in Sec.4.1 the constituent approximation for the spin–wave functions consists in writing  $A(k,K,v)^{\alpha\beta}_{\gamma\delta} = A(k,K,v)\delta^{\alpha}_{\gamma}\delta^{\beta}_{\delta}$  such that the  $\Lambda$ -type and  $\Sigma$ -type states become related. In the language of collinear  $SU(6)_W$  the diquark is the 21–dimensional  $\square$ -representation of the  $SU(6)_W$  symmetry, where  $21 = 1_a \otimes 3_a^* + 3_s \otimes 6_s$  is the  $SU(2)_{spin} \otimes SU(3)_{flavour}$  decomposition of the 21–dimensional representation. The spin 0 antisymmetric  $3^*$  representation is made up by the three antisymmetric combinations of u, d and s while the spin 1 symmetric 6 representation is made up by the six symmetric combinations of u, d and s.

The diquark transition will now be resolved into a pair of quark–quark transitions. A first simplification occurs when the quark–quark transitions are taken to be superpositions of a scalar and a vector interaction which are parameterized by the form factors  $f(\omega)$  and  $g(\omega)$ , respectively, as drawn in Fig.6. A spin–spin interaction term could be due to an effective one–gluon exchange force as described in [32] or, alternatively, would show up as a remnant of the fermionic propagator effect in the Bethe–Salpeter approach of [39]. It is then a simple matter to

Figure 6: Light-side diquark transition resolved into constituent quark transitions. Reduced form factors  $f(\omega)$  and  $g(\omega)$  multiply scalar-scalar and vector-vector constituent quark transitions. Zero recoil normalization condition for elastic case is f(1) + g(1) = 1.

calculate the resolved diquark transition using the spin wave functions (65) and the transition operator

$$I(\omega) = f(\omega)1 \otimes 1 + g(\omega)\gamma^{\mu} \otimes \gamma_{\mu} \tag{132}$$

One finds

$$\bar{\hat{\chi}}^0(v_2)I(\omega)\hat{\chi}^0(v_1) = \frac{\omega+1}{2}f(\omega) + (2-\omega)g(\omega)$$
(133)

$$\bar{\hat{\chi}}_{\nu}^{1}(v_{2})I(\omega)\hat{\chi}_{\mu}^{1}(v_{1}) = -\left(\frac{\omega+1}{2}f(\omega)+g(\omega)\right)g_{\mu\nu}+\frac{1}{2}f(\omega)v_{2\mu}v_{1\nu}$$
 (134)

with the zero recoil normalization condition

$$f(1) + g(1) = 1. (135)$$

Eq.(134) is understood to be taken between the spin polarization vector  $\varepsilon_2^{*\nu}$  and  $\varepsilon_1^{\mu}$ . In terms of the elastic form factors defined in Eqs.(112) and (120) one finds

$$\Lambda_Q: \qquad f^{(0)}(\omega) = \frac{\omega + 1}{2} f(\omega) + (2 - \omega) g(\omega) \tag{136}$$

$$\{\Sigma_Q\}: \qquad g_1^{(0)}(\omega) = \frac{\omega+1}{2}f(\omega) + g(\omega) \tag{137}$$

$$g_2^{(0)}(\omega) = \frac{1}{2}f(\omega)$$
 (138)

It will not be easy to experimentally test the above relation between the  $\Lambda$ -type and the  $\Sigma$ -type form factors in semileptonic decays. In the test one would have to compare  $\Lambda_b \to \Lambda_c$  and  $\Omega_b \to \Omega_c$  transitions where there are additional SU(3) breaking effects. However going to the  $e^+e^-$ -production channel, one can predict the relative rates of heavy baryon pair production from (136–138). For example, close to the threshold the contribution of  $f(\omega)$  is strongly suppressed and one obtains [39] <sup>3</sup>

$$\sigma_{\Lambda_Q\bar{\Lambda}_Q} : \sigma_{\Sigma_Q\bar{\Sigma}_Q} : \sigma_{\Sigma_Q\bar{\Sigma}_Q^*} + \sigma_{\Sigma_Q^*\bar{\Sigma}_Q} : \sigma_{\Sigma_Q^*\bar{\Sigma}_Q^*} = 27 : 1 : 16 : 10$$

$$(139)$$

<sup>&</sup>lt;sup>3</sup>The spin coupling factor  $(\omega + 1)/2$  multiplying the scalar form factor  $f(\omega)$  in (136) and (137)has a simple interpretation in the crossed  $e^+e^-$ -channel where  $(\omega + 1) \to -(\omega - 1)$  after crossing. Each factor of  $\sqrt{\omega - 1}$  in  $(\omega - 1) = (\sqrt{\omega - 1})^2$  accounts for one p-wave suppression for each of the light quark-antiquark pairs that are independently produced [39].

In the so called spectator quark model one sets the spin–spin interaction term to zero. In this case one finds

$$f^{(0)}(\omega) = g_1^{(0)}(\omega) = \frac{\omega + 1}{2}f(\omega)$$
 (140)

$$g_2^{(0)}(\omega) = \frac{1}{2}f(\omega)$$
 (141)

All three reduced form factors are now related to one single form factor  $f(\omega)$ . We shall refer to  $f(\omega)$  as the residual quark model form factor since the spin coupling factor  $(\omega + 1)/2$  has been factored out. When Eq.(140) and (141) is substituted into either of the Bjorken sum rules (124) or (127) one now finds

$$f(\omega) \le \frac{2}{\omega + 1} \tag{142}$$

for the residual form factor  $f(\omega)$ . Since  $2/(\omega+1)$  is the normalized monopole form factor in the heavy quark limit one finds that the residual form factors  $f(\omega)$  has to fall at least as fast as a monopole form factor in the heavy quark limit. The form factor  $f(\omega)$  used in the spectator quark model calculation of [67] and [65] is consistent with the bound (142).

Carone, Georgi and Osofsky [69] have recently presented arguments that the light constituent quarks have no spin interactions to leading order in  $1/N_C$  ( $N_C$  is the number of colours). This would lend support to the viability of the constituent spectator approach (light constituent quarks plus absence of spin interactions of light quarks). This would have dramatic implications for threshold production of heavy baryon pairs in  $e^+e^-$  –interactions because of the extra  $|\vec{p}|^4$  threshold suppressions present in the spectator model as argued before. In the absence of spin interactions of the light constituent quarks there are no spin singlet – spin triplet transitions because of the orthogonality of the spin wave functions  $\hat{\chi}^0$  and  $\hat{\chi}^1_{\mu}$ . Consequently one would predict e.g. that the s-wave to p-wave transitions  $\Lambda_{Q_1} \to \{\Lambda_{Qk1}\}$  and  $\Sigma_{Q_1} \to \{\Sigma_{Qk1}\}$  vanish (see also [65] and [70]). This would imply that only two of the seven  $\Lambda_c$ -type p-wave states contribute to the Bjorken sum rule (124). If there is only little rate into  $\Lambda_c^{**}$ 's much of the inclusive rate must go into the elastic  $\Lambda_b \to \Lambda_c$  channel. One would then conclude that the elastic channel has a large branching ratio, or, in the light of the sum rule of Bjorken, that the elastic transition form factor  $f^{(0)}(\omega)$  should be quite flat.

Finally, the simplest quark model configuration is given by the "independent quark motion approximation" where each light quark moves around the heavy quark source independently with no interaction between the light quarks. The analogue of this configuration in atomic physics is the "unperturbed" helium atom configuration where the interaction between the electrons has been switched off. This approximation corresponds to a totally factorized form of the diquark wave function [39]

$$A_{\alpha\gamma}^{\beta\delta}(k,K,v) = A(p_1,v)A(p_2,v)\delta_{\alpha}^{\beta}\delta_{\gamma}^{\delta}.$$
 (143)

In this approximation the baryonic form factor is nothing but the square of the mesonic reduced form factor  $\xi(\omega)$  with  $\xi(1) = 1$ , i.e.

$$f(\omega) = \xi^2(\omega). \tag{144}$$

Substituting (144) into (142) one obtains

$$\xi(\omega) \le \sqrt{\frac{2}{\omega + 1}} \tag{145}$$

which, not surprisingly, is just the Bjorken bound for the heavy meson reduced form factor [64].

Figure 7: Allowed pion transitions between p-wave and s-wave charm baryon states. For the one-pion transitions drawn in the figure there are no orbital angular momentum selection rules from Heavy Quark Symmetry. The transitions  $\{\Lambda_{cK1}\} \to \Lambda_c$  are via two-pion transitions. One-pion transitions are forbidden for these transitions by isospin and, in the case  $\frac{3}{2}^- \to \frac{1}{2}^+ + \pi^-$ , also by parity in the heavy quark limit.

## 4.5 Pion Transitions Between Heavy Baryons

A look at the spectrum of the s-wave charm baryon states shows that there is enough phase space for the two members of the  $\{\Sigma_c\}$  doublet to decay into  $\Lambda_c$  via pion emission. In fact the  $1/2^+$   $\Sigma_c$ -states revealed themselves as peaks in the  $(\Lambda_c\pi)$  invariant mass spectrum. Last year the SCAT collaboration reported evidence for the corresponding one-pion decay mode of the  $3/2^+$   $\Sigma_c^*$  state via the decay  $\Sigma_c^* \to \Lambda_c\pi$  [29].

Further interest in pion transitions between heavy charm baryons has been triggered by the recent observation of two excited  $\Lambda$ -type charm baryon states at  $\simeq 2593$  MeV and at  $\simeq 2627$  MeV by the ARGUS [53], CLEO [52] and E687 [54] collaborations. These states show up as peaks in the  $(\Lambda \pi \pi)$  invariant mass distribution. The resonances are narrow, in fact too narrow to be resolved by the experiments.

The lower resonance of the two appears to be dominantly decaying via the decay chain  $\Lambda_c(2593) \to \Sigma_c(\to \Lambda_c\pi) + \pi$ . For the higher lying resonance state ARGUS reports on some evidence for the existence of the decay chain  $\Lambda_c(2627) \to \Sigma_c(\to \Lambda_c\pi) + \pi$  [53] which, however, is not corroborated by the other experiments.

The two new states are very likely the two  $J^P = 1/2^-$  and  $3/2^-$  members of the p-wave multiplet  $\{\Lambda_{cK1}\}$ . In fact, an early quark model calculation [51] predicted mass values of 2.53 GeV and 2.61 GeV for the  $1/2^-$  and  $3/2^-$  members <sup>4</sup>, respectively, of the  $\{\Lambda_{cK1}\}$  multiplet which are quite close to the experimental mass values. A direct experimental determination of the  $J^P$ 

<sup>&</sup>lt;sup>4</sup>The numerical mass values were adjusted upward such that the input  $\Lambda_c$  mass agrees with its measured value.

Figure 8: One–pion (left) and one–photon (right) transitions between heavy baryons in the heavy quark limit. The pion and the photon couple only to the light–side diquark which makes a transition from spin–parity  $j_1^{P_1}$  to  $j_2^{P_2}$  at the same velocity v. The heavy quark is not affected by the transition. Pion transitions are labelled by pion's orbital momentum. Photon transitions are labelled in terms of electric  $(EJ_{\gamma})$  and magnetic  $(MJ_{\gamma})$  multipoles.

quantum numbers of the two new states is still outstanding. However, there is some indirect evidence for the validity of the  $J^P = 1/2^-$  and  $3/2^-$  assignments of the two new states from the existence or nonexistence of the intermediate state  $(\Sigma_c \pi)$  in the  $\Lambda_c(2593)$  and  $\Lambda_c(2627)$  decays. The argument goes as follows (see Fig.7). Both decays  $\Lambda_c(2593) \to \Sigma_c \pi$  and  $\Lambda_c(2627) \to \Sigma_c \pi$  are kinematically allowed. Although the phase space for  $\Lambda_c(2627) \to \Sigma_c \pi$  is larger than for  $\Lambda_c(2593) \to \Sigma_c \pi$  the former channel is not seen by two of the three experiments. This would find a natural explanation if  $\Lambda_c(2627) \to \Sigma_c \pi$  is a very much suppressed  $3/2^- \to 1/2^+ + \pi$  d—wave decay and  $\Lambda_c(2593) \to \Sigma_c \pi$  is an unhindered  $1/2^- \to 1/2^+ + \pi$  s—wave decay.

The physics of the one-pion transitions between heavy baryons is depicted in Fig.8. The pion is emitted from the light diquark while the heavy quark propagates unaffected by the pion emission process. Since the heavy baryon is infinitely heavy the heavy baryon will not recoil in the pion emission process, i.e. the velocity of the heavy quark and thereby the heavy baryon remains unchanged, as indicated in Fig.8.

The number of independent amplitudes describing the one-pion transitions on the light side can be determined by the same reasoning as in Sec.4.3. When counting the number N of independent helicity amplitudes one has to distinguish again between the two cases that the product of the normalities of the diquark states is even or odd. One obtains

i) 
$$n_1 \cdot n_2 = 1$$
  $N = j_{min}$   
ii)  $n_1 \cdot n_2 = -1$   $N = j_{min} + 1$  (146)

or, in closed form,  $N = j_{min} - \frac{1}{2}(n_1n_2 - 1)$ . The counting of amplitudes can of course equally well be done using the LS-coupling scheme.

In fact, in Table 6 we list the relevant forms of the covariant couplings of the pions in a definite orbital state  $l_{\pi}$ . In the heavy quark limit the orbital momenta of the pion relative to the diquark  $l_{\pi}$  and relative to the baryon  $L_{\pi}$  are identical, i.e.  $l_{\pi} = L_{\pi}$ . As we shall see at the end of Sec.4.5 the couplings listed in Table 6 can easily be transcribed into chiral invariant couplings.

Table 6: Tensor structure of pion couplings to diquark states. The pion is in a definite orbital state  $l_{\pi}$ . Tensor structure of transitions with  $(j_1^{P_1}, j_2^{P_2}) \rightarrow (j_1^{-P_1}, j_2^{-P_2}) \rightarrow (j_2^{P_2}, j_1^{P_1}) \rightarrow (j_2^{P_2}, j_1^{-P_1})$  are identical and are not always listed here.

diquark transition	orbital wave	covariant coupling
$j_1^{P_1} \to j_2^{P_2} + \pi$	$l_{\pi}$	$t^i_{\mu_1\mu_{j_1};\nu_1\nu_{j_2}}$
$0^+ \to 0^+ + \pi$	forbidden	-
$1^+ \rightarrow 0^+ + \pi$	1	$p_{\mu_1}^\perp$
$1^+ + \pi$	1	$\frac{1}{\sqrt{2}}\varepsilon(\mu_1\nu_1pv)$
$0^- \rightarrow 0^+ + \pi$	0	1 (scalar)
$1^+ + \pi$	forbidden	-
$0^{-} + \pi$	forbidden	-
$1^- \rightarrow 0^+ + \pi$	forbidden	-
$1^+ + \pi$	0	$rac{1}{\sqrt{3}}g^{\perp}_{\mu_1 u_1}$
	2	$\frac{\frac{1}{\sqrt{3}}g^{\perp}_{\mu_1\nu_1}}{\sqrt{\frac{3}{2}}(p^{\perp}_{\mu_1}p^{\perp}_{\nu_1} - \frac{1}{3}p^{2}_{\perp}g^{\perp}_{\mu_1\nu_1})}$
$0^{-} + \pi$	1	$p_{\mu_1}^\perp$
$1^{-} + \pi$	1	$\frac{1}{\sqrt{2}}\varepsilon(\mu_1\nu_1pv)$
$2^- \rightarrow 0^+ + \pi$	2	$\sqrt{\frac{3}{2}}p_{\mu_1}^\perp p_{\mu_2}^\perp$
$1^+ + \pi$	2	$p_{\mu_2}^{\perp} \varepsilon(\mu_1 \nu_1 p v)$
$0^- + \pi$	forbidden	
$1^- + \pi$	1	$\sqrt{rac{3}{5}}g^{\perp}_{\mu_1 u_1}p^{\perp}_{\mu_2}$
	3	$\sqrt{\frac{5}{2}} \{ p_{\mu_1}^{\perp} p_{\mu_2}^{\perp} p_{\nu_1}^{\perp} - \frac{1}{5} (p_{\perp}^2 g_{\mu_1 \mu_2}^{\perp} p_{\nu_3}^{\perp} + \text{cycl.}(\mu_1 \mu_2 \nu_1)) \}$
$2^{-} + \pi$	1	$\sqrt{\frac{2}{5}}g^{\perp}_{\mu_1\nu_1}\varepsilon(\mu_2\nu_2pv)$
	3	$\sqrt{\frac{2}{5}}(p_{\mu_1}^{\perp}p_{\nu_1}^{\perp} - \frac{1}{5}g_{\mu_1\nu_1}p_{\perp}^2)\varepsilon(\mu_2\nu_2pv)$

The one-pion transition amplitudes between heavy baryons can then be written as

$$M^{\pi} = \langle \pi(\vec{p}), B_{Q2}(v) \mid T \mid B_{Q1}(v) \rangle$$

$$= \bar{\psi}_{2}^{\nu_{1} \dots \nu_{j_{2}}}(v) \psi_{1}^{\mu_{1} \dots \mu_{j_{1}}}(v) (\sum_{l_{\pi}} f_{l_{\pi}} t_{\mu_{1} \dots \mu_{j_{1}}; \nu_{1} \dots \nu_{j_{2}}}^{l_{\pi}})$$
(147)

where the heavy–side baryon wave functions  $\psi^{\mu_1...\mu_j}$  have been given in Tables 4 and 5 and the relevant light–side tensors  $t^{l_{\pi}}_{\mu_1...\mu_{j_1};\nu_1...\nu_{j_2}}$  are listed in Table 6. They are tensors of rank  $(j_1+j_2)$  build from the building blocks  $g_{\perp\mu\nu}=g_{\mu\nu}-v_{\mu}v_{\nu},~p_{\perp\mu}=p_{\mu}-p_{\nu}vv_{\mu}$  and, depending on parity, from the Levi–Civita tensor. They are put together such that they have the correct parity and project out the correct partial wave amplitude with amplitude  $f_{l_{\pi}}$ . The normalization of the amplitudes  $f_{l_{\pi}}$  is such that a given partial wave amplitude  $f_{l_{\pi}}$  contributes as  $|f_{l_{\pi}}|^2 |\vec{p}|^{2l_{\pi}}$  to the spin summed square of the diquark transition amplitude.

As a first application we consider the ground state to ground state transition  $\{\Sigma_c\} \to \Lambda_c + \pi$ . The one–pion transition amplitudes are easily written down using Eq.(147), the relevant heavy–side spin wave functions from Tables 4 and 5, and the  $1^+ \to 0^+ + \pi$  covariant pion coupling in Table 6. One has

$$M^{\pi} = \bar{u}_2(v) \left\{ \begin{array}{c} \frac{1}{\sqrt{3}} \gamma_{\perp}^{\mu} \gamma_5 u_1(v) \\ u_1^{\mu}(v) \end{array} \right\} f_p p_{\mu}^{\perp} \tag{148}$$

The decay rates can be calculated using the general rate formula

$$\Gamma = \frac{1}{2J_1 + 1} \quad \frac{|\vec{p}|}{8\pi M_1^2} \sum_{spins} |M^{\pi}|^2.$$
 (149)

One then obtains

$$\Gamma_{\Sigma_c^* \to \Lambda_c + \pi} = \Gamma_{\Sigma_c \to \Lambda_c + \pi} = \frac{1}{6\pi} \frac{M_2}{M_1} |f_p|^2 |\vec{p}|^3$$
(150)

where  $|\vec{p}|$  is the CM momentum of the pion. The equality of the rates for  $\Sigma_c^* \to \Lambda_c + \pi$  and  $\Sigma_c \to \Lambda_c + \pi$  true in the heavy quark mass limit (when  $M_{\Sigma_c^*} = M_{\Sigma_c}$ ) is a general result for transitions into a Heavy Quark Symmetry spin singlet state. This general result is most easily derived in the 6-j symbol formalism discussed at the end of this section.

Differences in the phase space factors  $|\vec{p}|^3$  in the two decays constitute  $\mathcal{O}(1/m_c)$  effects which may be important when one wants to model  $1/m_c$ –effects in phenomenological applications. Similarly the final form of the rate (150) depends on at what stage of the rate calculation one has dropped the zero recoil approximation inherent to the Heavy Quark Symmetry approach. This explains the  $\mathcal{O}(1/m_c)$  differences between the results of [71] and Eq.(150). We have retained the zero recoil approximation in the calculation of the squared matrix element  $|M^{\pi}|^2$ .

An estimate of the coupling strength  $f_p$  can be obtained in the constituent quark model approximation [71]. The one-pion transition between the dipion states is resolved into one-pion transitions of the constituent quarks as drawn in Fig.9. The coupling of the pion to the constituent quarks can be obtained from PCAC and is given by  $g_A f_{\pi}^{-1} \not p_{\perp} \gamma_5$  ( $f_{\pi} = 93 \text{ MeV}$ ) where  $g_A$  is a phenomenological factor ( $g_A = 0.75$ ) which is introduced to get the  $g_A/g_V$  ratio in neutron  $\beta$ -decay right. The coupling strength  $f_p$  can then be computed by using the constituent spin wave functions  $\hat{\chi}^0$  and  $\hat{\chi}^{1,\mu}$  introduced in Sec.4.1. For the transition  $1^+ \to 0^+ + \pi$  one needs the trace

$$Tr\{\bar{\hat{\chi}}^0 p_{\perp} \gamma_5 \hat{\chi}_{\mu}^1\} = p_{\mu}^{\perp}.$$
 (151)

and for the  $1^+ \to 1^+ + \pi$  transition one needs the trace

$$Tr\{\bar{\hat{\chi}}_{\nu}^{1} p_{\perp} \gamma_{5} \hat{\chi}_{\mu}^{1}\} = i\varepsilon(\mu \nu p v). \tag{152}$$

Returning to Eq.(148) one then obtains  $f_p = g_A f_{\pi}^{-1}$  from a comparison with Eq.(151). This results in a width value of e.g.

$$\Gamma_{\Sigma_c^0 \to \Lambda_c \pi^-} = 2.45 \,\text{MeV} \tag{153}$$

where we quote the numerical result of the calculation of [71]. A QCD sum rule calculation results in a width value which includes the constituent quark model value within its large error bound [72]. A slightly different value is obtained upon using the rate formula (150), due to a difference in the treatment of recoil corrections, as remarked on earlier. From the width estimate Eq.(153) one concludes that the  $\Sigma_c$  is very likely so narrow that it will not be an easy task to experimentally determine its absolute width.

As a further application consider the transition  $\{\Lambda_{CK1}\} \to \{\Sigma\} + \pi$  with  $J^P$  quantum numbers  $\{\frac{1}{2}^-, \frac{3}{2}^-\} \to \{\frac{1}{2}^+, \frac{3}{2}^+\} + 0^-$ . The transition matrix element can easily be written down using Eq.(147) and reads

$$M^{\pi} = \left\{ \begin{array}{c} -\frac{1}{\sqrt{3}} \bar{u}_{2} \gamma_{5} \gamma_{\perp}^{\nu} \\ \bar{u}_{2}^{\nu} \end{array} \right\} \left\{ \begin{array}{c} \frac{1}{\sqrt{3}} \gamma_{\perp}^{\mu} \gamma_{5} u_{1} \\ u_{1}^{\mu} \end{array} \right\} \left( \frac{1}{\sqrt{3}} f_{s} g_{\mu\nu}^{\perp} + \sqrt{\frac{3}{2}} f_{d} (p_{\mu}^{\perp} p_{\nu}^{\perp} - \frac{1}{3} g_{\mu\nu}^{\perp} p_{\perp}^{2}) \right)$$
 (154)

As mentioned above, the decays  $\frac{1}{2}^- \to \frac{1}{2}^+ + \pi$  and  $\frac{3}{2}^- \to \frac{1}{2}^+ + \pi$  are kinematically allowed and are thus interesting from the experimental point of view. Their matrix elements can be read off from (154) and are

$$M^{\pi}(\frac{1}{2}^{-} \to \frac{1}{2}^{+} + \pi) = -\frac{1}{\sqrt{3}} f_{s} \bar{u}_{2} u_{1} M^{\pi}(\frac{3}{2}^{-} \to \frac{1}{2}^{+} + \pi) = \frac{1}{\sqrt{2}} f_{d} \bar{u}_{2} \gamma_{5} p_{\mu}^{\perp} p^{\perp} u_{1}^{\mu}$$

$$(155)$$

As expected the covariant couplings project out the correct orbital angular momenta  $l_{\pi} = L_{\pi}$ . Using the rate formula (149) one obtains

$$\Gamma\left(\frac{1}{2}^{-} \to \frac{1}{2}^{+} + \pi\right) = f_{s}^{2} \frac{|\vec{p}|}{6\pi} \frac{M_{2}}{M_{1}}$$
 (156)

$$\Gamma\left(\frac{3}{2}^{-} \to \frac{1}{2}^{+} + \pi\right) = f_d^2 \frac{|\vec{p}|^5}{8\pi} \frac{M_2}{M_1}.$$
 (157)

One notes that the rates (156) and (157) exhibit the correct threshold behaviour  $|\vec{p}|^{2L_{\pi}+1}$  where  $\vec{p}$  is the CM momentum of the pion.

Using  $M_{\Sigma_c}=2.453~{\rm GeV}$  one finds  $|\vec{p}|=1.62\times 10^{-2}~{\rm GeV}$  and  $|\vec{p}|^5=1.06\times 10^{-5}~{\rm GeV}$  for the two respective threshold factors. If the scale of the coupling constants were 1 GeV one would in fact have a  $10^{-3}$  suppression of  $\Lambda_c(2627)\to \Sigma_c\pi$  relative to  $\Lambda_c(2593)\to \Sigma_c\pi$  in agreement with the observation [52,54]. However, for the soft pion emission in these decay processes  $f_\pi\cong m_\pi$  is frequently a more appropriate scale. One would then have  $|\vec{p}|/m_\pi=0.117$  and  $|\vec{p}|^5/m_\pi^5=0.204$ . In such a case the d-wave decay in  $\Lambda_c(2593)\to \Sigma_c\pi$  would not be suppressed as seems to be the case in the ARGUS result [53]. Hopefully future experiments can clarify the situation about the  $\Lambda_c(2593)\to \Sigma_c\pi$  branching fraction.

Next consider the one-pion transitions from the p-wave multiplet  $\{\Lambda_{Ck2}\}$  down to the ground state multiplet  $\{\Sigma\}$ . In terms of  $J^P$  quantum numbers one has the transitions  $\{\frac{3}{2}^-, \frac{5}{2}^-\} \to \{\frac{1}{2}^+, \frac{3}{2}^+\} + \pi$ . Here the pion is emitted in a d-wave. For the transition amplitude one now has

$$M^{\pi} = \left\{ \begin{array}{c} -\frac{1}{\sqrt{3}} \bar{u}_{2} \gamma_{5} \gamma_{\perp}^{\nu_{1}} \\ \bar{u}_{2}^{\nu_{1}} \end{array} \right\} \left\{ \begin{array}{c} \frac{1}{\sqrt{10}} \gamma_{5} (\gamma_{\perp}^{\mu_{1}} u_{1}^{\mu_{2}} + \gamma_{\perp}^{\mu_{2}} u_{1}^{\mu_{1}}) \\ u_{1}^{\mu_{1}\mu_{2}} \end{array} \right\} f_{d}^{\prime} p_{\mu_{1}}^{\perp} \varepsilon (\mu_{2} \nu_{1} p^{\perp} v)$$
 (158)

Figure 9: Light-side one-pion transition resolved into constituent quark transitions. Equal velocities of diquark and quarks are implied.

One can then use the amplitude (158) to calculate the ratio of the four one-pion transitions described by (158). After a little bit of algebra [73] one obtains

$$\Gamma_{\frac{3}{2}^{-} \to \frac{1}{2}^{+} + \pi} : \Gamma_{\frac{3}{2}^{-} \to \frac{3}{2}^{+} + \pi} : \Gamma_{\frac{5}{2}^{-} \to \frac{1}{2}^{+} + \pi} : \Gamma_{\frac{5}{2}^{-} \to \frac{3}{2}^{+} + \pi} = 9 : 9 : 4 : 14 \tag{159}$$

and

$$\Gamma_{\frac{3}{2}^{-} \to \frac{1}{2}^{+} + \pi} + \Gamma_{\frac{3}{2}^{-} \to \frac{3}{2}^{+} + \pi} = \Gamma_{\frac{5}{2}^{-} \to \frac{1}{2}^{+} + \pi} + \Gamma_{\frac{5}{2}^{-} \to \frac{3}{2}^{+} + \pi}.$$
 (160)

This result agrees with the conventional approach using Clebsch–Gordan coefficients [74] or, in a more recent and compact guise, using 6–j symbols [75,76]. The sum rule (160) is a general result for Heavy Quark Symmetry doublet to doublet transitions and is easily derived in the 6–j coupling approach.

Let us briefly review the reasoning of Ref.[74–76] that leads to the introduction of Wigner's 6-j symbols. Having Fig.8 in mind one first compounds the spins in the initial and final state  $j_1 + S_Q \to J_1$  and  $j_2 + S_Q \to J_2$ , where  $S_Q = 1/2$  is the heavy quark spin, and then combines these with the transition  $j_1 \to j_2 + l_\pi$  ( $l_\pi = L_\pi$ ) using the appropriate Clebsch-Gordan coefficients. One then obtains

$$M^{\pi}(J_{1}J_{1}^{z} \to J_{2}J_{2}^{z} + L_{\pi}m) = M_{L_{\pi}} \sum_{s^{z}, j_{1}^{z}, j_{2}^{z}} \langle J_{2}J_{2}^{z} \mid j_{2}j_{2}^{z}S_{Q}S_{Q}^{z} \rangle \langle L_{\pi}mj_{2}j_{2}^{z} \mid j_{1}j_{1}^{z} \rangle$$

$$\langle j_{1}j_{1}^{z}S_{Q}S_{Q}^{z} \mid J_{1}J_{1}^{z} \rangle$$

$$= M_{L_{\pi}}(-1)^{L_{\pi}+j_{2}+S_{Q}+J}(2j_{1}+1)^{1/2}(2J_{2}+1)^{1/2}$$

$$\left\{ \begin{array}{cc} j_{2} & j_{1} & L_{\pi} \\ J_{1} & J_{2} & S_{Q} \end{array} \right\} \langle L_{\pi}mJ_{2}J_{2}^{z} \mid J_{1}J_{1}^{z} \rangle. \tag{161}$$

The reduced matrix elements  $M_{L_{\pi}}$  correspond to the coupling factors  $f_{l_{\pi}}$  used in Eq.(147). In the second step of Eq.(161) one has rewritten the first part of Eq.(161) in terms of the Wigner 6–j symbol.

After spin-averaging over the initial spin and summing over final spins one obtains the rate

$$\frac{1}{2J_1+1} \sum_{snins} |M^{\pi}(L_{\pi})|^2 = (2j_1+1)(2J_2+1) \left| \left\{ \begin{array}{ccc} L_{\pi} & j_2 & j_1 \\ S_Q & J_1 & J_2 \end{array} \right\} \right|^2 |M_{L_{\pi}}|^2$$
 (162)

for a transition involving a given orbital angular momentum  $L_{\pi}$  of the pion. Using the standard orthogonality relation for 6–j symbols

$$\sum_{J_2} (2j_1 + 1)(2J_2 + 1) \left| \left\{ \begin{array}{cc} L_{\pi} & j_2 & j_1 \\ S_Q & J_1 & J_2 \end{array} \right\} \right|^2 = 1 \tag{163}$$

one can immediately appreciate the significance of the result Eq.(160). The total rate of pionic decays from any of the two doublet states  $J_1 = j_1 \pm S_Q$  is independent of  $J_1$ . Also one immediately concludes that the transitions into a heavy quark symmetry singlet state from any of the two heavy quark symmetry doublet states are identical to one another. A general proof of the equivalence of the covariant coupling scheme and the 6-j coupling scheme (161) is presently being worked out [77].

It is quite apparent that the 6-j approach to one-pion transitions is much easier to handle from a calculational point of view and is structurally more transparent than the covariant approach. In the covariant approach, on the other hand, one may more readily include  $\mathcal{O}(1/m_c)$ recoil and phase space corrections according to one's own intuition and experience (or prejudice). Also the covariant approach lends itself more easily to a transcription into the usual field theoretic formulation of the pion's coupling in terms of effective Lagrangians. In fact one can easily turn the covariant couplings written down in this section into chirally invariant pion couplings. This can be done by enacting the following substitutions in Table 6

$$\begin{array}{rcl}
p_{\mu_1} \dots p_{\mu_k} & \Rightarrow & \frac{1}{F} \partial_{\mu_1} \dots \partial_{\mu_k} \Phi_{\pi} + \dots \\
g_{\mu_1 \mu_2} & \Rightarrow & g_{\mu_1 \mu_2}
\end{array} \tag{164}$$

and, for k=0, constant  $\Rightarrow \frac{1}{F}v \cdot \partial \Phi_{\pi}$ . The ellipses in Eq.(164) stand for higher order contribution in the chiral expansion (see [73]).

## 4.6 Photon Transitions Between Heavy Baryons

In addition to the pion transitions between heavy baryons treated in Sec.4.5 photon transitions between heavy baryon states are also of interest. In fact, because of phase space limitations there are many more levels that can be reached via photon transitions than via pion transitions for a given higher lying heavy baryon initial state. In some cases where the pion mode is not available the total rate of the heavy baryon state is entirely in terms of the photon decay mode. Examples are the  $\Xi'_c$  and  $\Omega^*_c$  charm baryon states which are expected to decay electromagnetically because pion emission is kinematically forbidden according to present mass estimates (see Fig.10). Furthermore hyperfine splitting effects can be expected to have become so small in the bottom sector that transitions between the two partners in a heavy quark spin multiplet can be mediated by photons alone.

In the following we set up the formalism necessary to describe photon transitions between heavy baryon states in the heavy quark limit. Our discussion will be limited to the treatment of leading effects in the  $1/m_Q$  expansion, although a consideration of nonleading effects certainly warrants future attention [78]. In the heavy mass limit the (real!) photon couples only to the light diquark side since the photon coupling to the heavy quark involves a spin-flip transition down by  $1/m_Q$ . Although the formalism in this section applies both to the heavy charm and bottom sectors we shall stay in the charm sector when we work out a few definite one photon transition examples. The reason is clearly experimental. While we are just at the threshold of being able to observe photon transitions in the charm baryon sector the corresponding physics in the bottom sector lies a few years ahead of us.

The photon transition amplitude between heavy baryon states can be written down in complete analogy to the corresponding one-pion transition amplitude Eq.(147) in Sec.4.5. The physics underlying the heavy quark description of one-photon transitions is depicted in Fig. 8. The photon is emitted from the light diquark side while the heavy quark remains unaffected. The transition amplitude can thus again be written in a factorized form

$$M^{\gamma} = \langle \gamma(k), B_{Q_2}(v) \mid T \mid B_{Q_1}(v) \rangle = \bar{\Psi}_2^{\nu_1 \dots \nu_{j_2}}(v) \Psi_1^{\mu_1 \dots \mu_{j_1}}(v) (\sum_{J_{\gamma}} f^{J_{\gamma}} t_{\mu_1 \dots \mu_{j_1}; \nu_1 \dots \nu_{j_2}}^{J_{\gamma}})$$
(165)

where the appropriate spin coupling factors are determined by performing the tensor contractions in Eq.(165). The index  $J_{\gamma}$  in (165) denotes the total angular momentum of the photon (spin of the photon plus its orbital angular momentum). We choose to work in terms of multipole amplitudes  $f^{J_{\gamma}}$  with multipolarities  $2^{J_{\gamma}}$  with  $J_{\gamma} = J_{\gamma min}$ ,  $(J_{\gamma min} + 1), \ldots J_{\gamma max}$ . The tensors  $t^{J_{\gamma}}_{\mu_1 \ldots \mu_{j_1}; \nu_1 \ldots \nu_{j_2}}$  project onto the multipole amplitudes. The reason for working in terms of multipole amplitudes is simply that the multipole amplitudes  $f^{J_{\gamma}}$  contribute to the decay rate with definite powers of the photon momentum  $|\vec{k}|^{2J_{\gamma}+1}$ . This allows one to classify the transitions in terms of decreasing importance. The reasoning is similar to the one–pion transition case treated in Sec.4.5 where we used an orbital momentum classification.

In Table 7 we list explicit forms of the covariant multipole tensors for radiative diquark transitions  $j_1^{P_1} \to j_2^{P_2} + \gamma$  for the cases of interest. The covariant tensors project onto magnetic  $(MJ_{\gamma})$  or electric  $(EJ_{\gamma})$  multipole transitions. The nature of the multipole transition is determined by the parity of the photon in a given multipole state which is  $P(EJ_{\gamma}) = (-1)^{J_{\gamma}}$  and  $P(MJ_{\gamma}) = (-1)^{J_{\gamma}+1}$ . For example, for  $P_1 \cdot P_2 = +1$  parity conservation implies an even and an odd  $J_{\gamma}$  for electric and magnetic multipole transitions, respectively. The covariants are written in terms of the momentum representation of the field strength tensor  $F_{\alpha\beta} = k_{\alpha}\varepsilon_{\beta} - k_{\beta}\varepsilon_{\alpha}$  or its dual  $\frac{1}{2}\tilde{F}_{\alpha\beta} = \varepsilon_{\alpha\beta\gamma\delta}F^{\gamma\delta}$  where  $\varepsilon_{\alpha}$  is the polarization vector of the photon. The use of the field strength tensor guarantees the appropriate coupling to (three-) transverse photons as can be easily appreciated by rewriting the antisymmetric field strength tensor as an one-index object  $F_{\alpha\beta} \to \varepsilon_{\mu\alpha\beta\gamma}k^{\alpha}\varepsilon^{\beta}v^{\gamma}$ , in analogy to Eq.(92). Whether the coupling is to  $F_{\alpha\beta}$   $(n_1n_2 = +)$  or to its dual  $F_{\alpha\beta}$   $(n_1n_2 = -)$  is determined by the product of normalities  $n_1 \cdot n_2$  also listed in Table 4. The counting of covariants and thereby the counting of the number of multipole amplitudes can be done by helicity or multipole amplitude counting and is given by

i) 
$$j_1 = j_2 : N = 2j$$
  
ii)  $j_1 \neq j_2 : N = 2j_{min} + 1$  (166)

The normalization is such that a given multipole amplitude  $f^{J_{\gamma}}$  contributes as  $|f^{J_{\gamma}}|^2 |\vec{k}|^{2J_{\gamma}+1}$  to the spin summed square of the diquark transition amplitude [79].

It is then an easy matter to derive the heavy quark symmetry structure of photon transitions between heavy baryon states using Eq.(165) and Tables 4,5 and 7. As a first application we write down the amplitude for the ground state transition  $\{\Sigma_Q\} \to \Lambda_Q + \gamma$ . One has

$$M^{\gamma} = \bar{u}_2 \left\{ \begin{array}{c} \frac{1}{\sqrt{3}} \gamma_{\perp}^{\mu_1} \gamma_5 u_1 \\ u_1^{\mu_1} \end{array} \right\} \frac{1}{\sqrt{2}} f^{M1} \tilde{F}_{\alpha\beta} g_{\mu_1}^{\alpha} v^{\beta} \tag{167}$$

Using standard  $\varepsilon_{\alpha\beta\gamma\delta}$ —tensor identities one obtains

$$\Sigma_c \to \Lambda_c + \gamma : \qquad M^{\gamma} = i \frac{1}{\sqrt{6}} f^{M1} \bar{u}_2 \not k \not \epsilon^* u_1 \tag{168}$$

$$\Sigma_c^* \to \Lambda_c + \gamma : M^{\gamma} = \frac{1}{\sqrt{2}} f^{M1} \bar{u}_2 \varepsilon (\mu_1 v k \varepsilon^*) u_1^{\mu_1}$$
 (169)

Table 7: Tensor structure of photon couplings to diquark states. Photon is in definite multipole state EJ (electric) MJ (magnetic). Sign of the product of naturalities determines whether coupling is to field strength tensor  $F_{\alpha\beta}$   $(n_1 \cdot n_2 = +1)$  or to its dual  $\tilde{F}_{\alpha\beta}$   $(n_1 \cdot n_2 = -1)$ . Tensor structure of transitions with  $(j_1^{P_1}, j_2^{P_2}) \rightarrow (j_1^{-P_1}, j_2^{-P_2}) \rightarrow (j_2^{P_2} j_1^{P_1}) \rightarrow (j_2^{-P_2} j_1^{-P_1})$  are identical and are not always listed separately.

diquark transition	multipolog	m m	covariant coupling
$j_1^{P_1} \rightarrow j_2^{P_2} + \gamma$	multipoles	$n_1 n_2$	$t^i_{\mu_1\mu_{j_1}; u_1 u_{j_2}}$
$ \begin{array}{ccc} 0^+ \to & 0^+ + \gamma \\ 1^+ \to & 0^+ + \gamma \end{array} $	forbidden	+1	r1··rrJ   5· 1···· J2
$1^+ \rightarrow 0^+ + \gamma$	M1	<u> </u>	$\frac{1}{\sqrt{2}}\tilde{F}_{\alpha\beta}g^{\alpha}_{\mu_1}v^{\beta}$
$1 + \gamma$ $1^+ + \gamma$		_	V Z FI
$1' + \gamma$	M1	+1	$\frac{1}{2}F_{\alpha\beta}g^{\alpha}_{\mu_1}g^{\beta}_{ u_1}$
-	E2	+1	$\frac{1}{2}F_{\alpha\beta}(2k_{\mu_1}g^{\alpha}_{\nu_1}v^{\beta} + k \cdot vg^{\alpha}_{\mu_1}g^{\beta}_{\nu_1})$
$\begin{array}{ccc} 0^{-} & 0^{+} + \gamma \\ \hline 1^{-} & 0^{+} + \gamma \end{array}$	forbidden	-1	
$1^- \to 0^+ + \gamma$	E1	+1	$rac{1}{\sqrt{2}}F_{lphaeta}g^{lpha}_{\mu_1}v^{eta}$
$1^+ + \gamma$	E1	-1	$rac{1}{2} ilde{F}_{lphaeta}g^{lpha}_{\mu_1}g^{eta}_{ u_1}$
	M2	-1	$\frac{1}{2}\tilde{F}_{\alpha\beta}(2k_{\mu_1}g^{\alpha}_{\nu_1}v^{\beta} + k \cdot vg^{\alpha}_{\mu_1}g^{\beta}_{\nu_1})$
$2^- \rightarrow 0^+ + \gamma$	M2	$-1 \\ -1$	$ ilde{F}_{lphaeta}k_{\mu_1}g^lpha_{\mu_2}v^eta$
$1^+ + \gamma$	E1	+1	$\sqrt{rac{3}{10}}F_{lphaeta}g^lpha_{\mu_1}g_{\mu_2 u_1}v^eta$
	M2	+1	$\sqrt{\frac{1}{6}}F_{\alpha\beta}(v \cdot kg_{\mu_2\nu_1}g^{\alpha}_{\mu_1}v^{\beta} + 2k_{\mu_2}g^{\alpha}_{\mu_1}g^{\beta}_{\nu_1})$
	E3	+1	$\sqrt{\frac{1}{30}} F_{\alpha\beta} ((v \cdot k)^2 g_{\mu_2 \nu_1} g_{\mu_1}^{\alpha} v^{\beta} + \frac{5}{4} v \cdot k k_{\mu_2} g_{\mu_1}^{\alpha} g_{\nu_1}^{\beta}$
			$+\frac{15}{4}v^{\beta}k_{\mu_2}(k_{\nu_1}g^{\alpha}_{\mu_1}+k_{\mu_1}g^{\alpha}_{\nu_1}))$
$2^- \rightarrow 0^- + \gamma$	E2	+1	$F_{lphaeta}k_{\mu_1}g^lpha_{\mu_2}v^eta$
$1^- + \gamma$	M1	-1	$\sqrt{rac{3}{10}} ilde{F}_{lphaeta}g^{lpha}_{\mu_1}g_{\mu_2 u_1}v^{eta}$
	E2	-1	$\sqrt{\frac{1}{6}}\tilde{F}_{\alpha\beta}(v \cdot kg_{\mu_2\nu_1}g^{\alpha}_{\mu_1}v^{\beta} + 2k_{\mu_2}g^{\alpha}_{\mu_1}g^{\beta}_{\nu_1})$
	M3	-1	$\sqrt{\frac{1}{30}}\tilde{F}_{\alpha\beta}((v \cdot k)^2 g_{\mu_2\nu_1} g_{\mu_1}^{\alpha} v^{\beta} + \frac{5}{4} v \cdot k k_{\mu_2} g_{\mu_1}^{\alpha} g_{\nu_1}^{\beta}$
			$+\frac{15}{4}v^{\beta}k_{\mu_2}(k_{\nu_1}g^{\alpha}_{\mu_1}+k_{\mu_1}g^{\alpha}_{\nu_1}))$
$2^- + \gamma$	M1	+1	$\sqrt{rac{1}{5}}F_{lphaeta}g_{\mu_1 u_1}g_{\mu_2}^lpha g_{ u_2}^eta$
	E2	+1	$\sqrt{\frac{3}{7}}F_{\alpha\beta}g_{\mu_1\nu_1}(2k_{\mu_2}v^{\beta}g^{\alpha}_{\nu_2} + v \cdot kg^{\alpha}_{\mu_2}g^{\beta}_{\nu_2})$
	M3	+1	$\sqrt{\frac{3}{10}} F_{\alpha\beta} g^{\alpha}_{\mu_2} g^{\beta}_{\nu_2} ((v \cdot k)^2 g_{\mu_1 \nu_1} + \frac{5}{2} k_{\mu_1} k_{\nu_1})$
	E4	+1	$\sqrt{\frac{1}{14}} F_{\alpha\beta} (2k_{\mu_2} v^{\beta} g^{\alpha}_{\nu_2} + v \cdot k g^{\alpha}_{\mu_2} g^{\beta}_{\nu_2})$
			$((v \cdot k)^2 g_{\mu_1 \nu_1} + \frac{7}{2} k_{\mu_1} k_{\nu_1})$

Figure 10: Light-side one-photon transition resolved into constituent quark transitions. Equal velocities of light diquark and heavy quark are implied.

The transition (169) can be checked to have the correct M1 coupling structure. The rate follows from the two body decay rate formula Eq.(149). In the degeneracy limit  $M_{\Sigma_c^*} = M_{\Sigma_c}$  one finds

$$\Gamma_{\Sigma_c \to \Lambda_c + \gamma} = \Gamma_{\Sigma_c^* \to \Lambda_c + \gamma} = \frac{1}{6\pi} |f^{M1}|^2 \frac{M_2}{M_1} |\vec{k}|^3$$

$$(170)$$

where  $|\vec{k}| = (M_1^2 - M_2^2)/2M_1$ . The equality of the decay rates of heavy quark symmetry partners into the ground state  $\Lambda_c$  is again a general result that can easily be derived in the 6–j formalism as applied to photon transitions.

The photonic coupling  $(\Lambda_c; \Lambda_c \gamma)$  vanishes in the heavy quark limit as Table 7 shows. The reason is simply that a (real!) photon cannot couple to the  $0^+$  diquark state. For the ground state transition  $\{\Sigma_Q\} \to \{\Sigma_Q\} + \gamma$  we calculate the M1 contribution to the kinematically accessible transition  $\Sigma_c^* \to \Sigma_c + \gamma$ . One obtains

$$\Sigma_c^* \to \Sigma_c + \gamma : M^{\gamma} = \frac{1}{2\sqrt{3}} f'^{M1} \bar{u}_2 \gamma_5 \gamma^{\alpha} u_1^{\mu_1} (k_{\mu_1} \varepsilon_{\alpha}^* - k_{\alpha} \varepsilon_{\mu_1}^*)$$
 (171)

where we denote the M1 diquark amplitude by  $f'^{M1}$  to set it aside from the amplitude  $f^{M1}$  used in Eq.(167). It can again be checked that Eq.(171) has the correct M1 coupling structure even though the proportionality of the M1–covariants in Eq.(169) and (171) is not apparent. The rate of the transition (171) can be computed to be

$$\Gamma_{\Sigma_c^* \to \Sigma_c + \gamma} = \frac{1}{36\pi} |f'^{M1}|^2 \frac{M_2}{M_1} |\vec{k}|^3$$
(172)

It is quite clear that heavy quark symmetry can tell us nothing about the strength of the "reduced matrix elements"  $f^{M1}$  and  $f'^{M1}$ . In order to obtain a rough estimate for the magnitude of the couplings  $f^{M1}$  and  $f'^{M1}$  we resort to the constituent quark model as has been done in [71]. In the constituent quark model the coupling of the photon to the diquark state is resolved into the sum of the couplings of the photon to the constituent quarks as shown in Fig.11. The photon couples to the constituent quarks with a M1 coupling structure and a known coupling strength  $\frac{1}{2}\mu_q\sigma_{\alpha\beta}F^{\alpha\beta}$  where  $\mu_q$  is the magnetic moment of the quark q given by  $\mu_q=e_qe/2m_q$ . The diquark coupling strengths  $f^{M1}$  and  $f'^{M1}$  can then be obtained by evaluating the photonic quark coupling sandwiched between the spin 0 and spin 1 constituent diquark states  $\hat{\chi}^0$  and  $\hat{\chi}^1_{\mu_1}$  introduced in Sec 4.1. One obtains

$$Tr\{\bar{\hat{\chi}}^0 \frac{1}{2} \mu_q \sigma_{\alpha\beta} F^{\alpha\beta} \chi^1_{\mu}\} = \mu_q \tilde{F}^{\alpha\beta} g_{\mu\alpha} v_{\beta}$$
 (173)

$$Tr\{\bar{\chi}_{\nu}^{1} \frac{1}{2} \mu_{q} \sigma_{\alpha\beta} F^{\alpha\beta} \chi_{\mu}^{1}\} = i \mu_{q} F^{\alpha\beta} g_{\nu\alpha} g_{\mu\beta}$$
 (174)

for the photon coupling to one of the quark lines.

From comparing (173) and (174) with the covariant structure in Table 7 one finds

$$f^{M1} = \sqrt{2}e \left( \frac{e_{q_1}}{2m_{q_1}} - \frac{e_{q_2}}{2m_{q_2}} \right) \tag{175}$$

$$f'^{M1} = 2ie\left(\frac{e_{q_1}}{2m_{q_1}} + \frac{e_{q_2}}{2m_{q_2}}\right) \tag{176}$$

after adding in flavour factors and the contribution of the second constituent quark. Note that the constituent quark model approach predicts a vanishing E2 amplitude for the  $\{\Sigma_Q\} \to \{\Sigma_Q\}$  transitions.

Using standard values for the constituent quark masses the authors of [80] have calculated the photonic width of  $\Sigma_c^+ \to \Lambda_c + \gamma$ . They obtain

$$\Gamma_{\Sigma_c^+ \to \Lambda_c + \gamma} = 93 \text{ keV}.$$
 (177)

Comparing with the pionic width  $\Gamma_{\Sigma_c^+ \to \Lambda_c + \pi^0} = 2.43$  MeV calculated in the same constituent approximation one finds a photonic branching ratio of  $\cong 4\%$  for the  $\Sigma_c^+$  which compares favourably with the  $\cong 0.5\%$  branching ratio found for  $\Delta \to N + \gamma$ . From the minus sign in Eq.(175) one predicts a severe rate suppression for  $\Xi_c'^0 \to \Xi_c^0 + \gamma$  relative to  $\Xi_c'^+ \to \Xi_c^+ + \gamma$  due to an almost complete cancellation of the contributions of the d and s quarks. From [80] the two  $\Xi_c' \to \Xi_c + \gamma$  rates are in the ratio 0.3/16.

In Fig.10 we have drawn all possible one–photon transitions involving the ground state charm baryons. We have included the two newly discovered  $\Lambda$ -type p-wave states in the plot. The multipole structure of the photonic transitions indicated in Fig.10 refers to the multipole structure predicted by Heavy Quark Symmetry. For example, the decay  $\Lambda_{cK1} \to \Lambda_c + \gamma$  can in general be a E1 and M2 transition but Heavy Quark Symmetry tells us that the transition is purely E1. This will not be an easy task to check experimentally. The remaining E2 and M2 quadrupole transitions indicated in Fig.10 are not forbidden by Heavy Quark Symmetry but are expected to be small in the constituent quark model approximation.

As a last application consider the one-photon transitions  $\{\Lambda_{cK1}\} \to \Lambda_c + \gamma$ . Using again Table 4 and 7 we find

$$\Lambda_{cK1} \to \Lambda_c + \gamma \quad : \qquad M^{\gamma} = -\frac{1}{\sqrt{6}} f^{E1} \bar{u}_2 \not\in \gamma_5 u_1 \mid \vec{k} \mid$$
 (178)

$$\Lambda_{cK1}^* \to \Lambda_c + \gamma : M^{\gamma} = -\frac{1}{\sqrt{2}} f^{E1} \bar{u}_2 \varepsilon_{\mu_1}^* u_1^{\mu_1} \mid \vec{k} \mid$$
 (179)

One can check that Eqs.(178) and (179) have the correct E1 coupling structure. In the mass degeneracy limit the two rates are equal as remarked on before. One finds

$$\Gamma_{\Lambda_{cK1} \to \Lambda_c + \gamma} = \Gamma_{\Lambda_{cK1}^* \to \Lambda_c + \gamma} = |f^{E1}|^2 \frac{1}{6\pi} \frac{M_2}{M_1} |\vec{k}|^3$$

$$\tag{180}$$

When phase space effects are taken into account the ratio of rates of  $\Lambda_{cK1} \to \Lambda_c + \gamma$  and  $\Lambda_{cK1}^* \to \Lambda_c + \gamma$  gets lowered by  $\cong 25\%$ . A very rough estimate of the rate for  $\Lambda_{cK1}^{+*} \to \Lambda_c + \gamma$  can be obtained by comparison with the rate estimate for  $\Sigma_c^+ \to \Lambda_c + \gamma$  given in Eq.(177). Phase space enhances the former rate by a factor of  $\cong$  7. Setting  $f^{E1} \cong f^{M1}$  one can thus



expect a rate of  $\mathcal{O}(700 \text{ keV})$  for the decay  $\Lambda_{cK1}^{+*} \to \Lambda_c + \gamma$ . If the hadronic width of the  $\Lambda_{cK1}^*$  is suppressed as much as is argued for in [81] one can indeed expect a substantial one–photon branching fraction of the  $\Lambda_{cK1}^*$ . At any rate, one can hope to extract a great deal of interesting physics from the analysis of one–photon transitions between charm baryon states in the future.

We close this subsection by expressing the photonic transition amplitudes in terms of 6–j symbols, in complete analogy to the pionic case discussed in Sec.4.5. In fact one just needs to replace  $L_{\pi}$  in Eqs.(161) and (163) by the total angular momentum of the photon  $J_{\gamma}$ . Skipping the first step in the derivation of Eq.(161) one now has

$$M^{\gamma}(J_{1}J_{1}^{z} \to J_{2}J_{2}^{z} + J_{\gamma}m) = M_{J_{\gamma}}(-1)^{J_{\gamma}+j_{2}+S_{Q}+J_{1}}(2j_{1}+1)^{\frac{1}{2}}(2J_{2}+1)^{\frac{1}{2}}$$

$$\begin{cases} J_{\gamma} & j_{2} & j_{1} \\ S_{Q} & J_{1} & J_{2} \end{cases} \langle J_{\gamma}mJ_{2}J_{2}^{z} \mid J_{1}J_{1}^{z} \rangle$$

$$(181)$$

The symbols appearing in (181) are explained at the end of Sec.4.5. The reduced matrix elements  $M_{J_{\gamma}}$  correspond to the multipole amplitudes  $f^{J_{\gamma}}$  in Eq.(165). As discussed in the beginning of this subsection parity determines whether the transition  $M^{\gamma}(J_{\gamma})$  is a magnetic or electric multipole transition.

# 5 Semileptonic Decays

### 5.1 Inclusive Semileptonic Rates

The main motivation for studying the inclusive semileptonic decays of bottom hadrons is to learn more about the two fundamental constants of the Standard Model  $V_{cb}$  and  $V_{ub}$ . To extract these parameters, it is important to have a precise calculation of the electron spectrum in the inclusive decays  $b \to \{c, u\}e\bar{\nu}$ . The simplest description of these processes assumes that the lepton spectrum is that of the free heavy quark decay (FQD). The light quark is assumed to play no role at all and is regarded as being just a "spectator". Refinements of this approach include taking into account the one-loop radiative corrections and of the internal motion (Fermi motion) of the heavy quark inside of the hadron in the framework of a nonrelativistic bound-state model. It is, however, only recently that a systematic calculation of the nonperturbative corrections to this picture has become possible, in terms of an expansion in powers of the inverse heavy quark mass  $m_b^{-1}$ . The aim of this chapter is to give a brief account of these developments.

We begin by presenting the predictions of the FQD picture for the decay of a polarized b quark. This provides a lowest–order description to be improved upon and is useful for understanding the gross features of the lepton spectrum. The weak interaction Lagrangian responsible for the decays we are considering is

$$\mathcal{L}_W = V_{jb} 2\sqrt{2} G_F J_{\mu} [\bar{\ell} \gamma^{\mu} \frac{1}{2} (1 - \gamma_5) \nu_{\ell}]$$
(182)

where  $J_{\mu} = \bar{j}\gamma_{\mu}\frac{1}{2}(1-\gamma_5)b$  is the charged current and  $j=u,c,\ \ell=e,\mu,\tau$ .  $V_{jb}$  is the corresponding Kobayashi–Maskawa matrix element. This yields for the decay rate of the process  $b(m_b v) \rightarrow j(p_j)e(p_e)\bar{\nu}(p_{\nu})$  the following expression (under the assumption that the lepton mass vanishes  $m_{\ell} = 0$ )

$$d\Gamma = 32G_F^2 |V_{jb}|^2 (p_e \cdot p_j) [(p_\nu \cdot v) + (p_\nu \cdot s)] dLips.$$
(183)

The heavy quark spin s satisfies  $v \cdot s = 0$ . The phase space element of the final state particles is

$$dLips = (2\pi)^4 \delta^{(4)} (p_B - p_e - p_\nu - p_j) \frac{d^3 p_e}{(2\pi)^3 2E_e} \frac{d^3 p_\nu}{(2\pi)^3 2E_\nu} \frac{d^3 p_j}{(2\pi)^3 2E_j}$$

$$\to \frac{E_e E_\nu dE_e d\Omega_e d\Omega_\nu}{8(2\pi)^5 [m_b + E_e (\cos \theta_{e\nu} - 1)]}.$$
(184)

We have chosen to parameterize the final state by giving the electron energy  $E_e$  and the flight directions of the electron and neutrino in the b-quark rest frame with  $d\Omega = d\cos\theta d\phi$ .

In some applications it might be more convenient to choose the neutrino energy  $E_{\nu}$  as an independent variable. This is done most easily by choosing  $p_e$  as the z-axis and specifying the neutrino direction by giving  $\theta_{e\nu}$  and a polar angle  $\phi_{\nu}$  whose origin might be chosen corresponding to the configuration where the three vectors  $p_e$ ,  $p_{\nu}$ , s are coplanar. The direction of  $p_e$  is given with respect to  $\vec{s}$  by  $(\theta, \phi)$  and will be considered for the moment being as fixed. Now  $\theta_{e\nu}$  can be replaced by  $E_{\nu}$  by making use of

$$E_{\nu} = \frac{m_b^2 - m_j^2 - 2m_b E_e}{2[m_b + E_e(\cos\theta_{e\nu} - 1)]}, \qquad dE_{\nu} = \frac{E_e E_{\nu} d\cos\theta_{e\nu}}{m_b + E_e(\cos\theta_{e\nu} - 1)}$$
(185)

and (183) can be rewritten as

$$d\Gamma = 2G_F^2 |V_{jb}|^2 (m_b^2 - m_j^2 - 2m_b E_\nu) (1 + \cos \theta_{s\nu}) \frac{E_\nu dE_e dE_\nu d\Omega_e d\phi_\nu}{(2\pi)^5}$$
(186)

with

$$\cos \theta_{s\nu} = \cos \theta_{e\nu} \cos \theta + \sin \theta_{e\nu} \sin \theta \cos \phi_{\nu} \tag{187}$$

It is a simple matter now to integrate over  $\phi_{\nu}$ . The  $\phi$ -integration is also trivially performed. The result can be most conveniently represented in terms of the scaled variables

$$y_e = \frac{2E_e}{m_b}, \qquad y_\nu = \frac{2E_\nu}{m_b}, \qquad \rho = \frac{m_j^2}{m_b^2}$$
 (188)

and is

$$\frac{\mathrm{d}\Gamma}{\mathrm{d}y_e \mathrm{d}y_\nu \mathrm{d}\cos\theta} = \frac{G_F^2 m_b^5 |V_{jb}|^2}{4(2\pi)^3} y_\nu (1 - \rho - y_\nu) \left[ 1 + \frac{2\cos\theta}{y_e y_\nu} \left( 1 - \rho - y_e - y_\nu + \frac{1}{2} y_e y_\nu \right) \right] . \quad (189)$$

An integration over the neutrino energy within the limits  $y_{\nu_{min}} = 1 - \rho - y_e$  and  $y_{\nu_{max}} = 1 - \rho/(1 - y_e)$  gives

$$\frac{\mathrm{d}\Gamma}{\mathrm{d}y_e \mathrm{d}\cos\theta} = \frac{G_F^2 m_b^5 |V_{jb}|^2}{24(2\pi)^3} \frac{y_e^2 (1-\rho-y_e)^2}{(1-y_e)^3} \left( \left[ (1-y_e)(3-2y_e) + \rho(3-y_e) \right] + \cos\theta \left[ (1-y_e)(1-2y_e) - \rho(1+y_e) \right] \right).$$
(190)

The total decay rate is obtained after integrating this distribution over  $\theta$  and over  $y_e$  from 0 to  $1 - \rho$  with the result

$$\Gamma_b = \frac{G_F^2 m_b^5 |V_{jb}|^2}{24(2\pi)^3} (1 - 8\rho + 8\rho^3 - \rho^4 - 12\rho^2 \log \rho).$$
 (191)

The corrections to these predictions are of three types: i) radiative corrections of order  $\alpha_s(m_b)$  due to hard gluon exchange between the initial and final state quarks; ii) corrections of order  $\Lambda/m_b$  due to the interaction of the heavy quark with the light quarks in the hadron and their gluon field; iii) corrections proportional to the lepton mass of order  $\mathcal{O}(m_\ell^2/m_b^2)$ .

The radiative corrections have been computed in [82,83] and their effect is to change the electron spectrum (190) into

$$\frac{\mathrm{d}\Gamma}{\mathrm{d}y_e} = \frac{\mathrm{d}\Gamma^{(0)}}{\mathrm{d}y_e} \left( 1 - \frac{2\alpha_s}{3\pi} G(y_e, \rho) \right) . \tag{192}$$

Figure 12: Inclusive semileptonic  $H_b \to X_c$  decays in QCD. The squared transition amplitude is expressed as the absorptive part of the handbag diagram where the b quark interacts with the light degrees of freedom in  $H_b$  and the c quark propagates in the background field of the light constituents.

Here  $d\Gamma^{(0)}/dy_e$  is the FQD spectrum of an unpolarized b quark and  $G(y_e, \rho)$  is in general a complicated function of its arguments. For  $\rho \simeq 0.08$ , corresponding to a  $b \to c$  transition, it is almost constant ( $\simeq 2.5$ ) for  $y_e < 0.7$  and diverges logarithmically for  $y_e \to 1 - \rho$ . However, this divergence is not very problematic in this case, because in this region the uncorrected spectrum vanishes and furthermore, the bound–state effects average the effect away. The situation is more serious for the  $b \to u$  case, where the divergence is doubly–logarithmic

$$G(y_e, 0) = \ln^2(1 - y_e) + \frac{7}{2}\ln(1 - y_e) + \text{terms regular as } y_e \to 1,$$
 (193)

and the FQD spectrum (190) does not vanish for  $y_e = 1$  (actually at this point it has a very steep fall, which in the limit  $m_u \to 0$  is described by a step-function  $\theta(1 - y_e)$ ). The authors of [84] have therefore proposed to change the correction (192) into

$$\frac{\mathrm{d}\Gamma}{\mathrm{d}y_e} = \frac{\mathrm{d}\Gamma^{(0)}}{\mathrm{d}y_e} \left( 1 - \frac{2\alpha_s}{3\pi} \tilde{G}(y_e, \rho) \right) \exp\left( -\frac{2\alpha_s}{3\pi} \ln^2(1 - y_e) \right) . \tag{194}$$

Here the exponential sums the double-logarithms of the form  $\alpha_s^n \ln^{2n}(1-y_e)$  (Sudakov logarithms) to all orders in  $\alpha_s$  and  $\tilde{G}(y_e, 0)$  is the remainder of  $G(y_e, 0)$  (193) after the first term has been subtracted away. After this modification, the QCD corrected spectrum vanishes at the end-point  $y_e = 1 - \rho$  in a smoother way than a step-function  $\theta(1 - y_e)$ . We mention that the  $\mathcal{O}(\alpha_s)$  radiative corrections to the electron spectrum (190) in semileptonic decays of polarized b quarks have recently been calculated [85].

The corrections proportional to  $\Lambda/m_b$  are partly due to the internal motion of the b quark inside of the heavy hadron, which Doppler shifts the FQD predictions (190,192) and partly to the interactions of the b quark with the background gluonic field created by the light constituents of the hadron (see Fig.12). Recent theoretical advances have made it possible to study these effects in an essentially model-independent way [86,87]. We present in the following a brief account of the method, as applied to the inclusive semileptonic decays of polarized  $\Lambda_b$  baryons.

The decay rates and the lepton angular distributions can be expressed in terms of the hadronic tensor

$$W^{\mu\nu} = (2\pi)^{3} \sum_{X} \delta^{(4)}(p_{\Lambda_{b}} - q - p_{X}) \langle \Lambda_{b}(v, s) | J^{\mu\dagger} | X \rangle \langle X | J^{\nu} | \Lambda_{b}(v, s) \rangle =$$

$$-g^{\mu\nu} W_{1} + v^{\mu} v^{\nu} W_{2} - i \epsilon^{\mu\nu\alpha\beta} v_{\alpha} q_{\beta} W_{3} + q^{\mu} q^{\nu} W_{4} + (q^{\mu} v^{\nu} + q^{\nu} v^{\mu}) W_{5}$$

$$-q \cdot s [-g^{\mu\nu} G_{1} + v^{\mu} v^{\nu} G_{2} - i \epsilon^{\mu\nu\alpha\beta} v_{\alpha} q_{\beta} G_{3} + q^{\mu} q^{\nu} G_{4} + (q^{\mu} v^{\nu} + q^{\nu} v^{\mu}) G_{5}]$$

$$(s^{\mu} v^{\nu} + s^{\nu} v^{\mu}) G_{6} + (s^{\mu} q^{\nu} + s^{\nu} q^{\mu}) G_{7} + i \epsilon^{\mu\nu\alpha\beta} v_{\alpha} s_{\beta} G_{8} + i \epsilon^{\mu\nu\alpha\beta} q_{\alpha} s_{\beta} G_{9} ,$$

$$(195)$$

with q the total momentum of the lepton pair, s the spin vector of the  $\Lambda_b$  and  $W_{1-5}(q^2, q \cdot v)$ ,  $G_{1-9}(q^2, q \cdot v)$  invariant form-factors.

The hadronic tensor  $W^{\mu\nu}$  (195) can be expressed as the discontinuity across the physical cut of the transition amplitude

$$T^{\mu\nu} = -i \int d^4x e^{-iq\cdot x} \langle \Lambda_b(v,s) | T J^{\mu\dagger}(x) J^{\nu} | \Lambda_b(v,s) \rangle$$
 (196)

which can be decomposed into covariants  $T_{1-5}$ ,  $S_{1-9}$  similarly to (195) and are related to  $G_i$  by

$$W_i = -\frac{1}{\pi} \text{Im} \, T_i \qquad G_i = -\frac{1}{\pi} \text{Im} \, S_i \,.$$
 (197)

The physical cut for the inclusive process under consideration extends from  $q \cdot v = \sqrt{q^2}$  up to  $q \cdot v = (m_{\Lambda_b}^2 + q^2 - m_{j_{min}}^2)/(2m_{\Lambda_b})$  with  $m_{j_{min}}$  the mass of the lightest hadron containing a j-type quark.

The time ordered product in (196) can be expanded into an operator product expansion (OPE) [86]. In momentum space, the operators of higher dimension which appear are suppressed by increasing (inverse) powers of  $m_b$  and  $\Delta = (m_b v - q)^2 - m_j^2$ , so the OPE can be meaningfully applied only in regions of the phase space where the second parameter is large enough, in comparison with the QCD scale  $\Lambda$ . In particular, this is not true near the boundaries of the allowed phase space, where special methods have been devised to deal with this problem [88].

The leading order term in the OPE consists of the operators  $\bar{b}\gamma_{\mu}b$  and  $\bar{b}\gamma_{\mu}\gamma_{5}b$ , whose matrix elements in a polarized  $\Lambda_{b}$  state are given by  $v_{\mu}$  and  $s_{\mu}$ , respectively, to leading order in  $1/m_{b}$ . By taking the imaginary part of the transition matrix element (196) according to (197), the old results of the FQD picture (183-191) are recovered. This procedure is shown in graphical form in Fig.12.

The operators contributing to the next order in the  $1/m_b$  expansion have dimension five. Actually, their contribution can be shown to vanish, which gives the remarkable prediction that the FQD results obtain corrections only at order  $\Lambda^2/m_b^2$  [86]. This is a constraint set by QCD on any model–dependent description of the inclusive semileptonic of heavy hadrons. It has been recently shown [89] that the ACCMM model [84] can accommodate this feature.

Up to now, the OPE method has been pushed up to order  $1/m_b^2$ . The corrections which appear to this order arise from two sources: i) from the matrix element of the kinetic energy of the b quark  $\bar{h}_{v_1}^{(b)}(iD)^2 h_{v_1}^{(b)}$ ; ii) the corrections to the matrix element of the axial current in a polarized  $\Lambda_b$  state. The first one has been calculated with the help of constituent quark models or from QCD sum rules, whereas the second one has only been estimated from a constituent quark model in [90]. For the case of the inclusive bottom meson decays, there is one more source of corrections, due to the chromomagnetic interaction operator  $\bar{h}_{v_1}^{(b)} g\sigma \cdot F h_{v_1}^{(b)}$ , whose

Figure 13: Electron spectrum in inclusive semileptonic decays of bottom mesons for  $b \to c$  and  $b \to u$  transitions. The spectra are normalized to  $\Gamma_b(\rho = 0)$ . Full line: the free quark decay result (190). Dashed line:  $\mathcal{O}(1/m_b^2)$  nonperturbative corrections included.

matrix elements can be determined in a model—independent way from the hyperfine splitting  $m_{B^*} - m_B$ . The effect of these corrections on the lepton spectrum is shown on Fig.13 for the two cases  $b \to c$  and  $b \to u$ .

Finally, the last type of corrections to the FQD predictions which we discuss are due to a nonvanishing lepton mass. As said before, they are of order  $\mathcal{O}(m_\ell^2/m_b^2)$ . Therefore they are most important for the case  $\ell = \tau$  and, to a lesser extent, for  $\ell = \mu$ . The combined corrections of order  $\mathcal{O}(\Lambda^2/m_b^2, m_\ell^2/m_b^2)$  have been calculated, to all orders in  $m_\ell^2/m_b^2$ , in [91]. The combined effect of these corrections is to lower the total FQD decay rate for  $B \to X_c \tau \bar{\nu}_\tau$  by 6.5%, whereas the neglect of the  $\tau$  mass would have given a decrease of only 3.7%.

On the experimental side, the totally inclusive semileptonic branching ratio for  $\Lambda_c \to e^+ + X$  has been measured by the Mark II collaboration [92] as  $(4.5 \pm 1.7)\%$ . This then leads to the inclusive rate

$$\Gamma^{sl}_{\Lambda_c}(\text{inclusive}) = (22.5 \pm 8.7) \times 10^{10} s^{-1} .$$
 (198)

The corresponding inclusive semileptonic charm meson rates are [26]  $\Gamma_{D^{\pm}}^{sl}$  (inclusive) =  $(16.1 \pm 1.54) \times 10^{10} s^{-1}$  and  $\Gamma_{D^0}^{sl}$  (inclusive) =  $(18.5 \pm 2.9) \times 10^{10} s^{-1}$ .

We mention that the Mark II collaboration [92] has also given results on semileptonic semi-inclusive branching ratios. They find  $BR_{\Lambda_c \to pe^+ + X} = (1.8 \pm 0.9)\%$  including protons from  $\Lambda$  decay, and  $BR_{\Lambda_c \to \Lambda e^+ + X} = (1.2 \pm 0.4)\%$ .

# 5.2 Exclusive Semileptonic Decays

### 5.2.1 Amplitudes, Rates and Angular Decay Distributions

Let us first stake out the spin complexity of the problem that one is concerned with. This entails an enumeration of the number of independent amplitudes in exclusive semileptonic decays and a discussion of how to measure them. To set the scope we remind the reader that

the separate determination of the three respective form factors in semileptonic  $B \rightarrow D^*$  [93–96] and  $D \rightarrow K^*$  [97] transitions through angular measurements has been eminently important for the development of a plausible theory for heavy meson transition form factors [98–104].

Let us begin our discussion by defining a standard set of invariant form factors for the weak current–induced baryonic  $1/2^+ \to 1/2^+$  and  $1/2^+ \to 3/2^+$  transitions. One has

$$\langle \Lambda_s(P_2) | J_{\mu}^{V+A} | \Lambda_c(P_1) \rangle = \bar{u}(P_2) [\gamma_{\mu} (F_1^V + F_1^A \gamma_5) + i \sigma_{\mu\nu} q^{\nu} (F_2^V + F_2^A \gamma_5) + q_{\mu} (F_3^V + F_3^A \gamma_5)] u(P_1)$$
(199)

$$\langle \Omega^{-}(P_{2})|J_{\mu}^{V+A}|\Omega_{c}(P_{1})\rangle = \bar{u}^{\alpha}(P_{2})[g_{\alpha\mu}(G_{1}^{V}+G_{1}^{A}\gamma_{5})+P_{1\alpha}\gamma_{\mu}(G_{2}^{V}+G_{2}^{A}\gamma_{5}) + P_{1\alpha}P_{2\mu}(G_{3}^{V}+G_{3}^{A}\gamma_{5})+P_{1\alpha}q_{\mu}(G_{4}^{V}+G_{4}^{A}\gamma_{5})]\gamma_{5}u(P_{1})$$
(200)

where  $J^V_\mu$  and  $J^A_\mu$  are vector and axial vector currents and  $q_\mu = (P_1 - P_2)_\mu$  is the 4-momentum transfer. We have found it convenient to use particle labels from baryonic  $c \to s$  decays instead of generic names. The form factors  $F^{V,A}_i$  and  $G^{V,A}_i$  are functions of  $q^2$ .

The invariants  $F^V_3, F^A_3, G^V_4$  and  $G^A_4$  multiplying  $q_\mu$  contribute to semileptonic decays at

The invariants  $F_3^V$ ,  $F_3^A$ ,  $G_4^V$  and  $G_4^A$  multiplying  $q_{\mu}$  contribute to semileptonic decays at  $\mathcal{O}(m_{\ell}^2/q^2)$  and are thus difficult to measure. Muon effects have been investigated in the corresponding semileptonic D $\to$ K(K\*) decays and have been found to be  $\leq 5\%$  in the total rate [100]. Muon effects in charm baryon decays are of similar size. The biggest effect occurs for the longitudinal rate, where the muon mass effect amounts to  $\mathcal{O}(10\%)$ , and is largest at small  $q^2$ . This is different in semileptonic  $b \to c$  decays where lepton mass effects can be conveniently probed in the  $\tau$ -channel [105,106]. The branching ratio into the  $\tau$ -modes is typically  $\simeq 20\text{-}30\%$  of the e-mode and now there can be large contributions from the  $q_{\mu}$ -form factor terms. Nevertheless, the invariants  $F_3^{V,A}$  and  $G_4^{V,A}$  multiplying  $q_{\mu}$  are important in nonleptonic decays where they contribute through the so-called factorizing contributions in the nonleptonic  $B_{Q_1} \to B_{Q_2} + M(0^-)$  decays.

Rates and angular decay distributions are given in terms of bilinear forms of the form factors. We first consider the (cascade) decay of an unpolarized charm baryon  $B_c \to B(\to B'M) + l^+ + \nu_l$  where the cascade decay  $B(\to B'M)$  is used as an analyzer of the polarization of the daughter baryon B. For semileptonic  $1/2^+ \to 1/2^+$  transitions the full four-fold decay distribution differential in the momentum transfer squared  $q^2$  and the angles  $\Theta, \chi$  and  $\Theta_B$  shown in Fig.14 reads [107,108]

$$\frac{\mathrm{d}\Gamma(\Lambda_c^+ \to \Lambda(\to p\pi^-) + l^+ + \nu_l)}{\mathrm{d}q^2 \mathrm{d}\cos\Theta \mathrm{d}\chi \mathrm{d}\cos\Theta_{\Lambda}} = B_{\Lambda \to p\pi^-} \frac{1}{2\pi}$$

$$\left[ \frac{3}{8} (1 + \cos^2\Theta) \frac{\mathrm{d}\Gamma_U}{\mathrm{d}q^2} (1 + \alpha_c^U \alpha_{\Lambda} \cos\Theta_{\Lambda}) + \frac{3}{4} \sin^2\Theta \frac{\mathrm{d}\Gamma_L}{\mathrm{d}q^2} (1 + \alpha_c^L \alpha_{\Lambda} \cos\Theta_{\Lambda}) \right.$$

$$- \frac{3}{2\sqrt{2}} \sin(2\Theta) \cos\chi \sin\Theta_{\Lambda} \alpha_{\Lambda} \frac{\mathrm{d}\Gamma_I}{\mathrm{d}q^2} - \frac{3}{4} \cos\Theta \frac{\mathrm{d}\Gamma_P}{\mathrm{d}q^2} (1 + \frac{\mathrm{d}\Gamma_U}{\mathrm{d}\Gamma_P} \alpha_{\Lambda} \cos\Theta_{\Lambda})$$

$$\frac{3}{\sqrt{2}} \sin\Theta \cos\chi \sin\Theta_{\Lambda} \alpha_{\Lambda} \frac{\mathrm{d}\Gamma_A}{\mathrm{d}q^2} \right] \tag{201}$$

where

$$\frac{\mathrm{d}\Gamma_i}{\mathrm{d}q^2} = \frac{1}{2} \frac{G^2}{(2\pi)^3} |V_{cs}|^2 \frac{pq^2}{12M_1^2} H_i \tag{202}$$

and where G is the Fermi coupling constant  $(G = 1.026 \cdot 10^{-5} m_{\rm p}^{-2})$  and p is the momentum of the daughter baryon in the B<sub>c</sub> rest frame,  $p = \sqrt{Q_+ Q_-}/2M_1$  with  $Q_{\pm} = 2(P_1 P_2 \pm M_1 M_2) =$ 

Figure 14: Definition of polar angles  $\theta_{\Lambda}$  and  $\theta$  and azimuthal angle  $\chi$  in the decay  $\Lambda_c^+ \to \Lambda(\to p\pi) + W^+(\to \ell^+\nu_{\ell})$ . For  $b \to c$  decays change the lepton side to  $W^-(\to \ell^-\bar{\nu}_{\ell})$ .

 $(M_1 \pm M_2)^2 - q^2$ . Again we have used particle labels in Equation (201) instead of a generic notation.

The helicity rates (or structure functions)  $H_i$  in Equation (201) are defined as follows

$$H_{U} = |H_{\frac{1}{2},1}|^{2} + |H_{-\frac{1}{2},-1}|^{2}$$

$$H_{L} = |H_{\frac{1}{2},0}|^{2} + |H_{-\frac{1}{2},0}|^{2}$$

$$H_{I} = \frac{1}{2} \operatorname{Re} \left( H_{-\frac{1}{2},0} H_{\frac{1}{2},1}^{*} - H_{\frac{1}{2},0} H_{-\frac{1}{2},-1}^{*} \right)$$

$$H_{P} = |H_{\frac{1}{2},1}|^{2} - |H_{-\frac{1}{2},-1}|^{2}$$

$$H_{A} = \frac{1}{2} \operatorname{Re} \left( H_{-\frac{1}{2},0} H_{\frac{1}{2},1}^{*} + H_{\frac{1}{2},0} H_{-\frac{1}{2},-1}^{*} \right)$$
(203)

where the  $H_{\lambda_2,\lambda_W} = H_{\lambda_2,\lambda_W}^V + H_{\lambda_2,\lambda_W}^A$  are the helicity amplitudes of the current induced transition,  $\lambda_W$  is the helicity of the current ( $\lambda_W = 0$  longitudinal,  $\lambda_W = \pm 1$  transverse) or, equivalently, of the off-shell W-boson and  $\lambda_2$  is the helicity of the daughter baryon. The relation between the set of helicity and invariant form factors is given by

$$\sqrt{q^2}H_{\frac{1}{2},0}^V = \sqrt{Q_-}\left((M_1 + M_2)F_1^V - q^2F_2^V\right) \tag{204}$$

$$H_{\frac{1}{2},1}^{V} = \sqrt{2Q_{-}} \left( -F_{1}^{V} + (M_{1} + M_{2})F_{2}^{V} \right)$$
 (205)

$$\sqrt{q^2}H_{\frac{1}{2},0}^A = \sqrt{Q_+}\left((M_1 - M_2)F_1^A + q^2F_2^A\right) \tag{206}$$

$$H_{\frac{1}{2},1}^{A} = \sqrt{2Q_{+}} \left( -F_{1}^{A} - (M_{1} - M_{2})F_{2}^{A} \right)$$
 (207)

The remaining helicity amplitudes can be obtained with the help of the parity relations

$$H_{-\lambda_2,-\lambda_W}^{V(A)} = +(-)H_{\lambda_2,\lambda_W}^{V(A)}.$$
 (208)

The labeling of the helicity rates  $H_i$  describes the polarization of the off-shell W boson in the decay: U (unpolarized transverse), L (longitudinal), I (transverse-longitudinal interference), P

(parity odd), A (parity asymmetric). For semileptonic decays involving the leptons  $\ell^- + \bar{\nu}_{\ell}$  (as in  $\bar{c} \to \bar{s}$  and  $b \to c$  transitions) the sign in the last two terms of Eq.(201) have to be reversed.

We have also introduced  $\alpha_c^U$  and  $\alpha_c^L$ , the  $q^2$ -dependent transverse and longitudinal asymmetry parameters

$$\alpha_c^U = \frac{|H_{\frac{1}{2},1}|^2 - |H_{-\frac{1}{2},-1}|^2}{|H_{\frac{1}{2},1}|^2 + |H_{-\frac{1}{2},-1}|^2}$$
(209)

$$\alpha_c^L = \frac{|H_{\frac{1}{2},0}|^2 - |H_{-\frac{1}{2},0}|^2}{|H_{\frac{1}{2},0}|^2 + |H_{-\frac{1}{2},0}|^2}.$$
(210)

 $\alpha_{\Lambda}$  is the asymmetry parameter in the parity–violating nonleptonic decay  $\Lambda \to p + \pi^-$  defined in analogy to Eq.(210). Its experimental value is  $\alpha_{\Lambda} = 0.64$  [26]. Triple, double and single decay distributions as well as the rate may be obtained from Eq.(201) by the appropriate integrations. For example, integrating over the azimuthal angle  $\chi$  and the lepton–side polar angle  $\theta$  one obtains

$$\frac{\mathrm{d}\Gamma}{\mathrm{d}q^2\mathrm{d}\cos\Theta_{\Lambda}} \propto 1 + \alpha\alpha_{\Lambda}\cos\Theta_{\Lambda} \tag{211}$$

where the asymmetry parameter  $\alpha$  is defined by

$$\alpha = \frac{|H_{\frac{1}{2},1}|^2 - |H_{-\frac{1}{2},-1}|^2 + |H_{\frac{1}{2},0}|^2 - |H_{-\frac{1}{2},0}|^2}{|H_{\frac{1}{2},1}|^2 + |H_{-\frac{1}{2},-1}|^2 + |H_{\frac{1}{2},0}|^2 + |H_{-\frac{1}{2},0}|^2}.$$
(212)

The asymmetry parameter  $\alpha$  is nothing but the longitudinal ("alignment") polarization of the daughter baryon  $\Lambda$  which is being analyzed by its subsequent decay according to the above polar angle distribution (211). For example the ARGUS [109] and CLEO [110] Collaborations have recently measured the mean of the asymmetry parameter  $\alpha$  in the semileptonic  $\Lambda_c \to \Lambda + \ell^+ + \nu_\ell$  decay using the above polar decay distribution. They found a large negative value of the asymmetry parameter  $\alpha$  in agreement with earlier theoretical predictions. We shall return to this point in Sec.5.2.2.

In Eq.(201) we have assumed that the form factors and helicity amplitudes are real since the physical threshold is at  $q^2 = (M_1 + M_2)^2 > q_{max}^2 = (M_1 - M_2)^2$ . We have thus omitted so-called T-odd contributions in the decay distribution which are proportional to  $\sin \Theta \sin \chi \sin \Theta_{\Lambda}$  and  $\sin(2\Theta) \sin \chi \sin \Theta_{\Lambda}$  [107]. We note in passing that the presence of such contributions could signal possible CP-violations in the decay process [108].

The structure of the decay distribution Eq.(201) is quite similar to the corresponding four-fold decay distribution for the cascade decay  $D \to K^*(\to K\pi) + l^+ + \nu_l$  [100],[102–104] which has been proven so useful in disentangling the form factor structure in the semileptonic  $D \to K^*$  decays [67,97]. The angular distribution Eq.(201) defines a set of eight observables which are bilinears in the four independent  $q^2$ -dependent real form factors. A measurement of these eight observables would considerably overdetermine the form factors. Note though that the complexity of the problem is reduced close to the phase space boundaries. At zero recoil  $q^2 \approx q_{max}^2$  only the s-wave contribution remains, and at  $q^2 \approx 0$  only the longitudinal contribution survives. The relevant dynamical information may be extracted by either one of the following methods: (i) moment analysis (ii) analysis of suitably defined asymmetry ratios as in [111] or (iii) angular fits to the data as in [97] depending on the quantity and quality of the data. All of this carries over to the  $b \to c$  sector with the requisite sign changes as mentioned after Eq.(208).

An additional set of polarization observables can be defined for the decay of polarized charm and bottom baryons. For example, bottom and charm quarks produced on the  $\mathbb{Z}^0$  resonance are

Figure 15: Definition of polar angles  $\theta_{\Lambda}$  and  $\theta_{p}$  and azimuthal angle  $\chi$  in the decay of a polarized  $\Lambda_{c}^{+} \to \Lambda(\to \pi^{-}) + X$ . The left plane is determined by polarization vector  $\vec{P}_{\Lambda_{c}}$  of the  $\Lambda_{c}$ . The unobserved state X stands for  $W_{off-shell}$  in semileptonic decays and for a meson in nonleptonic decays.

94% and 67% negatively polarized. It is quite likely that some of this polarization is retained when the bottom and charm quarks fragment into bottom and charm baryons. This will be discussed in more detail in Sec.5.3.. Also, hadronically produced  $\Lambda$ 's have been observed to be polarized where the polarization necessarily has to be transverse to the production plane because of parity invariance in the production process. It may well be that hadronically produced  $\Lambda_c^+$ 's show a similar polarization effect [112,113]. Also, charm baryons from weak decays of bottom baryons are expected to be polarized.

For polarized  $\Lambda_c$ -decays one orients the decay products and the subsequent decay of the daughter baryon relative to the  $\Lambda_c$  polarization as drawn in Fig.15 where the orientation angles  $\Theta_p$ ,  $\Theta_{\Lambda}$  and  $\chi$  are defined. For the corresponding four-fold angular decay distribution one finds

$$\frac{\mathrm{d}\Gamma(\Lambda_c^{\uparrow} \to \Lambda(\to p\pi^-) + l^+ + \nu_l)}{\mathrm{d}q^2 \mathrm{d}\cos\Theta_p \mathrm{d}\chi \mathrm{d}\cos\Theta_{\Lambda}} = \frac{1}{8\pi} B_{\Lambda \to p\pi^-}$$

$$\left[ \frac{\mathrm{d}\Gamma_{U+L}}{\mathrm{d}q^2} + \alpha_{\Lambda}\cos\Theta_{\Lambda} \left( \alpha_c^U \frac{\mathrm{d}\Gamma_U}{\mathrm{d}q^2} + \alpha_c^L \frac{\mathrm{d}\Gamma_L}{\mathrm{d}q^2} \right) \right.$$

$$-P_c \cos\Theta_p \left( \alpha_c^U \frac{\mathrm{d}\Gamma_U}{\mathrm{d}q^2} - \alpha_c^L \frac{\mathrm{d}\Gamma_L}{\mathrm{d}q^2} \right) + P_c \alpha_{\Lambda}\cos\Theta_p \cos\Theta_{\Lambda} \left( -\frac{\mathrm{d}\Gamma_U}{\mathrm{d}q^2} + \frac{\mathrm{d}\Gamma_L}{\mathrm{d}q^2} \right)$$

$$-P_c \alpha_{\Lambda}\sin\Theta_p \sin\Theta_{\Lambda}\cos\chi \frac{\mathrm{d}\Gamma_{LI}}{\mathrm{d}q^2} \right] \tag{213}$$

where  $P_c$  is the degree of polarization of the  $\Lambda_c^+$ . The longitudinal interference rate is  $d\Gamma_{LI}/dq^2 = 2\text{Re}\left(H_{\frac{1}{2},0}H_{-\frac{1}{2},0}^*\right)$ . A corresponding four-fold angular decay distribution formula can be derived for the lepton-side [108].

Measurements of the angular decay distribution relative to the initial spin polarization vector would allow one to either measure the degree and sign of the polarization of the  $\Lambda_c$ 

Figure 16: Partial wave analysis of quasi-two body decay  $1/2^+ \rightarrow 1/2^+ + W_{off-shell}$ .

if its decay structure is known, or, vice versa, if  $P_c$  were known, further constrain the decay amplitudes of the  $\Lambda_c$ . The information contained in the "decay"  $W^+ \to \ell^+ + \nu_\ell$  has not been used in Equation (213), i.e. the angular dependence on the orientation angles  $(\Theta, \chi')$  of the  $W^+ \to \ell^+ + \nu_\ell$  decay have been integrated out. As the lepton–side angular distribution goes unanalyzed the distribution (213) holds for both  $\Lambda_c \to \Lambda$  and  $\Lambda_b \to \Lambda_c$  transitions without any sign change. If this angular dependence is kept one would have a six–fold differential distribution. Corresponding decay distributions for semileptonic  $1/2^+ \to 3/2^+$  transitions (polarized and unpolarized) can be found in [108]. Let us mention that the decay distributions Equations (201) and (213) can also be derived using a frame independent representation in terms of spin and momenta correlations [114].

#### **5.2.2** Model Results $c \rightarrow s$

The accessible  $q^2$ -range in semileptonic charm baryon decays is not small  $(m_\ell^2 \le q^2 \le (M_1 - M_2)^2)$ . One thus has a large experimental leverage to study the  $q^2$ -dependence of the form factors. Also, the full spin dependent form factor structure can be investigated as the C.M. momentum  $p = |\vec{p}|$  becomes large enough when  $q^2$  moves away from the zero recoil point (or pseudo-threshold point)  $q^2 = (M_1 - M_2)^2$  to populate all partial waves in the decay  $B_1 \to B_2 + W_{off-shell}(q^2)$ .

In fact the momentum dependence of the semileptonic transitions close to the zero recoil edge of phase space can be conveniently classified by doing a partial wave analysis of the two-body decay of  $1/2^+ \to 1/2^+ + W$  as drawn in Fig.16. Since the W is off-shell it has four degrees of freedom for each of its vector and axial components. The  $J^P$  content of the off-shell W are  $J^P = (1_V^-, 1_A^+)$  for the spin 1 pieces and  $J^P = (0_V^+, 0_A^-)$  for the spin 0 piece. We remind the reader that the spin 0 pieces are not active in the decay in the limit of zero lepton mass.

One can then determine the partial wave content of the decay  $1/2^+ \to 1/2^+ + W$ . For the spin 1 part one has (in brackets the final state spin sum  $S = S_1 + S_2$ )

whereas for the spin 0 pieces one has

$$\begin{array}{lll} \frac{1}{2}^+ \rightarrow \frac{1}{2}^+ + 0_V^+ : & \text{s-wave } (S=1/2) & \text{"allowed Fermi transition"} \end{array} \tag{215} \\ \frac{1}{2}^+ \rightarrow \frac{1}{2}^+ + 0_A^- : & \text{p-wave } (S=1/2) & \text{"first forbidden Gamow-Teller transition"} \end{array}$$

Let us limit our discussion to the case  $m_{\ell} = 0$  which is a very good approximation for e and a good approximation for  $\mu$  for  $c \to s$  decays. There are then two vector and axial amplitudes each for  $1/2^+ \to 1/2^+ + W(1_V^-)$  and  $1/2^+ \to 1/2^+ + W(1_A^-)$  in agreement with the number of covariant form factor in Eq.(199) when the  $q_{\mu}$  form factors are disregarded. As  $p \to 0$  and the phase space closes<sup>5</sup> only the axial vector s-wave contribution in  $1/2^+ \to 1/2^+ + W(1_A^+)$  survives. We want to call to mind that in nuclear physics parlance the vector and axial vector transitions are referred to as Fermi and Gamow-Teller transitions, respectively. They are further classified according to their partial wave threshold behaviour by "allowed", "first forbidden", etc. The nuclear physics classification has been included in Eq. (214, 215). In contrast to nuclear physics transitions (where the Q-values of the transitions are comparable to the electron mass and the spin 0 components do contribute) the Q-values of the  $c \to s$  transitions are so big that only the spin 1 pieces are active, to a good approximation. We shall return to the partial wave classification when discussing the measurement of the KM matrix element  $V_{bc}$  in the exclusive semileptonic decay  $\Lambda_b \to \Lambda_c + \ell^- + \bar{\nu}_\ell$  in Sec.5.2.3. Returning to the  $c \to s$  decays one can certainly state that for large enough momenta p all partial waves in the decay  $B_1 \to B_2 + W_{off-shell}(q^2)$  come into play. This is different in ordinary hyperon decays, where the accessible  $q^2$ -range is small and only the low partial waves contribute to any significant degree. How to actually extract the various form factors through polarization type measurements has been dealt with before in Section 5.2.1.

To begin with we discuss rates. There have been a number of theoretical attempts to model the form factors in the semileptonic  $1/2 \rightarrow 1/2^+$  and  $1/2^+ \rightarrow 3/2^+$  transitions employing flavour symmetry and/or quark models. In Table 8 we have listed the rate predictions of various models for the semileptonic decay  $\Lambda_c^+ \to \Lambda + \ell^+ + \nu_\ell$ ,  $\Xi_c^+ \to \Xi^0 + \ell^+ + \nu_\ell$  and the  $1/2^+ \to 3/2^+$  decay  $\Omega_c \to \Omega^- + \ell^+ + \nu_\ell$   $(m_\ell = 0)$ . The first column contains early predictions which exploited SU(4) flavour symmetry at  $q^2 = 0$  to relate  $\Delta C = 1$  to the known  $\Delta C = 0$ amplitudes [115]. The results were then continued to  $q^2 = 0$  by using suitable form factors. The predictions of [116] are similar. The rates come out too large due to the use of SU(4) at  $q^2 = 0$ . [117] and [118] have shown that there are large mass breaking corrections to the SU(4) limit at  $q^2 = 0$  which brings the rates down as column 2 in Table 8 shows. Flavour symmetry should rather be applied at  $q_{max}^2$ . Nonrelativistic quark model results calculated close to  $q_{max}^2$  and then continued to  $q^2 \neq q_{max}^2$  via form factors were presented in [119,120]. Explicit quark model calculations as the ones in [119,120] tends to show approximate unit overlap at zero recoil, regardless of the masses of the quarks involved in the transition. Thus they tend to mimic the HQET zero recoil normalization, even for  $c \to s$  decays. The model of [121] uses such a HQET zero recoil normalization and dipole form factors to continue to  $q^2 \neq q_{max}^2$ . In order to be able to compare predictions we have taken the liberty to rescale the results of [119] by taking away their assumed large QCD correction which must be considered to be unrealistically large. The rate values for  $\Lambda_c^+ \to \Lambda$  then scatter around  $20 \times 10^{10} s^{-1}$  except for the rate prediction of Singleton [120]. These rates would imply a saturation of the total semileptonic inclusive rate

<sup>&</sup>lt;sup>5</sup>Readers old enough will remember that the zero recoil point  $q_{max}^2 = (M_1 - M_2)^2$  used to be also called the pseudo-threshold. "Pseudo" because phase space closes when the zero recoil point is approached in contrast to the normal threshold where phase space opens.

Table 8:	Exclusive	semileptonic	decay	rates in	n units	of	$10^{10}$	$s^{-1}$	$^{1}.$
----------	-----------	--------------	-------	----------	---------	----	-----------	----------	---------

	Buras	Gavela	PHGA	PHGA	Singleton	HK
	[115]	[117]	NRQM [119]	MBM [119]	[120]	[121]
$\Lambda_c^+ \to \Lambda$	60(20)	15(5)	17(5.6)	13(4.3)	10	22(7.3)
$\Xi_c^+\to\Xi^0$	235(118)	28(14)	28(14)	22(11)	17	33(16.5)
$\Omega_c^0 \to \Omega^-$	280	49	=	_	_	48

by the exclusive mode. The semi–inclusive rates quoted in Sec.5.1, however, preclude such a possibility. A more precise measurement of the experimental semileptonic  $\Lambda_c^+ \to \Lambda$  (exclusive or inclusive) rate would help to pin down this issue.

The calculation of Singleton [120] (see also [122]) differs from the other calculations in one important respect in that he has taken a spin–flavour suppression factor in the  $\Lambda_c \to \Lambda$  and  $\Xi_c \to \Xi$  transitions into account which other authors have not included. In order to understand the spin–flavour suppression factor present in the calculation of [120] consider the amplitude  $c_s$  of the spin 0 light diquark configuration in the various charm and strange baryons. Whereas the spin 0 light diquark configuration has the amplitude  $c_s = 1$  in  $\Lambda_c$  and  $\Xi_c$  it is only one of the many possible diquark configurations in the light baryons  $\Lambda$  and  $\Xi$ . In order to determine the amplitude of the spin 0 diquark configuration in the  $\Lambda$  and  $\Xi$  state one appeals to SU(6) for guidance. Consider the spin–flavour wave functions of the  $\Lambda_c$ ,  $\Xi_c$ ,  $\Lambda$  and  $\Xi$ . They are given by (see e.g. [123])

$$\Lambda_c^{\uparrow} = c^{\uparrow}[ud]_0, \qquad \Xi_c^{+\uparrow} = c^{\uparrow}[us]_0 \tag{216}$$

$$\Lambda^{\uparrow} = \frac{1}{\sqrt{3}} s^{\uparrow} [ud]_{0} + \frac{1}{2\sqrt{3}} d^{\uparrow} [us]_{0} + \frac{1}{2\sqrt{3}} u^{\uparrow} [ds]_{0} - \frac{1}{2\sqrt{3}} d^{\uparrow} \{us\}_{0}$$

$$+ \frac{1}{2\sqrt{3}}u^{\uparrow}\{ds\}_{0} + \frac{1}{\sqrt{6}}d^{\downarrow}\{us\}_{+1} - \frac{1}{\sqrt{6}}u^{\downarrow}\{ds\}_{+1}$$
 (217)

$$\Xi^{0\uparrow} = \frac{1}{\sqrt{2}} s^{\uparrow} [us]_0 - \frac{1}{\sqrt{18}} s^{\uparrow} \{us\}_0 + \frac{1}{\sqrt{9}} s^{\downarrow} \{us\}_{+1} + \frac{1}{\sqrt{9}} u^{\uparrow} \{ss\}_0 - \sqrt{\frac{2}{9}} u^{\downarrow} \{ss\}_{+1}$$
 (218)

where the suffix label denotes the m-quantum number of the diquark states. The  $[ud]_0$  is the totally symmetric spin 0-isospin 0 combination  $[ud]_0 = \frac{1}{2}(u^{\dagger}d^{\dagger} - u^{\dagger}d^{\dagger} + d^{\dagger}u^{\dagger} - d^{\dagger}u^{\dagger})$  and the  $\{us\}_{0,+1}$  are the corresponding totally symmetric spin 1-flavour symmetric combinations with m=0,+1. The spin-flavour wave functions can be checked to be normalized to 1. The transitions  $\Lambda_c \to \Lambda$  and  $\Xi_c \to \Xi$  can be seen to acquire factors of  $\sqrt{\frac{1}{3}}$  and  $\sqrt{\frac{1}{2}}$  in amplitude, respectively, from the  $[ud]_0$  and  $[us]_0$  components in the  $\Lambda$  and  $\Xi^0$  wave functions. The authors of [117,118,119,121] instead used SU(8)-type wave functions for the charm baryons  $\Lambda_c$  and  $\Xi_c$  treating all quarks democratically, i.e. they used wave functions for  $\Lambda_c$  and  $\Xi_c$  that are identical to the above  $\Lambda$  and  $\Xi$  wave functions except for replacing s by c. In such an approach there are no a priori spin-flavour suppression factors. In order to be able to compare the rates we have accordingly multiplied the high rates by factors of 1/3 and 1/2 and have included the lowered rates in Table 8. One can only hope for more accurate measurements on exclusive semileptonic charm baryon rates in the near future to be able to resolve this issue. No such adjustment is required for the transition  $\Omega_c^0 \to \Omega^-$ . The semileptonic rates for  $\Omega_c^0 \to \Omega^- + \ell^+ + \nu_\ell$  are predicted to be quite large [121]. This is basically because there are several possibilities for

the initial c quark to make a transition to the final s quark, regardless of the model.

Next we turn to the polarization type observables measurable through the joint angular decay distributions Eqs.(201) and (213). First observe that the angular decay distributions become quite uninteresting close to zero recoil point  $q^2 \to q_{max}^2 = (M_1 - M_2)^2$  where the axial vector s-wave contribution dominates  $(H_{\lambda_2,\lambda_W}^V \to 0, H_{\frac{1}{2},1}^A \to -\sqrt{2}H_{\frac{1}{2},0}^A)$ . For example, the asymmetry Eq.(211) (or the polarization of the  $\Lambda$ ) vanishes at the zero recoil point and the corresponding polar angle distribution becomes flat. At the other end of phase space as  $q^2 \to 0$  (or more exactly  $q^2 \to m_\ell^2$ ) the longitudinal helicity amplitudes dominate as Eqs.(204–207) show. There exists a very interesting Heavy Quark Symmetry prediction for the structure of heavy to light  $\Lambda_c \to \Lambda_s$  transitions at  $q^2 = 0$ . Take the relevant heavy to light form factor structure from Eq.(122) and substitute it into Eq.(212). At  $q^2 = 0$  one finds  $H_{\frac{1}{2},0} = 0$ , i.e. the daughter baryon  $\Lambda$  is predicted to emerge 100% (negatively) polarized from the decay at  $q^2 = 0$ . For the mean value of the polarization averaged over  $q^2$  Ref.[107] quote a theoretical range -0.52 to -0.94 (depending on the assumed form factor ratio),  $\langle \alpha \rangle = -0.82$  being a preferred value.

There have been two recent measurements of the mean polarization of the  $\Lambda$  in semileptonic  $\Lambda_c \to \Lambda$  decays by ARGUS [109] and CLEO [110] who quote

$$\langle \alpha \rangle = \begin{cases} -0.91 \pm 0.49 & \text{ARGUS [109]} \\ -0.89^{+0.17+0.09}_{-0.11-0.05} & \text{CLEO [110]} \end{cases}$$
 (219)

where we refer to the original papers for a discussion of the phase space region in which the mean is taken. Both collaborations conclude that their results imply that  $\alpha$  is close to -1 at  $q^2 = 0$  in agreement with the Heavy Quark Symmetry prediction.

One can check that the 100% polarization prediction of Heavy Quark Symmetry remains intact even if one includes  $1/m_c$  and naively applied  $1/m_s$  corrections according to Eq.(54–59). This may be taken as an indication of the stability of the HQET result. A semiphenomenological analysis that includes terms of order  $1/m_c$  in the HQET expansion but still treats the  $\Lambda$  as light leads to a very small departure from -1 at  $q^2 = 0$  [124].

It will not be an easy task experimentally to completely disentangle the form factor structure of semileptonic baryonic  $c \to s$  transitions through the angular correlation measurements in Eq.(201) and (213). However, one can hope for more and better data in the future. The two recent measurements [109] and [110] on the polarization of the  $\Lambda$  in the  $\Lambda_c \to \Lambda + \ell^+ + \nu_\ell$  and their interpretation in terms of HQET foreshadow things to come.

#### 5.2.3 Model Results $b \rightarrow c$

For the heavy–to–heavy  $b \to c$  transitions it is more convenient to work entirely in terms of velocity variables. Correspondingly we define a new set of form–factors in terms of velocity covariants, which we can choose to be the six form–factors introduced in (52–53). Note that now all six "velocity" form–factors contribute to the transition in the zero lepton mass case, i.e. one has not separated out the two scalar form–factors (multiplying  $q_{\mu}$ ) as in the representation (199,200) used before. Let us first state the linear relation between the "velocity" form–factors defined in (52–53) and the helicity amplitudes that enter into the formulas for physical observables. One has

$$\sqrt{q^2} H_{\frac{1}{2},0}^{V,A} = \sqrt{2M_1 M_2(\omega \mp 1)} \left( (M_1 \pm M_2) f_1^{V,A} \pm M_2(\omega \pm 1) f_2^{V,A} \pm M_1(\omega \pm 1) f_3^{V,A} \right) 
H_{\frac{1}{2},1}^{V,A} = -2\sqrt{M_1 M_2(\omega \mp 1)} f_1^{V,A}$$
(220)

where  $H_{\lambda_2,\lambda_W}^{V,A}$  are the helicity amplitudes for the vector (V) and axial vector (A) current induced  $1/2^+ \to 1/2^+ + W_{off-shell}^-$  transitions. The upper and lower signs in (220) stand for the vector (V) current and axial vector (A) current contributions, respectively, where the total helicity amplitude is given by

$$H_{\lambda_2,\lambda_W} = H^V_{\lambda_2,\lambda_W} + H^A_{\lambda_2,\lambda_W} \tag{221}$$

The remaining helicity amplitudes are related to the above two helicity amplitudes by parity as given in Eq.(208). For the differential decay rate one then obtains

$$\frac{\mathrm{d}\Gamma}{\mathrm{d}\omega} = \frac{G_F^2}{(2\pi)^3} |V_{bc}|^2 \frac{q^2 p M_2}{12M_1} \left( |H_{\frac{1}{2},1}|^2 + |H_{-\frac{1}{2},-1}|^2 + |H_{\frac{1}{2},0}|^2 + |H_{-\frac{1}{2},0}|^2 \right) \tag{222}$$

where p is the CM momentum of the daughter baryon  $\Lambda_c$   $(p = M_2 \sqrt{(\omega + 1)(\omega - 1)})$ .

The structure of the rate formula becomes very simple at the zero recoil point  $\omega=1$ . Using again  $H^V_{\lambda_2,\lambda_W}\to 0$  and  $H^A_{\frac{1}{2},1}\to -\sqrt{2}H^A_{\frac{1}{2},0}$  one finds that

$$\frac{\mathrm{d}\Gamma}{\mathrm{d}\omega} = \frac{G_F^2}{(2\pi)^3} 2|V_{bc}|^2 M_2^3 (M_1 - M_2)^2 \sqrt{\omega^2 - 1} |f_1^A(1)|^2 + \cdots$$
 (223)

at  $\omega = 1$ . At zero recoil only the "allowed Gamow–Teller transition"  $f_1^A$  survives (see Eq.(214)). Since HQET predicts that  $f_1^A(1) = 1$  up to order  $\mathcal{O}(1/m_Q)$  (see Eq.(61)), this relation would allow one to extract the value of  $|V_{bc}|$  up to order  $\mathcal{O}(1/m_Q)$  accuracy from e.g. semileptonic  $\Lambda_b \to \Lambda_c$  transitions if the data can be reliably continued to the zero recoil point. In doing so one has to also account for the small change in normalization resulting from vertex renormalization as discussed in Sec.3. This and the corrections of order  $\mathcal{O}(1/m_Q^2)$  to (223) have been carefully discussed in [90].

It is interesting to keep in the rate formula (222) not only the terms corresponding to  $\omega = 1$  (as has been done in deriving (223)), but also the contributions linear in  $(\omega - 1)$  including also p—wave contributions (see Eq.(214)). Using the predictions of HQET (54–59) for the  $\mathcal{O}(1/m_Q)$  structure of the  $\Lambda_b \to \Lambda_c$  transition one obtains

$$\frac{\mathrm{d}\Gamma}{\mathrm{d}\omega} = \frac{G_F^2}{(2\pi)^3} 2|V_{bc}|^2 M_2^3 (M_1 - M_2)^2 \sqrt{\omega^2 - 1} 
\left(1 + (\omega - 1) \left[ -2\rho^2 + 1 - \frac{2}{3} \frac{M_1 M_2}{(M_1 - M_2)^2} + \bar{\Lambda} \frac{M_1 + M_2}{2M_1 M_2} \right] \right) + \cdots$$
(224)

where the ellipsis stand for  $\mathcal{O}((\omega-1)^2)$  contribution. Here  $\rho$  is the so-called "charge radius" of the  $f_1^A$  form-factor defined by

$$f_1^A(\omega) = f_1^A(1) - \rho^2(\omega - 1) + \mathcal{O}((\omega - 1)^2). \tag{225}$$

Eq.(224) is useful when one wants to extrapolate experimental  $\Lambda_b \to \Lambda_c$  data into the zero recoil point for a given model value of the charge radius  $\rho^2$ .

As concerns the joint angular decay distribution for unpolarized  $\Lambda_b \to \Lambda_c$  transitions it can be taken from Eq.(201) with the requisite sign changes when going from a final state  $\ell^+ + \nu_\ell$  to  $\ell^- + \bar{\nu}_\ell$ , as remarked on already there. The angular decay distribution for polarized  $\Lambda_b$  decay is identical to Eq.(213). Corresponding formulas including lepton mass effects relevant for semileptonic decays involving the  $\tau$ -lepton can be found in [108,125]. Rate formulas and

Table 9: Rate for semileptonic decay  $\Lambda_b \to \Lambda_c + e^- + \bar{\nu}_e$  and polarization  $\langle \alpha \rangle$  for daughter baryon  $\Lambda_c$  in the models [126,120], dipole form factor model and in the free quark decay model with  $m_b = m_{\Lambda_b} = 5.64$  GeV and  $m_c = m_{\Lambda_c} = 2.285$  GeV. We have used  $|V_{bc}| = 0.044$ .

Decay: $\Lambda_b \to \Lambda_c + e^- + \bar{\nu}_e$	$\Gamma [10^{10} \text{ s}^{-1}]$	$\langle \alpha \rangle$
Infinite momentum frame [126]		
$\mathcal{O}(1)$	3.70	-0.71
$\mathcal{O}(1) + \mathcal{O}(1/m_Q)$	4.57	-0.77
Dipole form factor	5.14	-0.72
Quark model [120]	3.48	-0.71
Free quark decay	11.73	-0.81

decay distributions for  $1/2^+ \to 3/2^+$  transitions relevant for the decay  $\Omega_b \to \Omega_c^* + \ell^- + \bar{\nu}_\ell$  have been worked out in [67,108].

There have been a number of attempts to calculate the decay properties of the semileptonic decays  $\Lambda_b \to \Lambda_c + \ell^- + \bar{\nu}_\ell$ ,  $\Xi_b \to \Xi_c + \ell^- + \bar{\nu}_\ell$  and  $\Omega_b \to \Omega_c + \ell^- + \bar{\nu}_\ell$  using a variety of model assumptions and elements of HQET as a guiding principle. We shall not attempt to provide an exhaustive discussion of all the model calculations, in particular since there is no data to compare with yet. Instead, we list the results of a few representative model calculations for  $\Lambda_b \to \Lambda_c + \ell^- + \bar{\nu}_\ell$  (in the zero lepton mass case) in Table 9.

The model of [126] uses infinite momentum frame wave functions and determines the transition form factors at  $q^2 = 0$  by making use of the  $\mathcal{O}(1)$  and  $\mathcal{O}(1/m_O)$  structure of HQET. The form factors are then continued to the whole  $q^2$ -region by using the HQET scaling properties of the form factors. The model of [127] is similar. For comparison we list the results of a very simple dipole form factor ansatz described after Eq. (228). The model of Singleton uses a constituent quark model approach with a harmonic oscillator potential [120]. The transition form factors are evaluated in the  $\Lambda_b$  rest frame. For comparison we also give the results of free quark decay where we have taken  $m_b = m_{\Lambda_b} = 5.64 \text{ GeV}$  and  $m_c = m_{\Lambda_c} = 2.285 \text{ GeV}$  in order to get the kinematics right. The free quark decay result corresponds to taking structureless form factors in the dipole model or in the  $\mathcal{O}(1)$  HQET calculation and shows the influence of the form factor effect on the rate and the polarization. If one takes  $m_b = 4.73$  GeV and  $m_c = 1.55 \text{ GeV}$  one obtains a rate of  $7.52 \times 10^{10} \text{ s}^{-1}$  instead. Judging from the numbers in Table 9 the exclusive semileptonic decay rate  $\Lambda_b \to \Lambda_c + \ell^- + \bar{\nu}_\ell$  would be predicted to amount to about 37%-73% of the total inclusive semileptonic rate if one compares to the above two parton model rates. The difference in rate between the form factor models and the "structureless" rate  $\Gamma_{tot} \simeq (7.52 - 11.73) \times 10^{10} \text{ s}^{-1}$  would have to be filled in by the contribution of higher  $\Lambda_c$ resonances and continuum states.

 $\mathcal{O}(1/m_Q)$  effects in the IMF model [126] are small and tend to increase the rates and the value of the polarization. The value of the polarization of the daughter baryon  $\Lambda_c$  does not appear to be very model dependent and is predicted to lie in the range -0.70 to -0.80, close to the polarization of the charm quark in the free quark decay. We shall return to the subject of the  $\Lambda_c$  polarization in semileptonic  $\Lambda_b$  decays in Sec.5.3 where we discuss attempts to determine

the chirality of  $b \to c$  transitions using polarized  $\Lambda_b$  decays.

To conclude this section we briefly discuss the  $\Sigma$ -type  $b \to c$  transitions  $\Omega_b^- \to \Omega_c^0$  and  $\Omega_b^- \to \Omega_c^{*0}$ . The leading order HQET structure of these decays can easily be worked out from the spinor expression Eq.(120). One obtains

$$\Omega_{b}^{-}(1/2^{+}) \to \Omega_{c}^{0}(1/2^{+}) : 
\langle \Omega_{c}(v_{2})|J_{\lambda}^{V+A}|\Omega_{b}(v_{1})\rangle = -\frac{1}{3}\bar{u}_{2}\left[F_{L}\gamma_{\lambda}(1-\gamma_{5}) - \frac{2}{\omega+1}(F_{L}+F_{T})(v_{1_{\lambda}}+v_{2_{\lambda}}) + \frac{2}{\omega-1}(F_{L}-F_{T})(v_{1_{\lambda}}-v_{2_{\lambda}})\gamma_{5}\right]u_{1}$$

$$\Omega_{b}^{-}(1/2^{+}) \to \Omega_{c}^{*0}(3/2^{+}) :$$
(226)

$$\langle \Omega_c^{*0}(v_2) | J_{\lambda}^{V+A} | \Omega_b(v_1) \rangle = \frac{1}{\sqrt{3}} \bar{u}_2^{\nu} \left[ 2F_T g_{\nu\lambda} (1 + \gamma_5) + \frac{1}{\omega + 1} (F_L + F_T) v_{1_{\nu}} \gamma_{\lambda} \gamma_5 - \frac{1}{\omega - 1} (F_L - F_T) v_{1_{\nu}} \gamma_{\lambda} + \frac{2}{\omega^2 - 1} (F_L - \omega F_T) v_{1_{\nu}} v_{2_{\lambda}} (1 + \gamma_5) \right] u_1,$$
(227)

where  $F_L(\omega) = g_1^{(0)}(\omega)$  and  $F_T(\omega) = \omega g_1^{(0)}(\omega) - (\omega^2 - 1)g_2^{(0)}(\omega)$  describe the longitudinal and transverse spin 1 diquark transitions. As remarked on earlier  $F_L$  and  $F_T$  diagonalize the transition rates. We have dropped any reference to the  $\omega$ -dependence in the form-factors in Eq.(226). In the heavy quark limit there are thus two universal form factors  $F_L$  and  $F_T$  compared to the many independent factors in the general covariant expansion (199,200) to which they can be related. The two form factors are normalized to one at zero recoil  $q^2 = q_{max}^2 = (M_1 - M_2)^2$  or  $\omega = 1$ , that is  $F_L(\omega = 1) = F_T(\omega = 1) = 1$ . The  $1/m_Q$  corrections to the limiting structure described by Eqs.(226) and (227) have been worked out in [49]. At  $\mathcal{O}(1/m_Q)$  there are altogether seven universal form factors compared to the two leading order form factors  $F_L$  and  $F_T$ . According to Luke's theorem [46,42] one retains the zero recoil normalization condition at  $\mathcal{O}(1/m_Q)$ .

In order to perform a quick appraisal of the structure of the  $\Sigma$ -type transitions and their rates we turn to the constituent quark model approximation discussed in Sec.4.3. The longitudinal and transverse form factors  $F_L$  and  $F_T$  can be seen to be related to the residual form factor  $f(\omega)$  by

$$F_L(\omega) = F_T(\omega) = \frac{\omega + 1}{2} f(\omega). \tag{228}$$

For the residual form factor we make a dipole ansatz, i.e. we write

$$f(\omega) = \left(1 + \frac{2M_1 M_2 (\omega - 1)}{m_{FF}^2 - (M_1 - M_2)^2}\right)^{-2}$$
 (229)

where  $f(\omega)$  is evidently normalized at  $\omega = 1$ . By writing this formula in terms of the momentum transfer variable  $q^2$  one recovers the familiar dipole representation  $F^{dipole}(q^2) = N(q^2)(1 - q^2/m_{FF}^2)^{-2}$  where  $N(q^2)$  normalizes the dipole form factor to one at the zero recoil point  $q^2 = (M_1 - M_2)^2$ . As pole masses we take  $m_{FF} = 6.34$  GeV and 6.73 GeV for the vector and axial vector form factors, respectively. These pole masses correspond to the expected masses of the

 $(b\bar{c})$  vector and axial vector mesons. Using  $|V_{bc}|=0.044$  one obtains the following rate values

$$\begin{array}{lll}
\Lambda_b^0 \to \Lambda_c^- & : & (5.14; 1.54) \times 10^{10} \mathrm{s}^{-1} \\
\Xi_b^0 \to \Xi_c^+ & : & (5.21; 1.55) \times 10^{10} \mathrm{s}^{-1} \\
\Omega_b^- \to \Omega_c^0 & : & (1.52; 0.52) \times 10^{10} \mathrm{s}^{-1} \\
\Omega_b^- \to \Omega_c^{*0} & : & (3.41; 0.99) \times 10^{10} \mathrm{s}^{-1}
\end{array} \tag{230}$$

In Eq.(230) we also list predictions for the  $\Lambda$ -type transitions in the same constituent approximation. We have also included the corresponding rate predictions for the  $\tau$ -mode which can be seen to be down by a factor of approximately three. Similar results have been obtained in [120]. The rate predictions of the QCM model are higher [66] due to the fact that the QCM form factors are much harder than our dipole form factors. As argued in Sec.4.3 the high rate predictions of [66] for the  $\Sigma$ -type transitions cannot be trusted since the QCD form factors violate one of the bounds due to Bjorken.

#### 5.3 Polarization effects

According to the Standard Model, b quarks from the  $Z^0$  resonance  $e^+e^- \to Z^0 \to b\bar{b}$  have almost complete longitudinal polarization, given by

$$P_L^b = \frac{(8x_W^2 - 4x_W + 1)2v_b a_b \beta(1 + \cos^2 \Theta) + 2(4x_W - 1)(v_b^2 + \beta a_b^2)\cos\Theta}{(8x_W^2 - 4x_W + 1)((v_b^2 + \beta^2 a_b^2)(1 + \cos^2 \Theta) + v_b^2(1 - \beta^2)\sin^2 \Theta) + 4(4x_W - 1)v_b a_b \beta\cos\Theta}$$
(231)

where  $v_b = -1 + \frac{4}{3}x_W$ ,  $a_b = 1$ ,  $x_W = \sin^2\Theta_W$ ,  $\beta^2 = 1 - 4m_b^2/m_Z^2$  and  $\Theta$  is the CM scattering angle relative to  $e^-$ . For  $x_W = 0.23$  this gives a mean value  $\langle P_L^b \rangle = -0.94$  with very little angular dependence. A small transverse polarization of order 0.02 is predicted in the scattering plane; there is no polarization normal to the plane if we neglect  $\gamma - Z$  interference and loop corrections. Noteworthy is the absence of a longitudinal component proportional to  $\sin^2 \Theta$  in the numerator of (231) which comes about because there is no axial vector induced amplitude into the positive helicity b (or  $\bar{b}$ ) to lowest order in QCD. The lowest order result for  $\langle P_L^b \rangle$  is not changed by soft or hard gluon emission, or by loop effects, to any order in  $\alpha_s$  if (and only if!) the b quark can be treated as massless. However, while doing the  $\mathcal{O}(\alpha_s)$  radiative corrections to  $\langle P_L^b \rangle$  [128], it was noticed that one cannot naively set the quark mass to zero ab initio when doing radiative corrections. There is a spin flip contribution proportional to  $m_b^2$  which survives the limit  $m_b \to 0$  since it gets promoted to a constant term by a would-be collinear singularity  $\propto m_b^{-2}$ . As a result  $\langle P_L^b \rangle$  is corrected at  $\mathcal{O}(\alpha_s)$  [128] even for  $m_b/m_{Z^0} \to 0$ . We mention that the orientation dependent  $P_L^b(\cos\Theta)$  will be changed by hard gluon emission regardless of the above spin flip contribution. For charm the Standard Model predicts a somewhat smaller value  $\langle P_L^c \rangle = -0.67$ .

The question is whether this big polarization can be exploited and whether b quark polarization can survive hadronization to give bottom hadron polarization [129,76]. Hadronization to mesons is hopeless for our purposes. It is possible that high–spin mesons formed from b quarks may retain some of the initial b polarization, but they will decay by parity–conserving processes (that cannot give polarization–dependent asymmetries) down to a spin–0 B meson that retains no spin information. It is instructive however to consider how the b spin information is lost. Suppose at t=0 a spin–up b combines with a spin–down  $\bar{q}$  forming the state  $b^{\dagger}\bar{q}^{\downarrow}$ . This is not an eigenstate of total spin S but can be decomposed into a sum of S=0 and S=1 eigenstates:

$$b^{\uparrow} \bar{q}^{\downarrow} = \frac{1}{\sqrt{2}} \left( \frac{b^{\uparrow} \bar{q}^{\downarrow} - b^{\downarrow} \bar{q}^{\uparrow}}{\sqrt{2}} \right) + \frac{1}{\sqrt{2}} \left( \frac{b^{\uparrow} \bar{q}^{\downarrow} + b^{\downarrow} \bar{q}^{\uparrow}}{\sqrt{2}} \right) \tag{232}$$

If we add a common space wave function, then these two terms represent a spin-0 meson and a spin-1 meson coherently superposed. If indeed the physical meson states were precisely degenerate (as in the  $M_Q \to \infty$  limit of HQET), the time evolution of the S=0 and S=1 terms would be identical and the coherence would be preserved; the spin wave function would then remain  $b^{\dagger}\bar{q}^{\dagger}$ , the coherent superposition of meson states would preserve the b spin and total spin S would be irrelevant. In reality however  $M_b \neq \infty$ ; the pseudoscalar B and vector  $B^*$  mesons have different masses and therefore different time evolutions; at times  $t \gg (M_{B^*} - M_B)^{-1}$ , the S=0 and S=1 amplitudes become effectively incoherent and the b quark is depolarized over a period of time by spin-spin forces within the mesons (indeed the same forces that generate the  $B-B^*$  mass splitting).

One can make this more precise by defining a decoherence time scale  $t_{decoherence} = (M_{B^*} - M_B)^{-1}$  and a decay time scale  $t_{decay} = \Gamma^{-1}$ . For the case in question one has

$$t_{decoherence} = \frac{1}{M_{B^*} - M_B} \cong 2 \cdot 10^{-2} \text{ MeV}^{-1}$$

$$t_{decay} = \frac{1}{\Gamma_{B^* \to B\gamma}} \cong (10^3 - 10^4) \text{ MeV}^{-1}$$
(233)

where the width of the  $B^*$  is determined by its one-photon decay. The  $B^*$  width can be estimated in the constituent model as described in Sec.4.6. The authors of [80] quote  $\Gamma(B_u^{*+} \to B_u^+ + \gamma) = 0.84$  keV and  $\Gamma(B_d^{*0} \to B_d^0 + \gamma) = 0.28$  keV similar to the estimates in [130,131]. Thus one has  $t_{decay} \gg t_{decoherence}$  for the B mesons, i.e. the t = 0 coherent superposition in Eq.(232) will have become completely decoherent by the time  $B^*$  decays (the B decays weakly and is much longer lived).

Hadronization to bottom baryons is more promising. The Pauli principle implies that if a b quark combines with a spin-0 combination of one u plus one d, a  $\Lambda_b$  is formed; if the light-quark pair has spin 1 then  $\Sigma_b$  or  $\Sigma_b^*$  result with total spin 1/2 or 3/2. The crucial feature of this system is that in the heavy-quark limit the  $\Sigma_Q$ ,  $\Sigma_Q^*$  become degenerate and some 200 MeV more massive than the  $\Lambda_Q$  with the result that they decay to  $\Lambda_Q$  by the strong interaction, preserving the b polarization.

Suppose first that the polarized b quark picks up a spin-0 ud pair to form a 'prompt'  $\Lambda_b$ . Due to its ud pair having spin 0, all of the  $\Lambda_b$  spin resides on the valence b quark and we expect b polarization to become  $\Lambda_b$ -polarization (in the heavy-quark limit where b spin-flip is suppressed during hadronization). Suppose instead that the polarized b quark had combined with a spin-1 ud pair. In this case we would have to decompose the bqq wave functions into superpositions of eigenstates of different total spin  $S = 1/2, 3/2(\Sigma, \Sigma^*)$ . Take e.g. the state  $b^{\dagger}\{uu\}_0$  which, at t = 0, is a coherent superposition of S = 1/2 and S = 3/2 states according to

$$b^{\uparrow}\{uu\}_{0} = \sqrt{\frac{1}{3}} \left( \sqrt{\frac{1}{3}} b^{\uparrow}\{uu\}_{0} - \sqrt{\frac{2}{3}} b^{\downarrow}\{uu\}_{+1} \right)_{S=1/2} + \sqrt{\frac{2}{3}} \left( \sqrt{\frac{2}{3}} b^{\uparrow}\{uu\}_{0} + \sqrt{\frac{1}{3}} b^{\downarrow}\{uu\}_{+1} \right)_{S=3/2}$$
(234)

At  $t > (M_{\Sigma_b^*} - M_{\Sigma_b})^{-1}$  the *b* quark would become depolarized in the  $\Sigma_b$ ,  $\Sigma_b^*$  systems for reasons analogous to those outlined for the *B*,  $B^*$  bottom mesons above (in the present case the depolarization is only partial). Subsequent decays to  $\Lambda_b$  would produce partially depolarized  $\Lambda_b$ .

Quantitatively one has

$$t_{decoherence} = (M_{\Sigma_b^*} - M_{\Sigma_b})^{-1} \cong 5 \cdot 10^{-2} \text{ MeV}^{-1}$$

$$t_{decay} = \Gamma_{(\Sigma_b^*, \Sigma_b) \to \Lambda_b + \pi}^{-1} \cong 5 \cdot 10^{-2} \text{ MeV}^{-1}$$
(235)

taking the constituent one-pion width estimate from [71] as discussed in Sec.4.5. That the two time-scales come out approximately equal is an accident since the width is independent of the heavy quark mass while  $\Delta M(\Sigma_b^*, \Sigma_b)$  is proportional to  $1/m_b$ . The outcome of the above estimate is that the b quark will have become partially depolarized when it finally ends up in the  $\Lambda_b$ , because of the  $t_{decoherence} \cong t_{decay}$ . The situation is more favourable for fragmentation into the higher lying excited  $\Sigma_b^{**}$ -states because of phase space, but may be less favourable for fragmentation into excited  $\Lambda_b^{**}$  since these can decay to  $\Lambda_b$  only via two-pion emission. According to a rough estimate presented in [76] the polarization transfer from b to  $\Lambda_b$  can be expected to be all in all about 70%.

The reason that there has been such a wide interest in the polarization of the b or the  $\Lambda_b$  from  $Z^0$ -decays is that one can hope to turn this polarization information into an effective tool to analyze bottom or  $\Lambda_b$ -decays. One of the issues that has been discussed in this context is the hope to be able to determine the  $b \to c$  chirality using polarized b-decay. In order to set the stage let us gather together pieces of information and arguments concerning  $b \to c$  chirality (see also the review of [132]).

The prediction of the Standard Model that the  $b \to c$  transition is left chiral has recently been confirmed by a determination of the sign of the lepton's forward–backward (FB) asymmetry in the  $(l^-\overline{\nu}_l)$  rest system in the semileptonic decay  $\overline{B} \to D^* + l^- + \overline{\nu}_l$  [95,96]. In this analysis one uses the Standard Model left–handedness of the lepton current as input. However, if one leaves the realms of the Standard Model, the same FB asymmetry would arise if both quark and lepton currents were taken to be right–chiral, i.e. if one would switch from a  $H_{\mu\nu}(V-A)L^{\mu\nu}(V-A)$  coupling to a  $H_{\mu\nu}(V+A)L^{\mu\nu}(V+A)$  coupling.<sup>6</sup>

The FB asymmetry measure alluded to above constitutes a momentum–momentum correlation measure  $\langle \vec{l} \cdot \vec{p} \rangle$  which clearly is not a truly parity–violating measure.<sup>7</sup> What is needed to distinguish between the two above options is to define truly parity–violating spin–momentum correlation measures of the type  $\langle \vec{\sigma} \cdot \vec{p} \rangle$ .

Some such possible parity-violating measures that have been discussed recently exploit the polarized bottom quarks produced on the  $Z_0$  resonance. One then defines spin-momentum correlations w.r.t. the longitudinal spin direction of the decaying b or  $\Lambda_b$  using the momenta of the decay products of the b or  $\Lambda_b$ . For the semileptonic decays  $\Lambda_b \to \Lambda_c + l^- + \bar{\nu}_l$  or  $b \to c + l^- + \bar{\nu}_l$  this has been done using the lepton momentum [129,134] and the c or  $\Lambda_c$  momentum [134,107]. The sign of these correlations or the sign of the correspondingly defined FB asymmetries allow one to differentiate the above two options which remain after the analysis of the mesonic experiments, [95,96], i.e. the  $H_{\mu\nu}(V-A)L^{\mu\nu}(V-A)$  or the  $H_{\mu\nu}(V+A)L^{\mu\nu}(V+A)$  option. A problem with the suggested analysis is that they require the reconstruction of the  $\Lambda_b$  rest frame which will be a difficult experimental task.

Alternatively one can consider the shape of the lepton spectrum directly in the lab system [135]. The spin–lepton–momentum correlation effects referred to above have the effect that the emitted leptons in the semileptonic decay  $\Lambda_b \to \Lambda_c + l^- + \bar{\nu}_l$  (or  $b \to c + l^- + \bar{\nu}_l$ ) tend to

 $<sup>^{6}</sup>$ A viable model involving a right-handed  $W_{R}$  that is consistent with all present data has recently been proposed [133].

<sup>&</sup>lt;sup>7</sup> For example, it is well–known that in  $e^+e^-$ –annihilation the two photon exchange contribution also gives rise to nonvanishing FB asymmetries despite of the fact that QED is parity conserving.

counteralign and align with the polarization of the b for  $H_{\mu\nu}(V-A)L^{\mu\nu}(V-A)$  and  $H_{\mu\nu}(V+A)L^{\mu\nu}(V+A)$  interactions, respectively, leading to harder and softer lepton spectra in the lab system relative to unpolarized decay allowing one to distinguish between the two options in principle. However, as has been emphasized in [129], a lack of knowledge of the precise form of the  $b \to \Lambda_b$  fragmentation function precludes a decision whether the lepton spectrum is harder or softer than that of unpolarized decay, in particular since there is no unpolarized decay sample to compare with.

Another possibility to distinguish between the  $H_{\mu\nu}(V-A)L^{\mu\nu}(V-A)$  and  $H_{\mu\nu}(V+A)L^{\mu\nu}(V+A)$  options via a parity-violating measure is to determine the polarization of the lepton in the semileptonic decays  $B \to D(D^*) + l^- + \overline{\nu}_l$  [136] or  $\Lambda_b \to \Lambda_c + l^- + \overline{\nu}_l$  [125]. This will be a difficult experiment but may be feasible in the not too distant future for semileptonic decays involving the  $\tau$ -lepton.

In [137] two of us together with B. König proposed yet a fourth variant of a truly parity-violating spin-momentum correlation measure in  $b \to c$  decays. They proposed to look at the decay cascade  $\Lambda_b \to \Lambda_c(\to a_1 + a_2 + \cdots) + l^- + \overline{\nu}_l$  to determine the chirality of  $b \to c$  decays where  $\Lambda_c \to a_1 + a_2 + \cdots$  are nonleptonic decays of the  $\Lambda_c$ . The weak nonleptonic decays of the  $\Lambda_c$  serve to analyze the polarization of the  $\Lambda_c$  through the correlation of their momenta with the polarization of the decaying  $\Lambda_c$ . Ideal in this regard are the nonleptonic decays  $\Lambda_c \to \Lambda \pi$  and  $\Lambda_c \to \Sigma \pi$  the analyzing power of which has recently been determined [96,95,138]. As a further analyzing channel they discussed the decay modes  $\Lambda_c^+ \to p\bar{K}^{*0}$  and  $\Lambda_c^+ \to \Delta^{++}K^-$  which could make up a large fraction of the dominant decay mode  $\Lambda_c \to pK^-\pi^+$ . The analyzing power of these channels has not yet been determined experimentally but can be estimated using the theoretical quark model ansatz of [139].

Consider the semileptonic decay of an unpolarized  $\Lambda_b$ . Possible polarization effects due to polarized  $\Lambda_b$ —decays average out if one integrates over all possible momentum directions of the  $\Lambda_c$  in the decay  $\Lambda_b \to \Lambda_c + l^- + \overline{\nu}_l$ . Possible  $\Lambda_b$  polarization effects due to incomplete averaging because of experimental cut biases have been found to be very small. From simple helicity arguments the longitudinal polarization  $P_L$  (also called  $\alpha$  in Sec.5.2.1) of the daughter baryon  $\Lambda_c$  is expected to be negative (positive) in most of the phase space region for left—chiral ( $\xi = 1$ ) (right—chiral ( $\xi = -1$ ))  $b \to c$  transitions, respectively. For the mean value of  $P_L$  one finds

$$\langle P_L \rangle = \xi \begin{cases} -0.77 & \text{IMF [126]} \\ -0.81 & \text{FQD} \end{cases}$$
 (236)

The two polarization values refer to the Heavy Quark Effective Theory (HQET) improved infinite momentum frame (IMF) model of Ref.[126] and free quark decay (FQD) where we use  $m_b = M_{\Lambda_b} = 5.64$  GeV and  $m_c = M_{\Lambda_c} = 2.285$  GeV in order to get the phase space right.

The longitudinal polarization of the  $\Lambda_c$  can be probed by looking at the angular distribution of its subsequent nonleptonic decays as written down in Eq.(211). Ideal in this regard are the nonleptonic modes  $\Lambda_c \to \Lambda \pi$  and  $\Lambda_c \to \Sigma \pi$  since the analyzing power of these decays has recently been determined. For  $\Lambda_c \to \Lambda \pi$  one has

$$\alpha_{\Lambda_c \to \Lambda \pi} = \begin{cases} -1.0_{-0.0}^{+0.4} & [96] \\ -0.96 \pm 0.42 & [95] \end{cases} . \tag{237}$$

For  $\Lambda_c \to \Sigma \pi$  we quote the preliminary value [138]

$$\alpha_{\Lambda_c \to \Sigma \pi} = -0.43 \pm 0.23 \pm 0.20$$
 (238)

In correspondence to the decay distribution Eq.(211) one can define a forward–backward (FB) asymmetry by averaging over the daughter baryons in the respective forward (F) ( $0^{\circ} \leq \Theta < 90^{\circ}$ ) and backward (B) ( $90^{\circ} \leq \Theta < 180^{\circ}$ ) hemispheres to obtain

$$A_{FB} = \frac{1}{2} P_L \alpha_{\Lambda_c} \quad . \tag{239}$$

Judging from the large numerical values of the mean of  $P_L$  Eq.(236) and of the asymmetry parameters  $\alpha_{\Lambda_c}$  Eqs.(237,238) a measurement of the sign of  $A_{FB}$  within reasonable errors should allow one to conclude for the sign of  $\xi$  and therefore for the chirality of the  $b \to c$  transition with a good certainty.

What has been said up to now requires the reconstruction of the  $\Lambda_b$  rest system. This will not be an easy task for the energetic  $\Lambda_b$  bottom baryons produced on the  $Z_0$  where the analysis suggested in this paper is most likely to be done first. There is some hope, though, that such a reconstruction can be done with the newly installed vertex detectors in the CERN detectors. At present it is more realistic to consider the LEP environment with energetic longitudinally polarized  $\Lambda_b$ 's whose rest frames cannot be reconstructed. The polarization of the  $\Lambda_c$ 's in the semileptonic decays takes a more complicated form in the laboratory frame than in the  $\Lambda_b$  rest frame as given by Eq.(212). In particular negatively polarized  $\Lambda_c$ 's emerging backward in the  $\Lambda_b$  rest frame will turn into positively polarized  $\Lambda_c$ 's in the lab frame because of the momentum reversal due to the requisite Lorentz boost. Also, because of experimental cuts and/or biases the  $\Lambda_c$ 's polarization dependence on the polarization of the  $\Lambda_b$  may no longer average out, i.e. one has to address the question of polarization transfer under realistic experimental conditions.

In order to study all these issues a Monte Carlo program has been written that generates semileptonic decay events of polarized  $\Lambda_b$  into polarized  $\Lambda_c$ . It is then a simple matter to adapt the calculation to the experimental conditions present in the LEP environment including longitudinal and transverse lepton momentum cuts. What one finds is that approximately 50% of the polarization information is retained when going from the  $\Lambda_b$  rest frame to the lab frame ( $Z^0$  rest frame). One obtains  $\langle P_L \rangle_{labframe} = -(0.3 - 0.4)\xi$  with little cut and  $\Lambda_b$  polarization sensitivity.  $\xi$  is the chirality parameter as before. With sufficient statistics it should not be too difficult to pin down the chirality of the  $b \to c$  transitions through some such measurements. We emphasize that the quality of this experiment is crucially dependent on the quality of the charm decay data that one is using to analyze the  $\Lambda_c$  polarization.

Regardless of what has been said about the potential use of polarized b or  $\Lambda_b$  decays to measure the chirality of the  $b \to c$  transitions there is a wealth of interesting physics to be investigated using polarized b quarks, and for that matter, polarized heavy baryon decays.

# 6 Lifetimes and Inclusive Nonleptonic Decays

#### 6.1 Experimental Lifetimes

Let us quote the charm baryon lifetime values from the 1992 Particle Data Group [26]. The  $\Lambda_c$  has a lifetime of  $\tau(\Lambda_c) = (1.91 \pm {0.15 \atop 0.12}) \times 10^{-13} \, s$ , the charged  $\Xi_c^+$  has a lifetime of  $\tau(\Xi_c^+) = (3.0 \pm {1.0 \atop 0.6}) \times 10^{-13} \, s$  and the neutral  $\Xi_c^0$  lifetime is quoted at  $\tau(\Xi_c^0) = (0.82 \pm {0.59 \atop 0.30}) \times 10^{-13} \, s$ . There exist no lifetime measurements for the  $\Omega_c^0$  yet. For comparison, the lifetimes of the charmed mesons are  $\tau(D^0) = (4.20 \pm 0.08) \times 10^{-13} \, s$ ,  $\tau(D^\pm) = (10.66 \pm 0.23) \times 10^{-13} \, s$  and  $\tau(D_s^\pm) = (4.50 \pm {0.30 \atop -0.26}) \times 10^{-13} \, s$ .

In the bottom baryon sector there exist lifetime measurements only for the  $\Lambda_b$ . R.Forty [140] quotes a LEP average of  $\tau(\Lambda_b^0) = (1.07 \pm 0.15) \times 10^{-12} \, s$ . Ironically one now has a lifetime measurement of the  $\Lambda_b$  although the  $\Lambda_b$  has not yet been seen with certainty. Contrast the  $\Lambda_b$  lifetime with the bottom meson averages quoted by the Particle Data Group [26]:  $\tau(B^{\pm}) = (1.62 \pm 0.13) \times 10^{-12} \, s$ ,  $\tau(B^0) = (1.43 \pm 0.12) \times 10^{-12} \, s$  and  $\tau(B_s^0) = (1.41 \pm 0.22) \times 10^{-12} \, s$ .

#### 6.2 Theoretical Lifetime Estimates

In the large mass limit, one expects all heavy hadrons of the same flavour to have identical lifetimes. The spread in the experimental lifetime values of the  $\Lambda_c^+$ ,  $\Xi_c^{0,+}$  and  $\Omega_c$  charm baryons signals that  $1/m_c$  effects are still important in the weak inclusive decays of charm baryons (as they are for charm mesons). The preasymptotic effects enter in the form of W-exchange contributions [141], and additional contributions come from the interference of decay quarks and spectator quarks. These are sensitive to the probability that the the charm and light quarks in the baryon wave function will come together at one point: to the square of the wave function at the origin  $|\Psi(0)|^2$  with mass dimension  $[m^3]$ .

From dimensional arguments, one then finds

$$\Gamma_{FQD} \approx G_F^2 m_c^5$$

$$\Gamma_{exch,int} \approx G_F^2 m_c^2 |\Psi(0)|^2$$
(240)

where  $\Gamma_{FQD}$  denotes the "free quark decay" parton model decay rate,  $\Gamma_{exch}$  and  $\Gamma_{int}$  denote the W-exchange and interference rates, and  $m_c$  refers to the charm quark mass.

Explicit calculations [142,143] show that  $\Gamma_{FQD} \approx \Gamma_{exch,int}$  in the charm baryon sector and that  $\Gamma_{FQD} \approx \Gamma_{int}$  in the charm meson sector [143]. Using the fact that the wave function at the origin of the heavy–light bound state becomes independent of the heavy quark mass as the heavy quark mass becomes large [144], one can scale Equation (240) to the bottom quark sector. One then finds  $\Gamma_{exch,int}/\Gamma_{FQD} \approx (m_c/m_b)^3 \approx \mathcal{O}(5\%)$ , which implies that the lifetime differences

in the bottom sector are expected to be quite small. To some extend this is corroborated by the present bottom lifetime measurements.

The difficulty in obtaining reliable rate and life time estimates for the charm baryons is clearly evidenced by the fact that the preasymptotic effects, which are down by several powers of  $1/m_c$ , are so important. This makes an analysis in terms of a  $1/m_c$  expansion difficult. Nevertheless one can attempt to obtain a qualitative picture of the life time differences of charm baryons in the form of a life time hierarchy [142,143].

The starting point in the analysis is the usual effective nonleptonic Hamiltonian

$$H_{eff} = \sqrt{2}G_F V_{cs} V_{ud}^* \left[ c_- O_- + c_+ O_+ \right] \tag{241}$$

where  $O_{\pm}$  are local 4-quark operators

$$O_{\pm} = (\bar{u}_L \gamma_\mu d_L)(\bar{s}_L \gamma^\mu c_L) \pm (\bar{s}_L \gamma_\mu d_L)(\bar{u}_L \gamma^\mu c_L) \tag{242}$$

with  $\bar{q}_L \gamma_\mu q_L = \frac{1}{2} \bar{q} \gamma_\mu (1 - \gamma_5) q$ , and  $V_{\bar{q}_\alpha q_\beta}$  are elements of the Kobayashi-Maskawa mixing matrix with  $V_{cs} \simeq V_{ud} \simeq \cos \Theta_c$  and  $\Theta_c$  the Cabibbo angle. The coefficients  $c_{\pm}$  describe the leading logarithmic evolution of the nonleptonic Hamiltonian from the W mass scale down to the charm mass scale  $\mu \simeq \mathcal{O}(m_c)$  [145]. We take  $c_+ = 0.74$  and  $c_- = 1.80$  as in the work of Guberina et al. [143].

The effective nonleptonic Hamiltonian Eq.(241) induces the inclusive nonleptonic decay contributions drawn in Fig.17 for e.g. the inclusive  $\Lambda_c^+$  decays. Simple expressions can be obtained for these rates when one neglects u, d, s quark masses and uses a nonrelativistic wave function for the charm baryons. For example, for the  $\Lambda_c^+$  decay one then has a nonleptonic (n.l.) rate [143]

$$\Gamma_{n.l.}^{\Lambda_c^+} = \Gamma_{FQD}^{\Lambda_c^+} + \Gamma_{exch}^{\Lambda_c^+} + \Gamma_{int}^{\Lambda_c^+} 
= (2c_+^2 + c_-^2) \frac{G_F^2 m_c^5}{192\pi^3} + c_-^2 \frac{G_F^2 m_c^2 |\Psi(0)|^2}{4\pi} - c_+ (2c_- - c_+) \frac{G_F^2 m_c^2 |\Psi(0)|^2}{4\pi} 
= (1.58 + 3.01R - 0.99R) \times 10^{-12} \text{s}^{-1}$$
(243)

with  $m_c = 1.6 \text{ GeV}$ ,  $c_{\pm}$ -values as above and  $R = |\Psi(0)|^2/10^{-2} \text{GeV}^3$ .

As is evident from Equation (243) the resulting nonleptonic rate is quite sensitive to the value of the wave function at the origin  $|\Psi(0)|^2$ . From a fit to the hyperfine splitting, as discussed in Sec.2, one has  $|\Psi(0)|^2 \simeq 10^{-2} \text{GeV}^3$ . Adding a nominal semileptonic rate value  $2 \times 15\%$  of the nonleptonic FQD rate one finds  $\tau_{\Lambda_c^+} = 2.46 \times 10^{-13} \text{s}$  which is somewhat larger than the experimental value  $\tau_{\Lambda_c^+}(exp.) = (1.91 \pm 0.15 \atop 0.12) \times 10^{-13} \text{s}$ . Smaller values of the wave function at the origin are obtained in a bag model [143]  $(|\Psi(0)|^2 \simeq 0.4 \times 10^{-2} \text{GeV}^3)$  or if one equates the baryon's and meson's wave function at origin [142]  $(|\Psi(0)|^2 \simeq 0.4 \times 10^{-2} \text{GeV}^3)$  with  $f_D = 165 \text{ MeV}$ . Values similar to the above  $|\Psi(0)|^2 \simeq 10^{-2} \text{GeV}^3$  are also obtained by using electromagnetic mass differences in the hyperfine formula [146]. It is clear that using the smaller values of  $|\Psi(0)|^2$  worsens the agreement with the experimental rate.

Applying the same calculation to the other weakly decaying charm baryons Guberina, Rückl and Trampetic [143] find a lifetime hierarchy  $\tau(\Omega_c) \approx \tau(\Xi_c^0) < \tau(\Lambda_c) < \tau(\Xi_c^+)$  whereas Voloshin and Shifman [142] obtained  $\tau(\Omega_c) < \tau(\Xi_c^0) < \tau(\Lambda_c) \approx \tau(\Xi_c^+)$ . In a more recent analysis Blok and Shifman estimate the lifetime ratios at  $\tau(\Xi_c^0) : \tau(\Lambda_c) : \tau(\Xi_c^+) \approx 0.36 : 0.77 : 1$  and point out that the lifetime of the  $\Omega_c$  can either be the most short–living and the most long–living among charmed baryons depending on the strength of the unknown spin–spin interaction in



the  $\Omega_c$  [147]. Present data favours the inequality chain of [143] and the new values of Blok and Shifman [147].

The main effects leading to the lifetime extremes in the inequality chains are easily identified: the large  $\Omega_c^0$ -rate is due to a large positive interference effect among the s-quarks (the s-quark from the weak decay vertex can interfere with either of the spectator s-quarks) and the small  $\Xi_c^+$ -rate is due to the absence of a W-exchange contribution in this case.

One must stress that there are a number of theoretical uncertainties in the lifetime calculations of [142] and [143] related to the size of the preasymptotic effects which could not be discussed in detail here. Nevertheless, the authors of [142] are optimistic and claim that their inequalities can be replaced by equality relations with multiplicative factors of 1.5 to 2.

The absence of large preasymptotic effects in bottom baryon nonleptonic decay rates is gratifying. Present evidence points to a somewhat larger difference in lifetimes between bottom mesons and the  $\Lambda_b$  bottom baryon than expected from the naive dimensional analysis (240). Clearly one needs better experimental data on bottom hadron lifetimes including the bottom baryons  $\Xi_b^{0,-}$  and  $\Omega_b$  to be able to ascertain how big the spread in lifetimes in the bottom sector is, and whether one can understand the lifetime hierarchy from first theoretical principles.

# 7 Exclusive Nonleptonic Decays

#### 7.1 Decay Rates and Decay Distributions

Let us begin by counting the number of independent amplitudes in the four classes of two–body nonleptonic ground-state to ground-state transitions

$$B_1(1/2^+) \to B_2(1/2^+, 3/2^+) + M(0^-, 1^-)$$
:

- (i)  $1/2^+ \rightarrow 1/2^+ + 0^-$ : 2 complex amplitudes
- (ii)  $1/2^+ \rightarrow 3/2^+ + 0^-$ : 2 complex amplitudes
- (iii)  $1/2^+ \rightarrow 1/2^+ + 1^-$ : 4 complex amplitudes
- (iv)  $1/2^+ \rightarrow 3/2^+ + 1^-$ : 6 complex amplitudes

Using standard methods (e.g. [148]) one can then derive angular decay distributions which, upon integration, give the decay rates. Again we prefer an explicit frame–dependent representation of the decay distributions instead of the frame independent representation discussed in [149]. We begin by considering the nonleptonic decay of unpolarized charm or bottom baryons. In the simplest case one has the decay  $1/2^+ \to 1/2^+ (\to 1/2^+ + 0^-) + 0^-$  as for example in  $\Lambda_c^+ \to \Lambda(\to p\pi^-) + \pi^+$ . Referring to Fig.14, one now sees a cascade only on one side as the pion's decay goes unobserved. Consequently one has only a single polar angle distribution. One obtains

$$\frac{\mathrm{d}\Gamma(\Lambda_c^+ \to \Lambda(\to p\pi^-) + \pi^+)}{\mathrm{d}\cos\Theta_{\Lambda}} = \frac{1}{2} B_{\Lambda \to p\pi^-} \Gamma_{\Lambda_c^+ \to \Lambda\pi^+} (1 + \alpha_c \alpha_{\Lambda} \cos\Theta_{\Lambda}) \tag{244}$$

where  $\alpha_c$  and  $\alpha_{\Lambda}$  are the asymmetry parameters in the decays  $\Lambda_c^+ \to \Lambda \pi^+$  and  $\Lambda \to p\pi^-$ , respectively, defined in analogy to Eqs.(209,210). The definition of the polar angle  $\Theta_{\Lambda}$  is given in Fig. 14 with the replacement  $W^+ \to \pi^+$ . The cascade decay  $\Lambda \to p\pi^-$  acts as an analyzer of the longitudinal polarization of the daughter baryon  $\Lambda$  whose polarization is given by the asymmetry parameter  $\alpha_c$ . This single angular decay distribution was utilized experimentally to measure the asymmetry parameter  $\alpha_c$  in the decay  $\Lambda_c \to \Lambda(\to p\pi^-) + \pi^+$  [96,95].

Somewhat more complicated is the decay distribution in the double cascade  $1/2^+ \to 1/2^+(\to 1/2^+ + 0^-) + 1^-(\to 0^+ + 0^-)$  as for example in  $\Lambda_c^+ \to \Lambda(\to p\pi^-) + \rho^+(\to \pi^+\pi^0)$ . One has [139,108]

$$\frac{\mathrm{d}\Gamma(\Lambda_c^+ \to \Lambda(\to p\pi^-) + \rho^+(\to \pi^+\pi^0))}{\mathrm{d}\cos\Theta\mathrm{d}\chi\mathrm{d}\cos\Theta_{\Lambda}} = \frac{1}{2\pi}B_{\Lambda\to p\pi^-}B_{\rho^+\to \pi^+\pi^0}\frac{p}{32\pi M_1^2} 
\cdot \left(\frac{3}{4}\sin^2\Theta H_U(1 + \alpha_c^U\alpha_{\Lambda}\cos\Theta_B) + \frac{3}{2}\cos^2\Theta H_L(1 + \alpha_c^L\alpha_{\Lambda}\cos\Theta_{\Lambda})\right) 
-\frac{3}{4\sqrt{2}}\sin(2\Theta)\cos\chi\cos\Theta_{\Lambda}\alpha_{\Lambda}H_I + \frac{3}{4\sqrt{2}}\sin(2\Theta)\sin\chi\cos\Theta_{\Lambda}\alpha_{\Lambda}H_{I'}\right)$$
(245)

where the helicity rates  $H_U$ ,  $H_L$ , and  $H_I$  and the asymmetry parameters  $\alpha_c^U$  and  $\alpha_c^L$  are defined in analogy to Eqs.(203,209,210). Angles are defined as in Fig.14 with the replacement of  $(W^+ \to l^+ \nu_l)$  by  $(\rho^+ \to \pi^+ \pi^+)$ . Clearly the six observables defined by the decay distribution do not suffice to determine the four complex decay amplitudes of the process.

The observable  $H_{I'}$  is proportional to the *imaginary* part of the longitudinal–transverse interference term (see the third line of Equation (203)) and is thus a so–called T–odd observable. It obtains contributions from CP–violating interactions and/or from effects of final–state interaction. The Standard Model CP–violating contributions are expected to be quite small and thus  $H_{I'}$  would be a good measure of the strength of final state interaction effects. Alternatively, one may extract possible CP–violating effects by comparing  $\Lambda_c^+$  and  $\bar{\Lambda}_c^+$  cascade decays.

We now briefly turn to the decays of polarized heavy baryons in which the cascade decay of the daughter baryon is used as an analyzer and the meson decay goes unanalyzed. The orientation angles are defined in Fig.15. The angular decay distribution for the  $1/2^+ \rightarrow 1/2^+ (\rightarrow 1/2^+ + 0^-) + 0^-$  transition is well known from the analysis of the nonleptonic decays of the cascade hyperon  $\Xi$  and reads [108,150]

$$\frac{\mathrm{d}\Gamma(\Lambda_c^{\uparrow} \to \Lambda(\to p\pi^-) + \pi^+)}{\mathrm{d}\cos\Theta_p \mathrm{d}\cos\Theta_\Lambda \mathrm{d}\sin\chi} = \frac{1}{8\pi} \Gamma_{\Lambda_c \to \Lambda\pi^+} B_{\Lambda \to p\pi^-} 
[1 + \alpha_c \alpha_\Lambda \cos\Theta_\Lambda + P_c(\alpha_c \cos\Theta_p + \alpha_\Lambda \cos\Theta_p \cos\Theta_\Lambda 
+ \alpha_\Lambda \sin\Theta_p \sin\Theta_\Lambda(\gamma_c \cos\chi + \beta_c \sin\chi))]$$
(246)

where  $\beta_c$  and  $\gamma_c$  are the usual nonleptonic decay parameters (e.g. [149]). In a noncascade charm baryon decay, for example  $\Lambda_c \to p\bar{K}^0$ , one would be left with a decay distribution  $W(\Theta_c) = (1 + P_c \alpha_c \cos \Theta_p)$ . This would allow for a determination of the asymmetry parameter  $\alpha_c$  only if  $P_c$  were known.

The remaining angular decay distributions involving the other nonleptonic decay processes (polarized and unpolarized) can be found in [108].

### 7.2 Symmetry Considerations

In the nonleptonic Hamiltonian Eq.(241) we included only the dominant contribution proportional to  $\simeq \cos^2\Theta_c$ . Once suppressed transitions proportional to  $\simeq \cos\Theta_c\sin\Theta_c$ , not written in Eq.(241), are the transition  $c\to du\bar{d}$  and  $c\to su\bar{s}$ , and the doubly suppressed decay  $c\to du\bar{s}$  proportional to  $\simeq \sin^2\Theta_c$ . The  $\Delta C=1$  SU(3) content of the antisymmetric representation 20" is  $3_a$  and  $6^*$ , and that of the symmetric representation 84 is  $3_s$  and 15. The dominant pieces are the  $6^*$  and 15 SU(3) representations. The I-, U-, and V-spin content of the dominant piece is  $\Delta I=1$ ,  $\Delta U=1$  and  $\Delta V=0$ , 1. Sum rules relating different charm changing nonleptonic amplitudes can be and have been written down using various techniques [151–155]; the simplest technique appears to be an analysis using the three SU(2)<sub>I,U,V</sub></sub> subgroups [151]. The I-spin sum rules are expected to be quite accurate. For example one predicts equal rates for  $\Lambda_c \to \Sigma^+\pi^0$  and  $\Lambda_c \to \Sigma^0\pi^+$  from the  $\Delta I=1$  rule [151] which is borne out by recent experiments [138]. The U-spin and V-spin sum rules are not expected to be as good because of SU(3) breaking effects. Nonet symmetry for the mesons can be incorporated in the usual way by excluding disconnected flavour flow diagrams (see e.g. [151]).

<sup>&</sup>lt;sup>8</sup> In the sum rule approach, one relates different nonleptonic decay amplitudes by using flavour symmetry relations based on the flavour symmetry group SU(4) and/or its SU(3) and SU(2) subgroups.

An interesting observation concerns the rates of the two members  $\Lambda_c^+$  and  $\Xi_c^0$  of the same U–spin doublet. In the case of 20" dominance of  $H_{eff}$  it has been shown from U–spin arguments that for the dominating  $c \to su\bar{d}$  transitions one can derive equality of total rates and partial rates into any particular spin channels [153]. Considering the present nonequality of  $\Lambda_c^+$  and  $\Xi_c^0$  life times shows that  $H_{eff}^{20"}$  dominance of the effective nonleptonic Hamiltonian may not be a good approximation.

Further sum rules may be obtained relating Cabibbo favoured, suppressed and doubly suppressed decay amplitudes when the Cabibbo suppression factors are removed. Similarly one may even attempt to relate charm changing  $\Delta C=1$  processes to ordinary  $\Delta C=0$  nonleptonic hyperon decays although the large mass difference between charm and ordinary baryons makes such an approach problematic.

Still another class of sum rules may be obtained by considering parity-conserving and parity-violating amplitudes separately and assuming the <u>full</u> SU(4) symmetry of the transition in conjunction with the charge conjugation symmetry of  $H_{eff}$  which is C=+1 and C=-1 for the parity-conserving and parity-violating parts, due to CP-conservation [151,152]. One then e.g. obtains the result that the parity-violating amplitude A in  $\Lambda_c^+ \to \Lambda \pi^+$  vanishes. This is in direct conflict with the recent nonvanishing asymmetry measurement in this decay [95,96]. One concludes that SU(4) is not a useful flavour symmetry for charm changing weak decays due to the large mass breaking factor  $(m_c - m_s)/m_c \simeq 70\%$ .

While SU(4) is not a useful symmetry, SU(3) flavour symmetry may still be useful for charm changing decays [151,154]. But even then one encounters the problem of which mass dimension the SU(3) flavour symmetric amplitude should carry. Related to this is the extraction of supposed flavour symmetric amplitudes from rates where one does not know which mass scale  $\tilde{M}$  is appropriate for the  $(p/\tilde{M})^{2l+1}$  phase space factor. In order to be able to answer this question reliably one is back to the dynamical problem. Hopefully one will learn more about the appropriate mass scaling factors for an amplitude in the future. Unfortunately one must conclude that the SU(3) flavour symmetry approach to nonleptonic and semileptonic decays involving  $\Delta C=1$  transitions provides a rule of thumb at best.

# 7.3 Quark Model and Current Algebra Results

In the quark model the effective current×current Hamiltonian (241) gives rise to the five types of flavour diagrams drawn in Fig.18. We have chosen to label the quark lines for the specific transition  $\Lambda_c^+ \to \Lambda \pi^+$  for illustrative purposes. The wavy lines are included in order to indicate how the effective quark currents of the Hamiltonian (241) act. As a next step, one wants to interpret the diagrams as Feynman diagrams possibly with additional gluon exchanges added. The general dynamical problem in all its complexity is far from being solved, so one has to resort to some approximation. The quark lines in Fig.18 transmit spin information from one hadron to the other. This is realized in the spectator quark model, which postulates that there is no spin communication between quark lines. Quark pairs are created from the vacuum with  $^3P_0$  quantum numbers. Finally, these postulates can be cast into a covariant form if the quarks in a hadron are assumed to propagate with equal velocity which is also the hadron's velocity.

In terms of quark model spin wave functions, the decay amplitudes for the process  $B_1 \rightarrow B_2 + M$  corresponding to Fig.18 can then be written as [151]

$$T_{B_1 \to B_2 + M} = H_1 \bar{B}_2^{ABC'} B_{1ABC} \bar{M}_D^{D'} (O_{C'D'}^{CD} - \frac{1}{N_c} O_{D'C'}^{CD})$$

Figure 18: Quark diagrams contributing to nonleptonic decay  $\Lambda_c \to \Lambda \pi^+$ , including colour–flavour weight factors.

$$+\frac{1}{N_{c}}H_{2}\bar{B}_{2}^{AB'D}B_{1ABC}\bar{M}_{D}^{D'}O_{B'D'}^{BC} 
+\frac{1}{N_{c}}H_{2}'\bar{B}_{2}^{AB'C'}B_{1ABC}\bar{M}_{D}^{B}O_{B'C'}^{CD} 
+\frac{1}{N_{c}}H_{3}\bar{B}_{2}^{A'B'C'}B_{1ABC}\bar{M}_{C'}^{C}O_{A'B'}^{AB} \tag{247}$$

where the first, second, third and fourth terms of (247) correspond to the contributions of diagrams Ia,b, IIa, IIb and III in Fig.18 in that order.  $B_{ABC}$  and  $M_A^B$  are quark model wave functions for the baryons and mesons. Each index A stands for a pair of indices  $(\alpha, a)$ , where  $\alpha$  and a denote the spin and flavour degrees of freedom. We have already summed over colour degrees of freedom which results in the typical factors  $1/N_c$  where  $N_c = 3$ . We emphasize that the limit  $N_c \to \infty$  cannot be taken naively for the last three contributions in (247) (IIa,b and III in Fig.18). We shall return to this point later on. The matrix  $O_{AB}^{CD}$  describes the spin-flavour structure of the effective current×current Hamiltonian (241).  $H_1, H_2, H'_2$  and  $H_3$  are wave function overlap integrals corresponding to diagrams I, IIa,b and III which are expected to depend on the masses of a particular decay process. Eq.(247) can be viewed as an algebraic realization of the diagrams shown in Fig.18: each line in Fig.18 corresponds to a contraction of doubly occurring spin-flavour indices in (247), where one sums over the spin-flavour indices.

The first term in (247) corresponds to the so-called factorization contribution and can be calculated in terms of the current matrix elements of Sec.5. Bringing the contributions of the non-factorizing diagrams IIa,b and III into tenable forms with the above assumptions does not preclude the possibility that (247) can be derived from a more general point of view dropping some of the above assumptions. One should note that in the case of transitions between ground state baryons, the non-factorizing diagrams IIa,b and III obtain contributions only from  $O^-$  (transforming as 20" in SU(4)) because of the symmetric nature of the ground state baryons [156]. Both operators  $O^+$  and  $O^-$  contribute to diagram Ia and Ib. The contributions of Ia and Ib add up such that the resulting contribution is proportional to  $\chi_{\pm} = (c_+(1+1/N_C) \pm c_-(1-1/N_C))/2$  depending on whether the final state meson is charged (+) or neutral (-).

The contribution of diagram Ib can be seen to be colour suppressed. Guided by the analysis

of exclusive nonleptonic charm and bottom meson decays [157,158] it seems to be appropriate to take the  $N_c \to \infty$  limit and accordingly drop the contribution of diagram Ib in Fig.18. Superficially also the contributions of diagrams IIa,b and III appear to be colour suppressed. But considering the fact that baryons contain  $N_c$  quarks as  $N_c \to \infty$  the denominator factor  $N_c$  is balanced by combinatorial numerator expressions such that diagrams IIa,b and III occur at  $\mathcal{O}(1)$  as  $N_c \to \infty$  and may not be dropped in this limit.

The results of calculating diagrams IIa, IIb, and III depend on the details of the quark model wave functions used as input. As a first approximation, one may use  $SU(2)_W$  spin wave functions [151]. They correspond to boosting static quark model wave functions to a collinear equal velocity frame as mentioned above [159]. When explicit mass factors are scaled out of the baryon wave functions according to the HQET, one can set  $H_2 = H'_2$  in Eq.(247), because of CP-invariance. After some straightforward algebraic manipulations involving the evaluation of the amplitude Eq.(247) with the  $SU(2)_W$  wave functions, one can calculate the nonleptonic transition amplitudes for the decays  $1/2^+ \rightarrow (1/2^+, 3/2^+) + (0^-, 1^-)$ .

In order to be able to discuss some general features of the solutions, we treat the decay  $1/2^+ \to 1/2^+ + 0^-$  in more detail. Writing the amplitude  $T_{B_1 \to B_2 + M} = \bar{u}_2(A + B\gamma_5)u_1$  one obtains the following amplitude expressions

$$A = A^{fac} + \frac{1}{3} \frac{H_2}{M_1 M_2 \sqrt{M_3}} \left( -\frac{3}{4} Q_+ (M_1 I_3 - M_2 \hat{I}_3) + \frac{3}{4} M_1 M_2 M_3 (I_3 - \hat{I}_3) \right)$$

$$B = B^{fac} + \frac{1}{3} \frac{H_2}{4M_1 M_2 \sqrt{M_3}} \left( Q_+ (M_1 (I_3 + 2I_4) + M_2 (\hat{I}_3 + 2\hat{I}_4)) \right)$$

$$+ \frac{1}{3} \frac{H_3}{M_1 M_2 \sqrt{M_3}} 3M_1 M_2 (M_1 + M_2 + M_3) I_5$$

$$(249)$$

where the factorizing contributions  $A^{fac}$  and  $B^{fac}$  (corresponding to diagrams Ia and Ib) are obtained from the current-induced form factors discussed in Section 5. We have defined  $Q_+ = (M_1 + M_2)^2 - M_3^2$ . The invariant flavour wave function contractions (Clebsch–Gordan coefficients) denoted by  $I_i$  and  $\hat{I}_i$  are defined in [151].  $I_3$  and  $I_4$  are associated with diagram IIa,  $\hat{I}_3$  and  $\hat{I}_4$  with diagram IIb, and  $I_5$  with diagram III. Diagram III can be seen to contribute only to the p.c. amplitude B, whereas diagrams I and II contribute to both parity–conserving and parity–violating amplitudes. The parity–conserving and –violating amplitudes can be seen to be even and odd with respect to the generalized charge conjugation operation  $(M_1; I_{3,4}; I_5) \to (M_2; \hat{I}_{3,4}; I_5)$  as expected from the CP-conserving property of the nonleptonic Hamiltonian. For example, for the decay  $\Lambda_c^+ \to \Lambda \pi^+$  one finds  $I_3 = \hat{I}_3$  and thus the parity–violating amplitude A in the symmetry limit  $M_1 = M_2$  vanishes, as remarked on earlier. With  $M_1 \gg M_2$  this statement no longer holds true.

The contributions of diagrams IIb and III are nonleading on the scale of the mass  $M_1$  of the parent baryon. As a helicity analysis shows, they are nonleading because the contributions IIb and III are suppressed by helicity as a result of the  $(V-A)\times (V-A)$  nature of the underlying quark transition [160]. This implies that only the factorizing contribution Ia and the non-factorizing contribution IIa survive when  $M_2/M_1 \to 0$ . This conclusion holds in general for all the ground state decay channels. These leading contributions can be seen to lead to an exclusive decay mode power behaviour  $\Gamma \sim 1/M_1$  when  $M_2$  and  $M_3$  are kept fixed. The helicity suppressed contributions are down by an additional factor  $(M_2/M_1)^2$ . The same power behaviour holds true in nonleptonic meson decays. Compared to the inclusive nonleptonic rate  $\Gamma^{nl}_{FQD} \sim M_1^5$ 

one infers that the exclusive branching ratio of a particular two-body channel decreases very rapidly as  $M_1$  becomes large and  $M_2$ ,  $M_3$  are kept fixed. When both  $M_1$  and  $M_2$  become large with their ratios fixed, and  $M_3$  kept fixed and small, one has again  $\Gamma \sim (M_1)^5 \cdot (M_2/M_1)^6$  with the helicity suppressed contributions diagrams IIb, III down by another factor  $(M_2/M_1)^2$ . We do not, however, see a mechanism that would suppress the non-factorizing contribution IIa relative to the factorizing contribution in this limit as is implicit in the analysis of [149,161].

The flavour structure in the parity violating amplitude A has a remarkable property: there exists a one—to—one flavour correspondence with terms arising in the current algebra plus soft pion approach. This was first noticed empirically in the  $\Delta C = 0$ ,  $\Delta Y = 1$  [162] and in the  $\Delta C = 0$ ,  $\Delta Y = 0$  [163] transitions and was later proven in general [151]. The correspondence between the quark model and current algebra approach works in the following way: the contributions proportional to  $I_3$  and  $\hat{I}_3$  have the flavour structure of the "equal time commutator" term when the symmetry limit  $M_1 = M_2$  is taken. The factorizing contribution  $A^{fac}$  has the same interpretation in both schemes. In a similar vein, the nonfactorizing parity—conserving contributions can readily be interpreted as baryon pole contributions.

In the past few years, many new nonleptonic charm-baryon decays have been observed [23]. By now about 25% of the  $\Lambda_c^+$  decay channels are accounted for; new nonleptonic decay modes of  $\Xi_c$  and  $\Omega_c$  have been seen recently. As for the bottom baryons, the experimental situation is meagre. Evidence for  $\Lambda_b$  in the exclusive nonleptonic mode  $\Lambda_b \to \Lambda J/\Psi$  was presented in [10] which, however, was not confirmed by other collaborations [164]. Low statistics evidence has been obtained for the mode  $\Lambda_b \to \Lambda_c^+ \pi^-$  [11]. Among the observed charm-baryon decay channels there are many two-body and quasi-two-body modes which can be compared with theoretical predictions. For the three- and four-body decay modes only a few theoretical analyses have been carried out: Using a chiral Lagrangian, the authors of [165] give predictions for decays of the type  $\Lambda_c^+ \to 1/2^+ + 0^- + 0^-$ , while a semiquantitative estimate of the decay channels  $\Lambda_c^+ \to p\overline{K^0}\pi^0$  and  $p\overline{K^0}\pi^+\pi^-$  has been made in [166]. Further theoretical work on the nonleptonic many-body decays is needed. In Table 10 we list some of the current-algebra and pole-model calculations for two-body modes and compare them to a quark model calculation with best fit values for the overlap parameters  $H_2 = H_2'$  and  $H_3$  in Eq.(247). Compared to the quark model calculation of [139] the calculations [167,68,168] include long-distance dynamics by considering the contributions of low-lying baryon intermediate states. The calculations differ in the details of how coupling factors in this approach are determined. In [167] the non-factorizing contribution has been evaluated by using the pole approximation, where the (parity-violating) s-wave amplitudes are dominated by the low-lying  $1/2^-$  resonances, while the (parity-conserving) p-wave ones are governed by the ground state 1/2<sup>+</sup> poles. The MIT bag model was employed to calculate the coupling constants, form factors and baryon matrix elements. The importance of including the  $1/2^-$  pole terms to the s-wave contributions has also been emphasized by the authors of [68]. They used symmetry arguments to relate their couplings to those from semileptonic hyperon decays as well as the diquark model to determine the parity-conserving amplitudes. As for the parity-violating contribution, the authors of [68] claim that they are completely determined by the current algebra commutator term and the masses of the relevant  $1/2^-$  resonances without introducing further new parameters. Zenczykowski [168] sums intermediate states contributing to the parity-violating amplitudes to obtain an effective current-algebra expression. He uses broken SU(4) to relate coupling factors in the charm sector to coupling factors in the hyperon sector similar to the calculation [68].

All calculations [167,68,139,168] use the  $N_c \to \infty$  approximation to determine the factorizing contributions ("new factorization"). The new factorization scheme is supported by the analysis

of the Cabibbo suppressed decay  $\Lambda_c^+ \to p\phi$  which only gets contributions from the factorizing diagram I. As was first noticed in [23,139], its measured rate can only be accounted for by dropping terms proportional to  $1/N_c$ . We reiterate that the quark model and pole model or current algebra approaches to nonleptonic charm baryon decays are not radically different from one another because of the equality of spin–flavour factors in both approaches [151].

In the next few years the advent of new data will certainly constrain the current algebra and quark model calculations further. Almost all model calculations predict negative asymmetry parameter values close to their maximum value of -1 for the decays  $\Lambda_c^+ \to \Lambda \pi^+$  and  $\Lambda_c^+ \to pK^-$ . They are thus in agreement with the measured asymmetry parameter in the decay  $\Lambda_c^+ \to \Lambda \pi^+$  [96,95]. The decays  $\Lambda_c^+ \to \Xi^0 K^+$  and  $\Lambda_c^+ \to \Sigma \pi$  are particularly interesting: they obtain contributions only from the nonfactorizing diagrams IIa and III in Fig.18 and thus give a measure of the nonfactorizing contributions to nonleptonic charm baryon decays. Their experimental observation proves that the nonfactorizing (or W–exchange) contributions can certainly not be neglected as is implicit in the analysis of [149,161].

Table 10. Current algebra and quark model predictions for nonleptonic charm baryon decays. The num (in units  $10^{11}s^{-1}$ ) and asymmetry parameters  $\alpha_c$  (in parentheses)

	Cheng and Tseng	Cheng and Tseng	Xu and Kamal	Żenczykowski	Quark N
	Current Algebra [167]	Pole Model [167]	[68]	[168]	[139]
$\Lambda_c^+ \to p\overline{K^0}$	1.82(-0.90)	0.63(-0.49)	0.60(0.51)	0.99(-0.90)	input(-1)
$\Lambda_c^+ \to p \overline{K^0}(892)$				1.19	1.54
$\Lambda_c^+ \to \Delta^{++} K^-$					1.35
$\Lambda_c^+ \to p\phi$				0.05	0.11
$\Lambda_c^+ \to \Lambda \pi^+$	0.73(-0.99)	0.44(-0.95)	0.81(-0.67)	0.31(-0.86)	input(-0)
$\Lambda_c^+ \to \Lambda \rho^+$				0.27	9.54
$\Lambda_c^+ \to \Sigma^0 \pi^+$	0.88(-0.49)	0.36(0.78)	0.17(0.92)	0.23(-0.76)	0.16(0.70
$\Lambda_c^+ \to \Sigma^+ \pi^0$	0.88(-0.49)	0.36(0.78)	0.17(0.91)	0.23(-0.76)	0.16(0.71)
$\Lambda_c^+ \to \Sigma^+ \rho^0$				0.28	1.56
$\Lambda_c^+ \to \Sigma^+ \omega$				0.18	2.01
$\Lambda_c^+ \to \Xi^0 K^+$			0.05(0)	0.04(0)	0.13(0)
$\Xi_c^+ \to \Sigma^+ \overline{K^0}$	0.01(0.43)	0.19(-0.09)	0.10(0.24)	0.15(0.68)	1.46(-1.
$\Xi_c^+\to\Xi^0\pi^+$	0.19(-0.77)	0.89(-0.77)	0.76(-0.81)	0.16(0.65)	0.80(-0.
$\Xi_c^0 \to \Lambda \overline{K^0}$	0.89(-0.88)	0.24(-0.73)	0.33(1.00)	0.21(-0.84)	0.11(-0.
$\Xi_c^0 \to \Sigma^0 \overline{K^0}$	0.02(0.85)	0.12(-0.59)	0.09(-0.99)	0.03(-0.89)	1.05(-0.
$\Xi_c^0 \to \Sigma^+ K^-$			0.11(0)	0.04(0)	0.11(0)
$\Xi_c^0 \to \Xi^0 \pi^0$	1.12(-0.78)	0.25(-0.54)	0.50(0.92)	0.15(-0.99)	0.03(0.92)
$\Xi_c^0 \to \Xi^- \pi^+$	0.74(-0.47)	1.12(-0.99)	1.55(-0.38)	0.46(-0.78)	0.93(-0.
$\Omega_c^0 \to \Xi^0 \overline{K^0}$	0.98(0.44)	0.13(-0.93)			1.75(0.51)

# 8 Summary and Outlook

In this review we have concentrated on the decay properties of ground state and excited state charm and bottom baryons, focussing on recent advances in the understanding of how QCD turns into a much simplified Heavy Quark Effective Field Theory when the quarks become much heavier than the QCD confinement scale. Present experiments are already proving the usefulness of the concepts of HQET. One can expect a wealth of data on heavy hadron physics in the future to be confronted with the predictions of HQET.

At present there are strong experimental programmes on heavy hadron physics at high energy laboratories all over the world. ARGUS at DESY has stopped running in 1993 after having produced a wealth of important results on charm and bottom physics during its lifetime. CLEO is very much alive and coping very well with CESR's present top performance at a design luminosity of  $3 \times 10^{33} \, cm^{-2} \, s^{-1}$  with further improvements lying ahead. LEP has begun to contribute to bottom physics in a significant way. There will be two more years of running on the  $Z^0$  peak and there is still data on the tapes of previous runs waiting to be analyzed. The hyperon beam experiment WA89 at CERN specializes on charm–strangeness baryons and has seen first signs of the  $\Xi_c'$  baryon. There have been detector improvements and there are more runs coming up. At Fermilab the collider mode detectors CDF and D0 have produced high statistics charm and bottom hadron results and further detector and machine improvements are being planned or have been installed. Then there are the photoproduction and hadroproduction fixed target experiments E653, E672, E687, E691, E771, E789 and E791 that have yielded some very accurate results on heavy hadron physics in general and on some specific decay modes in particular.

SLAC is tooling up with its approved B factory project which is expected to start its bottom physics program in 1999. The HERA-B project at DESY and the B factory project at KEK are awaiting approval. While the primary objective of these machines is to discover and study CP-violation in the bottom sector there certainly will be ample fall-off for heavy hadron physics in general.

All in all, we can expect an abundance of interesting new data on charm and bottom baryons in the next few years. The field is very much alive and one can be sure that there will be plenty of experimental and theoretical activity in heavy baryon physics in the future. As experience has shown, real progress is achieved when theoretical and experimental advances go hand in hand. In this sense the theoretical heavy quark physics community is looking forward to a lot of new experimental results on heavy quark physics in general and on heavy baryon physics in particular.

#### Acknowledgements.

We would like to thank J.Landgraf, M.Lavelle and H.W.Siebert for help and advice. Much of

the material presented in this review is drawn from work done in collaboration with S.Balk, P.Bialas, F.E.Close, A.Czarnecki, C.A.Dominguez, F.Hussain, A.Ilakovac, U.Kilian, M.Jezabek, B.König, P.Kroll, J.H.Kühn, J.Landgraf, R.Migneron, R.J.Phillips, A.Pilaftsis, K.Schilcher, D.J.Summers, G.Thompson, M.Tung, Y.L.Wu and K.Zalewski. Part of this work was done while J.G.K. was a visitor at the DESY theory group. He would like to thank W.Buchmüller for hospitality and the DESY directorate for support. J.G.K. acknowledges partial support by the BMFT, Germany under contract 06MZ730. M.K. is supported by the DFG and D.P. is supported by the Graduiertenkolleg "Teilchenphysik" in Mainz.

### References

- [1] J.J.Aubert et al., Phys.Rev.Lett. **33** (1974) 1404
- [2] J.E.Augustin *et al.*, Phys.Rev.Lett. **33** (1974) 1406
- [3] E.G.Cazzoli et al., Phys.Rev.Lett. **34** (1975) 1125
- [4] G.Goldhaber et al., Phys.Rev.Lett. **37** (1976) 255
- [5] I.Peruzzi et al., Phys.Rev.Lett. **37** (1976) 569
- [6] K.Niu, E.Mikumo and Y.Maeda, Prog. Theor. Phys. 46 (1971) 1644
- [7] S.W.Herb et al., Phys.Rev.Lett. 39 (1977) 252;
   W.R.Innes et al., Phys.Rev.Lett. 39 (1977) 1240, 1640(E)
- [8] S.Behrends et al., Phys.Rev.Lett. 50 (1983) 881;
   R.Giles et al., Phys.Rev. D30 (1984) 2279
- [9] H.Albrecht *et al.*, Phys.Lett. **B185** (1987) 218
- [10] UA1 Collaboration, C.Albajar et al., Phys.Lett. **B273** (1991) 540
- [11] OPAL Collaboration, OPAL Physics Note PN111 (1993), private communication
- [12] ALEPH Collaboration, D.Decamp et al., Phys.Lett. B278 (1992) 209;
  OPAL Collaboration, P.Acton et al., Phys.Lett. B281 (1992) 394;
  ALEPH Collaboration, D.Buskulic et al., Phys.Lett. B294 (1992) 145;
  DELPHI Collaboration, P.Abreu et al., Phys.Lett. B311 (1993) 379
- [13] ALEPH Collaboration, contribution to Europhysics Conference on High Energy Physics, Marseille 1993;
  DELPHI Collaboration, contribution to Europhysics Conference on High Energy Physics, Marseille 1993
- [14] M.Basile *et al.*, Lett.Nuovo Cimento **31** (1981) 97
- [15] F.Bloch and A.Nordsieck, Phys.Rev. **52** (1937) 54
- [16] N.Bogoliubov and D.V.Shirkov, Introduction to the Theory of Quantized Fields, Interscience Publishers Inc., N.Y. 1959

- [17] R.N.Cahn, ed., e<sup>+</sup>e<sup>-</sup>Annihilation: New Quarks and Leptons
   (A volume in the Annual Reviews Special Collections Program);
   Menlo Park: Benjamin-Cummings (1985)
- [18] W.Kwong, J.L.Rosner and C.Quigg, Ann.Rev.Nucl.Part.Sci. 37 (1987) 325
- [19] R.J.Morrison and M.S.Witherell, Ann.Rev.Nucl.Part.Sci. 39 (1989) 183
- [20] M.A.Shifman, Nucl. Phys. **B3** (Proc. Suppl.) (1988) 289
- [21] S.R.Klein, Int.J.Mod.Phys. **A5** (1990) 1457
- [22] S.Fleck and J.M.Richard, Particle World 1 (1990) 67
- [23] J.G.Körner and H.W.Siebert, Ann.Rev.Nucl.Part.Sci. 41 (1991) 511
- [24] B.Grinstein, Ann.Rev.Nucl.Part.Sci. 42 (1992) 101;
  N.Isgur and M.B.Wise, in *B Decays*, S.Stone (Ed.), World Scientific 1992;
  H.Georgi, HUPT-91-A039 (published in 1991 TASI Proceedings);
  J.G.Körner, in Proc.Int.Symp. "Extended Objects and Bound Systems", Karuizawa, Japan (1992), World Scientific, Singapore (1993) p.279
- [25] M.Neubert, SLAC-PUB-6263, September 1993
- [26] Particle Data Group, K.Hikasa et al., Phys.Rev. **D45** (1992) S1
- [27] ARGUS Collaboration, H.Albrecht et al., Phys.Lett. **B288** (1992) 367
- [28] E687 Collaboration, P.L.Frabetti et al., Phys.Lett. **B300** (1993) 190
- [29] SKAT Collaboration, V.V.Ammosov *et al.*, paper #42 submitted to XVI International Symposium on Lepton-Photon Interactions, Cornell University, Ithaca (1993)
- [30] W.Kwong and J.L.Rosner, Phys.Rev. **D44** (1991) 212
- [31] U.Aglietti, Phys.Lett. **B281** (1992) 341
- [32] A.De Rújula, H.Georgi and S.L.Glashow, Phys.Rev. **D12** (1975) 147
- [33] S.Capstick and N.Isgur, Phys.Rev. **D34** (1986) 2809
- [34] WA89 Collaboration, private communication
- [35] E.Eichten and F.Feinberg, Phys.Rev. **D23** (1981) 2724;
  E.V.Shuryak, Nucl.Phys. **B198** (1982) 83;
  S.Nussinov and W.Wetzel, Phys.Rev. **D36** (1987) 130;
  M.B.Voloshin and M.A.Shifman, Sov.J.Nucl.Phys. **45** (1987) 292; **47** (1988) 511
- [36] H.D.Politzer and M.B.Wise, Phys.Lett. B206 (1988) 681; B208 (1988) 504;
  N.Isgur and M.B.Wise, Phys.Lett. B232 (1989) 113; B237 (1990) 527;
  G.Lepage and B.A.Thacker, Nucl.Phys. B4 (1988) 199;
  E.Eichten and B.Hill, Phys.Lett. B234 (1990) 511;
  B.Grinstein, Nucl.Phys. B339 (1990) 253;
  H.Georgi, Phys.Lett. B240 (1990) 447;

- F.Hussain, J.G.Körner, K.Schilcher, G.Thompson and Y.L.Wu, Phys.Lett. **B249** (1990) 295
- [37] M.J.Savage and M.B.Wise, Phys.Lett. **B248** (1990) 177;
   M.White and M.J.Savage, Phys.Lett. **B271** (1991) 410
- [38] N.Isgur and M.B.Wise, Nucl.Phys. B348 (1991) 276;
  H.Georgi, Nucl.Phys. B348 (1991) 293;
  T.Mannel, W.Roberts and Z.Ryzak, Nucl.Phys. B355 (1991) 38
- [39] F.Hussain, J.G.Körner, M.Krämer and G.Thompson, Z.Phys. C51 (1991) 321
- [40] A.Falk, H.Georgi, B.Grinstein and M.B.Wise, Nucl. Phys. B343 (1990) 1
- [41] E.Eichten and B.Hill, Phys.Lett. **B243** (1990) 427;
   A.Falk, B.Grinstein and M.Luke, Nucl.Phys. **B357** (1991) 185
- [42] J.G.Körner and G.Thompson, Phys.Lett. **B264** (1991) 185
- [43] T.Mannel, W.Roberts and Z.Ryzak, Nucl. Phys. **B368** (1992) 204
- [44] S.Balk, J.G.Körner and D.Pirjol, Mainz preprint MZ-TH/93-13, 1993
- [45] A.Das, Univ. of Rochester preprint UR-1325, 1993
- [46] M.Luke, Phys.Lett. **B252** (1990) 447
- [47] H.Georgi, B.Grinstein and M.B.Wise, Phys.Lett. **B252** (1990) 456
- [48] C.G.Boyd and D.E.Brahm, Phys.Lett. **B254** (1991) 468
- [49] C.G.Boyd and D.E.Brahm, Phys.Lett. B257 (1991) 393
- [50] F.Hussain, J.G.Körner and G.Thompson, ICTP Preprint, IC/93/314, Mainz preprint MZ-TH/93-23 (1993)
- [51] L.A.Copley, N.Isgur and G.Karl, Phys.Rev.  $\mathbf{D20}\ (1979)\ 768$
- [52] D.Acosta et al. (CLEO Collaboration), CLEO CONF 93-7 and CLEO CONF 93-32, contributed to the International Symposium on Lepton and Photon Interactions, Ithaca 1993
- [53] ARGUS Collaboration, H.Albrecht et al., Phys.Lett. **B317** (1993) 227
- [54] P.L.Frabetti *et al.* (E687 Collaboration) Fermilab preprint FERMILAB-PUB-93-323-E (1993)
- [55] H.F.Jones, Groups, Representations and Physics, Adam Hilger, Bristol, N.Y., 1990
- [56] J.T.Gudehus, Phys.Rev. **184** (1969) 1788
- [57] A.F.Falk, Nucl.Phys. **B378** (1992) 79
- [58] J.G.Körner, Nucl.Phys. **B21** (Proc.Suppl.) (1991) 366

- [59] K.Zalewski, Phys.Lett. **B264** (1991) 432
- [60] N.Isgur, M.B.Wise and M.Youssefmir, Phys.Lett. **B254** (1991) 215
- [61] H.D.Politzer, Phys.Lett. **B250** (1990) 128
- [62] J.G.Körner and M.Kuroda, Phys.Lett. **B67** (1977) 455
- [63] F.Hussain, D.Liu, M.Krämer, J.G.Körner and S.Tawfiq, Nucl. Phys. **B370** (1992) 259
- [64] J.D.Bjorken, Invited talk given at "Les Recontre de la Vallee d'Aosta La Thuile", Editions Frontiers, Gif-sur-Yvette (1990) 583;
   J.D.Bjorken, I.Dunietz and J.Taron, Nucl.Phys. B371 (1992) 111
- [65] Q.P.Xu, Phys.Rev. **D48** (1993) 5429
- [66] G.V.Efimov, M.A.Ivanov, N.B.Kulimanova and E.Lyubovitskij, Z.Phys. C54 (1992) 349
- [67] F.Hussain, J.G.Körner and R.Migneron, Phys.Lett. **B248** (1990) 406
- [68] Q.P.Xu and A.N.Kamal, Phys.Rev. **D46** (1992) 270
- [69] C.Carone, H.Georgi and S.Osofski, Phys.Lett. **B322** (1994) 227
- [70] C.K.Chow and M.B.Wise, Caltech preprint CALT-68-1919 (1994)
- [71] Hai-Yang Cheng, Chi-Yee Cheung, Guey-Lin Lin, Y.C.Lin, Tung-Mow Yan and Hoi-Lai Yu, Phys.Rev. **D46** (1992) 5060
- [72] A.Grozin and O.Yakovlev, Novosibirsk Preprint BUDKERINP-94-3 (1994)
- [73] A.Ilakovac, U.Kilian, J.G.Körner and J.Landgraf, to be published
- [74] N.Isgur and M.B.Wise, Phys.Rev.Lett. **66** (1991) 1130
- [75] K.Zalewski, Plenary talk at the EPS HEP 93 Conference, Marseille 1993
- [76] A.F.Falk and M.E.Peskin, SLAC Preprint SLAC-PUB-6311 (1993)
- [77] A.Ilakovac, J.G.Körner and J.Landgraf, to be published
- [78] J.G.Körner, D.Pirjol and K.Schilcher, Phys.Rev. **D47** (1993) 3955
- [79] A.Ilakovac, J.G.Körner and J.Landgraf, to be published
- [80] Hai-Yang Cheng, Chi-Yee Cheung, Guey-Lin Lin, Y.C.Lin, Tung-Mow Yan and Hoi-Lai Yu, Phys.Rev. **D47** (1993) 1030
- [81] P.Cho, Caltech preprint CALT-68-1912 (1994)
- [82] A.Ali and E.Pietarinen, Nucl.Phys. B154 (1979) 519;
   N.Cabibbo, G.Corbo and L.Maiani, Nucl.Phys. B155 (1979) 83;
   G.Corbo, Nucl.Phys. B212 (1983) 99
- [83] M.Jezabek and J.H.Kühn, Nucl.Phys. **B320** (1989) 20

- [84] G.Altarelli, N.Cabibbo, G.Corbo, L.Maiani and G.Martinelli, Nucl.Phys. **B208** (1982) 365
- [85] A.Czarnecki, M.Jezabek, J.G.Körner and J.H.Kühn, Karlsruhe and Mainz preprint TTP 93-32, MZ-TH/93-35 (1993)
- [86] J.Chay, H.Georgi and B.Grinstein, Phys.Lett. **B247** (1990) 399
- [87] I.I.Bigi, M.Shifman, N.G.Uraltsev and A.Vainshtein, Phys.Rev.Lett. 71 (1993) 496;
  B.Blok, L.Koyrakh, M.Shifman and A.I.Vainshtein, NSF-ITP-93068, 1993;
  A.Manohar and M.Wise, Phys.Rev. D49 (1994) 1310;
  A.F.Falk, M.Luke and M.J.Savage, UCSD/PTH 93-23, 1993;
  T.Mannel, IKDA 93/26 (1993)
- [88] M.Neubert, CERN preprint CERN-TH.7087/93, November 1993;
  A.F.Falk, E.Jenkins, A.V.Manohar and M.Wise, UCSD-PTH-93-38, December 1993;
  M.Neubert, CERN preprint CERN-TH.7113/93, December 1993;
  I.I.Bigi, M.A.Shifman, N.G.Uraltsev and A.I.Vainshtein, TPI-MINN-93/60-T, UMN-TH-1231-93, CERN-TH.7129/93, December 1993
- [89] C.Csaki and L.Randall, preprint CTP-2262, 1993;
  G.Baillie, preprint UCLA/93/TEP/47;
  I.Bigi, M.Shifman, N.Uraltsev and A.Vainshtein, CERN-TH.7159/94, TPI-MINN-94/2-T, UMN-TH-1235-94, UND-HEP-94-BIG02, 1994
- [90] A.F.Falk and M.Neubert, Phys.Rev. **D47** (1993) 2982
- [91] L.Koyrakh, Minnesota preprint TPI-MINN-93/47-T;
   S.Balk, J.G.Körner, D.Pirjol and K.Schilcher, Mainz preprint MZ-TH/93-32;
   A.F.Falk, Z.Ligeti, M.Neubert and Y.Nir, Univ.of California, San Diego preprint UCSD/PTH 93-43
- [92] E.Vella et al., Phys.Rev.Lett. 48 (1982) 1515
- [93] H.Albrecht et al., Phys.Lett. **B219** (1989) 121
- [94] D.Bertoletto et al., Phys.Rev.Lett. 63 (1989) 1667
- [95] ARGUS Collab., H.Albrecht et al., Z.Phys. C57 (1993) 533
- [96] CLEO Collab., S.Songhera et al., Phys.Rev. **D47** (1993) 791
- [97] J.C.Anjos, et al., Phys.Rev.Lett. **65** (1990) 2630
- [98] J.G.Körner and G.A.Schuler, Z.Phys. C38 (1988) 511; erratum Z.Phys. C41 (1989) 690
- [99] J.G.Körner and G.A.Schuler, Phys.Lett. **B226** (1989) 185
- [100] J.G.Körner and G.A.Schuler, Z.Phys. C46 (1990) 93
- [101] B.Grinstein, N.Isgur, D.Scora and M.B.Wise, Phys.Rev. **D39** (1989) 799
- [102] K.Hagiwara, A.D.Martin and M.F.Wade, Phys.Lett. **B228** (1989) 144;
   Nucl.Phys. **B327** (1989) 569

- [103] F.J.Gilman and R.L.Singleton, Phys.Rev. **D41** (1990) 142
- [104] G.Köpp, G.Kramer, W.F.Palmer and G.A.Schuler, Z.Phys. C48 (1990) 327
- [105] J.G.Körner and G.A.Schuler, Phys.Lett. **B231** (1989) 306;
   C.A.Dominguez, J.G.Körner and K.Schilcher, Phys.Lett. **B248** (1990) 399
- [106] K.Hagiwara, A.D.Martin and M.F.Wade, Z.Phys. C46 (1990) 299
- [107] J.G.Körner and M.Krämer, Phys.Lett. **B275** (1992) 495
- [108] P.Białas, J.G.Körner, M.Krämer and K.Zalewski, Z.Phys. C57 (1993) 115
- [109] ARGUS Collaboration, H.Albrecht et al., Phys.Lett. **B326** (1994) 320
- [110] CLEO Collaboration, T.Bergfeld et al., Phys.Lett. B323 (1994) 219
- [111] J.G.Körner, K.Schilcher and Y.L.Wu, Phys.Lett. **B242** (1990) 119(1990)
- [112] A.N.Aleev et al., Yad.Fiz. 43 (1986) 619
- [113] P.Chauvat et al., Phys.Lett. **B119** (1987) 304
- [114] J.D.Bjorken, Phys.Rev. **D40** (1989) 1513
- [115] A.J.Buras, Nucl. Phys. **B109** (1976) 373
- [116] K.Yamada, Phys.Rev. **D22** (1980) 1676
- [117] M.B.Gavela, Phys.Lett. **B83** (1979) 367
- [118] C.Avilez and T.Kobayashi, Phys.Rev. **D19** (1979) 3448
- [119] R.Pérez-Marcial et al., Phys.Rev. **D40** (1989) 2955
- [120] R.Singleton, Phys.Rev. **D43** (1991) 2939
- [121] F.Hussain and J.G.Körner, Z.Phys. C51 (1991) 607
- [122] P.Kroll, B.Quadder and W.Schweiger, Nucl. Phys. **B316** (1989) 393
- [123] F.E.Close, An Introduction to Quarks and Partons, Academic Press 1979
- [124] G.L.Lin and T.Mannel, Phys.Lett. **B321** (1993) 417
- [125] B.König, J.G.Körner and M.Krämer, to be published
- [126] B.König, J.G.Körner, M.Krämer and P.Kroll, Mainz preprint MZ-TH/92-42
- [127] X.H.Guo and P.Kroll, Z.Phys. C59 (1993) 567;
   F.Hussain, D.S.Liu and S.Tawfiq, ITCP preprint IC-93-25 (1993)
- [128] J.G.Körner, A.Pilaftsis and M.Tung, Mainz Preprint MZ-TH/93-20
- [129] F.E.Close, J.G.Körner, R.J.N.Phillips and D.J.Summers, Journ.Phys. G18 (1992) 1716

- [130] J.F.Amundson et al., Phys.Lett. **B296** (1992) 415
- [131] P.Cho and H.Georgi, Phys.Lett. **B296** (1992) 408
- [132] M.Gronau, Technion preprint TECHNION-PH-94-6, 1994
- [133] M.Gronau and S.Wakaizumi, Phys.Lett. **B280** (1992) 79;
   M.Gronau and S.Wakaizumi, Phys.Rev.Lett. **68** (1992) 1814
- [134] M.Gronau, T.Hasuike, T.Hattori, Z.Hioki, T.Hayashi and S.Wakaizumi, Journ.Phys. G19 (1993) 1987
- [135] T.Mannel and G.A.Schuler, Phys.Lett. B279 (1992) 194;
  J.Amundson, J.L.Rosner, M.Worah and M.B.Wise, Phys.Rev. D47 (1993) 1260;
  B.Mele and G.Altarelli, Phys.Lett. B299 (1993) 345;
  M.Gronau and S.Wakaizumi, Phys.Rev. D47 (1993) 1262;
  M.Tanaka, Phys.Rev. D47 (1993) 4969;
  Z.Hioki, Phys.Lett. B303 (1993) 125;
  Z.Hioki, Z.Phys. C59 (1993) 555
- [136] S. Wakaizumi in Proc. Int. Workshop on B-Factories, KEK, Nov. 17-20, 1992, p.390 (1992)
- [137] B.König, J.G.Körner and M.Krämer, Phys.Rev. **D49** (1993) 2363
- [138] M.Procario, Talk given at the International Symposium on Heavy Flavour Physics, Montreal, Canada, July 6-10, 1993
- [139] J.G.Körner and M.Krämer, Z.Phys. C55 (1992) 659
- [140] R.Forty, Invited talk at the  $XIII^{th}$  International Conference on Physics in Collisions, Heidelberg (1993), to appear in the Proceedings.
- [141] V.Barger, J.P.Leveille and P.M.Stevenson, Phys.Rev.Lett. 44 (1980) 226
- [142] M.B.Voloshin and M.A.Shifman, Sov.Phys.JETP 64 (1986) 698;
   M.B.Voloshin and M.A.Shifman, Sov.J.Nucl.Phys. 41 (1985) 120
- [143] B.Guberina, R.Rückl and J.Trampetić, Z.Phys. C33 (1986) 297
- [144] H.D.Politzer and M.B.Wise, Phys.Lett. **B206** (1988) 681
- [145] M.K.Gaillard and B.W.Lee, Phys.Rev.Lett. 33 (1974) 108;
   G.Altarelli and L.Maiani, Phys.Lett. B52 (1974) 35
- [146] J.L.Cortes and J.Sanchez-Guillen, Phys.Rev. **D24** (1981) 2982
- [147] B.Blok and M.Shifman, Minnesota preprint TPI-MINN-93/55-T
- [148] J.D.Jackson in High Energy Physics,
   ed. C. de Witt and R.Gatto. New York, Gordon and Breach (1965), p.325;
   A.D.Martin and D.Spearman, Elementary Particle Theory.
   Amsterdam, North-Holland (1970);
   R.Pilkuhn, The Interactions of Hadrons. Amsterdam, North-Holland (1967)

- [149] J.D.Bjorken, Phys.Rev. **D40** (1989) 1513
- [150] R.Lednicky, Sov.J.Nucl.Phys. 43 (1986) 817
- [151] J.G.Körner, G.Kramer and J.Willrodt, Z.Phys. C2 (1979) 117
- [152] Y.Iwasaki, Phys.Rev.Lett. **34** (1975) 1407; (E) **35** (1975) 246
- [153] G.Altarelli, N.Cabibbo and L.Maiani, Phys.Lett. **B57** (1978) 277
- [154] M.J.Savage and R.P.Springer, Phys.Rev. **D42** (1990) 1527
- [155] S.Pakvasa, S.F.Tuan and S.P.Rosen, Phys.Rev. **D42** (1990) 3746
- [156] J.G.Körner, Nucl.Phys. B25 (1970) 282;
   J.G.Pati and C.H.Woo, Phys.Rev. D3 (1971) 2920; D42 (1990) 3746
- [157] M.Bauer and B.Stech, Phys.Lett. **B152** (1985) 380
- [158] A.J.Buras, J.M.Gérard and R.Rückl, Nucl. Phys. **B268** (1986) 16
- [159] F.Hussain, J.G.Körner and G.Thompson, Ann. Phys. **206** (1991) 334
- [160] J.G.Körner and G.R.Goldstein, Phys.Lett. **B89** (1979) 105
- [161] T.Mannel, W.Roberts and Z.Ryzak, Phys.Lett. **B255** (1991) 593;
   A.Acker, S.Pakvasa, S.P.Rosen and S.F.Khan, Phys.Rev. **D43** (1991) 3083
- [162] J.G.Körner and T.Gudehus, Nuovo Cim. **11A** (1972) 597
- [163] J.G.Körner, G.Kramer and J.Willrodt, Phys.Lett. **B81** (1979) 365
- [164] F.Pierre, DAPNIA/SPP 93-14, unpublished
- [165] Y.L.Kalinovsky, V.N.Pervushin and N.A.Sarikov, Phys. Lett. **B180** (1986) 141
- [166] S.Fajfer, A.Ilakovac, D.Tadić and K.Surulitz, Preprint Technische Universität München TUM-T31-51/93, to be published in Z. Phys. C
- [167] H.Y.Cheng and B.Tseng, Phys.Rev. **D48** (1993) 4188
- [168] P.Zenczykowski, INP-1643-PH, unpublished
- [169] CLEO Collaboration (P.Avery, et al.), CNLS 93/1260, CLEO 93-22, unpublished
- [170] M.Procario, in the 5th Internatiol Symposium on Heavy Flavour Physics, Montreal, 1993, unpublished
- [171] CLEO Collaboration (P.Avery, et al.), CNLS 93/1231, CLEO 93-10, unpublished
- [172] CLEO Collaboration (P.Avery, et al.), Phys.Rev.Lett. **71** (1993) 2291

This figure "fig1-1.png" is available in "png" format from:

This figure "fig2-1.png" is available in "png" format from:

This figure "fig1-2.png" is available in "png" format from:

This figure "fig2-2.png" is available in "png" format from:

This figure "fig1-3.png" is available in "png" format from:

This figure "fig2-3.png" is available in "png" format from:

This figure "fig1-4.png" is available in "png" format from: